

© 2006

Felisa Lauren Wolfe-Simon

ALL RIGHTS RESERVED

THE ROLE AND EVOLUTION OF SUPEROXIDE DISMUTASES IN ALGAE

by

FELISA LAUREN WOLFE-SIMON

A Dissertation submitted to the

Graduate School-New Brunswick

Rutgers, The State University of New Jersey

In partial fulfillment of the requirements

for the degree of

Doctor of Philosophy

Graduate Program in Oceanography

written under the direction of

Paul Falkowski and Oscar Schofield

and approved by

Paul Falkowski

Oscar Schofield

Jody Hey

John Reinfelder

Costantino Vetriani

Edward Stiefel

New Brunswick, New Jersey

*May 2006*

## ABSTRACT OF THE DISSERTATION

### **THE ROLE AND EVOLUTION OF SUPEROXIDE DISMUTASES IN ALGAE**

By FELISA LAUREN WOLFE-SIMON

Dissertation Directors:

Paul Falkowski and Oscar Schofield

Superoxide is a natural byproduct of normal cellular functions and is an important molecule to detoxify because it can obliterate key cellular components. Superoxide dismutases catalyze the destruction of the superoxide radical ( $O_2^{\cdot -}$ ) into molecular oxygen and hydrogen peroxide. There are four known varieties of SODs distinguished by their metal cofactor. These are the iron (Fe), manganese (Mn), copper-zinc (CuZn) and nickel (Ni) forms. This enzyme plays a particularly important role in photosynthetic eukaryotes because they have two sources of radical oxygen: photosynthesis and respiration.

This dissertation focuses on aspects of SODs in marine secondary red plastid derived algae. Photosynthetic eukaryotes evolved from a singular primary endosymbiosis where a heterotrophic cell engulf and enslaved a cyanobacterium-like plastid. These primary endosymbiotic eukaryotes diverged into the green and red plastid lineages. The secondary red plastid containing algae are the most successful in the modern ocean. Typically, photosynthetic eukaryotes have FeSOD within the plastid. However, laboratory results suggest that the secondary red alga diatom, *Thalassiosira*

*pseudonana*, posses an MnSOD in the plastid which can account for approximately 20% of the total Mn in a cell. This helps close the Mn budget for diatoms. This is a unique use for MnSOD and may contribute to the success of *T. pseudonana* in the Fe poor modern ocean.

This dissertation also addresses the molecular phylogeny of the Fe- and MnSOD family to further understand the extant physiological expression of this enzyme and also examine the phylogenetic position of secondary red algae with respect to the SODs. Because these enzymes are localized with in organelles the genes have likely derived from the original organelle endosymbiont. These data suggest that for all plastid derived eukaryotes FeSOD evolved from the primary endosymbiotic event and was transferred to the nucleus from the plastid because this is the last common ancestor of all these organisms. This includes currently amitochondrial or aplastidic parasites that have subsequently lost these organelles. The MnSOD sequences show monophyly for primary and secondary red algae with a basal relationship to the primary green alga. Because green plants cluster separately with the cyanobacteria, this suggests that the MnSOD of primary green, primary and secondary red plastid eukaryotes evolved from the primary endosymbiotic host cell (i.e. last common ancestor for these groups) and the green plants derived MnSOD from the primary endosymbiont plastid.

## ACKNOWLEDGEMENTS

There are so many people I owe a great deal of thanks to that I will just try and start from the beginning. Fundamental to my pursuit of a Ph.D. and was the influence of Dr. Gail Tucker-Griffith as my Advance Placement Biology teacher in high school. It was no small feat to teach this high level course at a performing arts high school! Dr. David Egloff was my undergraduate advisor who anticipated my foray into ocean sciences and algae so much so that he made sure to send me off to the jungles of Costa Rica to study Howler Monkeys. Just to make sure I knew what I wanted to do. I learned how to look up that summer- thanks. I also want to thank Dr. Ivan Valiela for turning me on to biogeochemistry as an undergraduate during a summer REU in Woods Hole.

Graduate school has been a tremendously intense learning experience and with out the support and guidance of my co-advisors: Dr. Paul Falkowski and Dr. Oscar Schofield this would never have been possible. Paul for being...Paul; a stimulating, extraordinary, and never predictable challenge. Oscar, for a warm-fuzzy sort of shot in the arm. I also want to thank my committee members for dealing with the interdisciplinary nature of both my project and myself. Drs. John Reinfelder, Costa Vetriani, Jody Hey, and Ed Stiefel. You all always made time for my questions and dire need for feedback. Thank you. Furthermore, I want to especially thank the financial support of the National Science Foundation and Rutgers University.

Of course, my fellow graduate students at IMCS are also integral to my success. Jason Sylvan and Grant Law - rock on. Steve Litvin, Tracy Wiegner, Tuo Shi, Sindia Sosdian, Alex Kahl, Carrie Fraser, Steve Tuorto, Rachel Sipler, and others. Thanks for being around when I most needed you! Also, I wish to thank the many post-docs that

have been through the Falkowski lab. I owe a huge amount of thanks to Drs. Yi-Bu Chen, Yi Sun, Daniel Grzebyk, Michal Koblizek, Diana Nemergut, Lin Jiang, and Ilana Berman-Frank. And of course, a great big thank you hug to Liti Haramaty and Kevin Wyman who put up with my need for constant instrument refresher courses!

Finally, my deepest gratitude to my besheert, Jonathan. Without whom none of this would have even been a thought.

## TABLE OF CONTENTS

ABSTRACT OF THE DISSERTATION	ii
ACKNOWLEDGEMENTS	iv
LIST OF TABLES	ix
LIST OF ILLUSTRATIONS	x
1.0 Introduction	1
1.1 Sources and Sinks of ROS in Algae	5
1.2 The SOD Defense System	9
1.2.1 Iron and Manganese SODs	10
1.2.2 Copper-Zinc SODs	12
1.2.3 Nickel SODs	16
1.3 Objectives of Dissertation Research	16
2.0 Review of SODs in Prokaryotic and Eukaryotic Algae	22
2.1 Environmental Regulation of SODs in Algae	23
2.1.1 Visible Light Stress	23
2.1.2. Ultraviolet Radiation	24
2.1.3 Nutrient Stress	25
2.1.4 Metal Toxicity	25
2.2 Algae SODs in an Evolutionary Context	26
2.3 Conclusions and Future Directions	31

3.0	Localization and Role of Manganese Superoxide Dismutase in a Marine	
	Diatom	34
3.1	Introduction	35
3.2	Materials and Methods	37
	3.2.1 Organisms, Culture Conditions, and Standard Protocols	37
	3.2.2 Cloning and Purification of Recombinant TpMnSOD	37
	3.2.3 Antibody Production Against TpMnSOD	38
	3.2.4 Immunoblot Analyses	38
	3.2.5 Immunogold Staining	39
3.3	Results	41
	3.3.1 Native Molecular Mass and Western Analyses	41
	3.3.2 MnSOD and the Cellular Manganese Budget in Diatoms	41
	3.3.3 Immunolocalization of MnSOD in Plastids	45
	3.3.4 Impact of Light on TpMnSOD Expression	45
3.4	Discussion	52
4.0	The Phylogenetic Position of Iron and Manganese Superoxide Dismutases in	
	Secondary Red Algae	58
4.1	Introduction	60
4.2	Materials and Methods	63
4.3	Results	65
	4.3.1 FeSOD Clade	70

4.3.2	MnSOD Clade	75
4.3.3	Phototroph Phylogeny	78
4.4	Discussion	80
4.4.1	Position of the primary and secondary plastid-containing eukaryotes	80
4.4.2	The secondary red-plastid puzzle	82
4.4.3	Evidence for LGT beyond endosymbiosis	84
4.4.4	Correlative relationship between the molecular evolution of Photosystems I and II and the Fe/MnSOD family	85
4.5	Conclusion	87
	References	95
	Curriculum Vita	109

## LIST OF TABLES

Table 1.1: The four one-electron reactions for the reduction of O <sub>2</sub> to H <sub>2</sub> O in aqueous solution and the corresponding reduction potentials.	20
Table 1.2: The basic superoxide dismutase ping-pong mechanism.	21
Table 3.1: Antibody cross reactivity.	56
Table 3.2: Statistics for MnSOD in <i>Thalassiosira pseudonana</i> CCMP1335	57
Table 4.1 All Fe- and MnSOD amino acid sequences used in analyses and their ID	89
Table. 4.2 Averages of similarity indices of Fe- and Mn Superoxide Dismutases.	93
Table 4.3 Prokaryotic and eukaryotic plastid-related sequences used in analyses.	94

## LIST OF ILLUSTRATIONS

Figure 1.1: Seasonal hydrogen peroxide and chlorophyll at the Hawaii Ocean Times

Series (HOT) station ALOHA. Data collected from Jan 1994 to Dec 1998 (Gasc et al., 2002). Color represents average chlorophyll in  $\text{ng}\cdot\text{L}^{-1}$  and contour lines are of equal hydrogen peroxide concentrations in nM. Within the water column algae are the most prominent source of ROS. Significant abiological ROS production would require the presence of free transition metals. At this location, the average trace metal concentrations are too low to produce (from Fenton reactions, see text) the level of ROS observed. Some work has suggested that in coastal and estuarine regions, CDOM may serve as both a source and a sink for ROS {Andrews, 2000 #432; Voelker, 2000 #431; Zepp, 1992 #430; Blough, 1995 #433}, Andrews et al. 2000, Voelker et al. 2000). However, the low nutrient- low chlorophyll waters at the HOT station are unlikely to experience the same levels of CDOM and abiotically produced ROS. 3

Figure 1.2: Synthetic distribution based on known evidence from biochemical and genetic data of the various superoxide dismutases over the tree of life (figure modified after Baldauf et al., 2004). All the potential routes for genetic inheritance are evident in SOD genes. FeSOD is widely distributed between all major clades while specifically MnSOD is more prevalent in Bacteria and Eukaryota. Fe and MnSOD have contrasting potential evolutionary histories. In eukaryotic photosynthetic autotrophs, the ancestral origin of FeSOD may be from

the GSB ancestor of PSI in cyanobacteria, while MnSOD has a variety of possible origins mainly the proteobacterial ancestor to PSII and mitochondria; both plastid metalloforms having been acquired through cyanobacteria. CuZnSOD demonstrates multiple lateral gene transfers. Furthermore, organisms often possess multiple copies of CuZnSOD in their genomes, which are in general significantly phylogenetically distant. Branches are colored according to known SODs: magenta- FeSOD, cyan- MnSOD, cyan/magenta- Fe/MnSOD (cambialistic), green- CuZnSOD, and grey- unknown form of SOD. \* NiSOD genes found in genomes of four cyanobacteria. CuZnSOD only found in *Gloeobacter* sp. †NiSOD and FeZnSOD found in *Streptomyces* spp. 6

Figure 1.3: Subcellular localization of superoxide dismutases. This conceptual scheme summarizes all known locations of SODs within eukaryotic cells. An important attribute of SODs is that they are poised and ready at metabolic the site of superoxide production. Soluble forms of SOD found in the cytoplasm are typically CuZnSOD in embryophytes. Occasionally, FeSOD can be found soluble but, both cytoplasmic and extracellular SODs are characteristic of multicellular organisms that have cell signaling pathways through which ROS are exchanged. The chloroplast can be associated with Fe, Mn, and/or CuZnSOD. In diatoms, MnSOD can be found here, most likely associated with the lumen side of PSII (Wolfe-Simon unpublished). CuZnSOD and FeSOD may fill the same role on the stromal side of PSI, with the former dominantly found in embryophytes and charophytes and the latter in the cyanobacteria, chlorophytes, and dinoflagellates.

Much research is still needed to completely understand the SODs with in other algal plastids. The mitochondria have MnSOD almost exclusively. No other SOD has been found associated with these organelles in photosynthetic autotrophs.

14

Figure 1.4: Phylogenetic tree of NiSOD genes. NiSODs have been biochemically characterized in the two *Streptomyces* sp. shown. The cyanobacteria sequences represented here are derived from genomic data, but no biochemical or physiological data are yet available for the activity of NiSODs in cyanobacteria. Interestingly, both *Prochlorococcus* sp. strains shown possess only the gene for NiSOD- they do not contain genetic information for any other known form of SOD. The evolutionary significance of NiSODs is not yet clear but, the increase in genomic data will help resolve this issue. This may prove to be a major sink for Ni in environments where these are the dominant organisms. This unrooted tree was generated using the Genetic Database Environment (GDE) sequence alignment editor (Smith et al., 1994) based on a DNA maximum likelihood approach using fastDNAm1 (Felsenstein, 1981; Olsen et al., 1994), the branching pattern is supported by bootstrap analysis (100 replicates). The tree has been modified for clarity. Accession numbers are given for the *Streptomyces* sp. and ORF identification numbers are give for all the cyanobacteria. Scale bar represents the number of substitutions per nucleotide site.

18

Figure 2.1: Unrooted phylogenetic tree for iron and manganese superoxide dismutase proteins. The phylogenetic clusters reflect the evolutionary history of these nuclear encoded genes. The MnSOD branches follow a mitochondrial origin while the FeSOD patterns are likely due to originating from the plastid symbiont. FeSOD likely derived from the ancestral progenitors of PSI in cyanobacteria, the GSB. Interestingly, MnSOD may have originated from the proteobacterial source of PSII, which is also associated with the origin of mitochondria. See text for full discussion. SOD amino acid sequences were aligned using CLUSTALX (Thompson et al., 1994; Thompson et al., 1997) and the Genetic Data Environment (GDE) (Smith et al., 1994) multiple sequence editor. A maximum-likelihood tree was constructed using PHYML (Guindon and Gascuel, 2003) employing an empirical model of evolution (Whelan and Goldman, 2001) and the branching pattern is supported by bootstrap analysis (100 replicates). The scale represents the expected number of substitutions per amino acid position. The tree has been modified for clarity. FeSOD representatives are indicated with magenta branches while MnSOD representatives are in cyan. Species text color key: green – chlorophytes and higher plants, red – rhodophytes, aqua – cyanobacteria, brown – chromophyte algae. Accession numbers of the sequences are next to each taxa.

28

Figure 3.1: Immunoblot of Selected Diatom Species.

Immunoblots showing the anti-TpMnSOD antibody we produced cross-reacted with multiple diatom species. The phylum specificity of this antibody suggests

that all diatoms have an MnSOD with similar structure. All lanes loaded with 30µg total protein (except control loaded with 10ng pure recombinant TpMnSOD): lane 1, *Ditylum brightwellii* CCMP358; lane 2, *Navicula incerta* CCMP542; lane 3, *Nitzschia brevirostris* CCMP551; lane 4, *Stephanopyxis turris* CCMP815; lane 5, *Thalassiosira pseudonana* CCMP1010; lane 6, *Skeletonema costatum* CCMP1332; con, control protein overexpressed and purified recombinant TpMnSOD. Note: *T. pseudonana* strain used in this immunoblot is CCMP1010 and different than CCMP1335, which is the one used for cloning and over-expression of *sodA*. Marker indicates molecular weight standards in kDa. 42

Figure 3.2: Immunoblot of *Thalassiosira pseudonana* CCMP1335 cells and cells treated with 10mg/ml cycloheximide, (Lc, Dc) to inhibit protein synthesis (all treatments also included 0.1% DMSO). After 27 hours the protein is below detection in the cells grown under light with protein synthesis inhibited. This suggests that the turnover of TpMnSOD is related to processes that occur when cells are exposed to light. Conversely, cells exposed to continuous darkness show evidence of TpMnSOD through out the experiment. Each lane is loaded with 8µg of total protein extracts. Antibody was specifically raised against recombinant protein in control lane. 43

Figure 3.3: Intracellular Distribution of Manganese for *Thalassiosira pseudonana* CCMP1335. Total cellular Mn ( $Mn_{tot}$ ) was estimated from the  $C_{org}$ -specific Mn quotas ( $\mu\text{mol Mn mol C}^{-1}$ ) of Sunda and Huntsman (1998, Fig. 7 and high light,

low Mn Table 2) and the  $C_{org}$  content of mid-log exponentially growing cells (0.89 pmols  $C_{org}$  cell<sup>-1</sup>). Mn in photosystem II ( $Mn_{PSII}$ ) is that modeled by Raven (1990). Mn in SOD was estimated as the average measured MnSOD concentration using the quantitative immuno-technique (mols of MnSOD cell<sup>-1</sup>, Table 3.2). Note that as  $C_{org}$  decreases in cells as light increases while moles of MnSOD cell<sup>-1</sup> stays constant across light levels, the percent of Mn in MnSOD may increase with irradiance (see also Fig. 3.5).

44

Figure 3.4: Immunogold localization of MnSOD in *Thalassiosira pseudonana*

CCMP1335. A, Osmium tetroxide stained electron micrograph of whole cell. B, Second different view of Osmium tetroxide stained cell. C, Immunogold labeling of the chloroplast with the anti-TpMnSOD antibody. D, Magnified view of delineated area in B. E, Immunogold labeling of the chloroplast in another cell of *T. pseudonana*. F, Magnified view of delineated area in E. Note the absence of labeling of mitochondrial and cytosolic regions. Key: c, chloroplast; p, pyrenoid; m, mitochondrion; n, nucleus; nc, nucleolus; v, vacuole. Arrows indicate black, electron dense gold label corresponding to TpMnSOD. Scale bars = length as indicated. Note, granules apparent in the pyrenoid of F are crystalline RUBISCO, clearly not as electron dense as the gold particles.

46

Figure 3.5: Comparison of growth rate, total cellular chlorophyll, and MnSOD per unit chlorophyll of *Thalassiosira pseudonana* CCMP1335 cells grown at different continuous light intensities. Western blot images above the graph are of protein

samples loaded according to equal chlorophyll. Growth rate (solid black circles and solid line) increases by two-fold over these light levels. Concurrently, cellular chlorophyll (solid black squares, dotted line) decreases. Although MnSOD is constant per unit protein (data not shown), MnSOD per unit chlorophyll (solid black triangles, dashed and dotted line; and western blot above image) increases. This supports the strong association of the relative contribution of MnSOD to protecting the photosynthetic machinery; especially as the light harvesting pigments decrease.

48

Figure 3.6. Diel expression of MnSOD in *Thalassiosira pseudonana* CCMP1335. Here is the quantum yield, A, of cells exposed to 12:12 L:D cycle under high light ( $800\mu\text{mol m}^{-2}\text{s}^{-1}$ , solid black triangles and dashed line) and control light ( $120\mu\text{mol m}^{-2}\text{s}^{-1}$ , solid black circles solid line) over time (x-axis). Fv/Fm decreases in the high light over the first 12 h when compared to the control and then recovered during and after the dark period. The dark period is represented by the shaded area. Immunoblot densitometric analysis, B, showed the TpMnSOD in the high light (hatched bars) treatment experienced a significant increase after the dark period as compared to the expression of TpMnSOD in the control light (solid bars) cultures (values are means,  $n=2\pm\text{SD}$ ). Asterisks denote significant differences between treatments ( $p=0.0105$ ).

50

Figure 4.1: Excerpts of amino acid sequence alignment of the Fe and MnSODs used in this study. The asterisks denote primary and secondary sphere amino acids

involved in either binding or coordination of the metal site. See text for discussion. A) N-terminal excerpt, B) Middle excerpt, C) C-terminal excerpt. 66

Figure 4.2: Bayesian based evolutionary relationship among the Fe/MnSOD family of proteins. Phylogeny representing all major taxa was inferred from a Bayesian analysis based on amino acid sequences. The tree elucidates the endosymbiotic origin of this family of SODs in eukaryotes. The Fe clade shows a clear primary photosynthetic endosymbiotic origin evolving from the cyanobacteria and green sulfur bacteria (GSB). The MnSOD clade shows a few different photosynthetic clusters most notably a separation of the single celled primary green and primary and secondary red plastid containing eukaryotes from the green plants. The monophyletic relationship of the MnSODs in red-plastid algae is congruent with other estimated relationships. The basal primary green plastid alga to this clusters suggests a common origin for these seuquences. Fe and Mn sequences were aligned using CLUSTALX and edited with BioEdit. This is the tree of highest likelihood identified in the Bayesian tree pool using the fixed rate WAG model (Ln likelihood = -37193.92). Numbers at the nodes represent posterior probabilities. Scale bar represents the number of substitutions per amino acid site.

71

Figure 4.3: Maximum likelihood based evolutionary relationship among the Fe/MnSOD family of proteins. This tree agrees to a large extent with the Bayesian inferred tree. Important regions of difference are the clustering of the green plants in the

FeSOD clade. Bootstrap support is weak for many of the internal nodes which are resolved in the Bayesian tree. However, this tree validates many of the same hypotheses in agreement with the Bayesian tree. Sequences were aligned as in Figure 4.2. A maximum likelihood tree was constructed using PHYML employing the WAG empirical fixed rate model of evolution. The scale bar represents the expected number of substitutions per amino acid position. 73

Figure 4.4: Bayesian based tree constructed as in Figure 4.2 based on plastid related organisms. Here the monophyly of plastid related eukaryotes to the cyanobacteria is better resolved for FeSOD. In the MnSOD clade, the cyanobacteria and green plants form a monophyletic cluster excluding primary green, and primary and secondary red algae. This is in contrast to the full trees including all organisms. The high posterior probability support (100%) for the divergence of these two groups before the inheritance of MnSOD suggests a closer, primary host relationship between the primary green, and primary and secondary red algae. Furthermore, this strongly supports the relationship between MnSODs of plants and cyanobacteria. Scale bar represents the expected number of substations per amino acid site. 76

## 1.0 Introduction

The evolution of oxygenic photosynthesis in the early Proterozoic Eon exerted a powerful selective pressure on life (Dismukes et al., 2001; Knoll, 2003; Falkowski et al., 2004a). Free atmospheric oxygen allowed metabolism to become “supercharged”, whereby the energy extraction efficiency per mole of glucose increased over 400% relative to anaerobic fermentation. However, this metabolic benefit came at the price of potential damage to the metabolic machinery (Koppenol, 1988). Reactive oxygen species (ROS), which, under anaerobic conditions were present but almost certainly at very low concentrations, became relatively abundant. ROS can react with lipids, membranes, and proteins to cause irreversible damage to a cell. The most notable culprit within the ROS family is the superoxide anion radical ( $O_2^-$ ), which is a metabolic by-product of aerobic respiration and oxygenic photosynthesis (Fridovich 1998, Falkowski and Raven 1997). Both processes leak ~ 1 to 4% of their electrons onto molecular oxygen to form superoxide (Halliwell, 1982; Apel and Hirt, 2004). Given the ubiquitous presence of ROS, it is not surprising that efficient defense mechanisms evolved to destroy ROS. In this paper we review the biochemistry, physiological function, and evolutionary history of the defense mechanisms in algae against ROS, focusing on the role of superoxide dismutase.

ROS accumulate both in the open ocean (Gasc et al., 2002) (Fig. 1.1) and in coastal zones (Zepp et al., 1992; Blough and Zepp, 1995; Voelker et al., 2000). In the ocean, production of ROS appears to be largely biological. For example, in coastal areas dinoflagellates and raphidophycean algae are both sources of ROS. These organisms can produce ROS in the dark when exposed to a variety of stimulants including lectins and

iron-limited environments (Oda et al., 1992; Oda et al., 1997; Kim et al., 1999a). This response is temperature dependent, associated with the presence of an NADPH oxidase-like cell surface enzyme (Kim et al., 1999a; Kim et al., 1999b; Twiner and Trick, 2000) and may be used as a cell signaling mechanism or in quorum sensing (Joint et al., 2002; Apel and Hirt, 2004). The extracellular target of ROS is not well known, however there is experimental evidence that these molecules can reduce competition by killing or inhibiting the growth of bacteria, as well as reducing Fe found in iron complexes in bulk water. Thus, while ROS are potentially toxic, aquatic organisms may have capitalized on the chemistry associated with ROS production to increase their fitness. In order to do so, however, the organisms must have defense mechanisms that prevent the ROS from inflicting damage to themselves.

One of the major biochemical protective systems against ROS is provided by the superoxide dismutases (SODs), found in all branches of the tree of life (Fig. 1.2). There are four known metalloforms of SOD, identified by their metal centers (Fe, Mn, CuZn, and Ni). Orthologs of all four forms have been found in photosynthetic organisms. The cellular SOD profile is variable between organisms and can change with ambient environmental conditions (Fee, 1991; Amanatidou et al., 2001). The majority of research on SODs has focused on either medical or agricultural applications, however, given the polyphyletic origins of eukaryotic algae (Baldauf, 2003), the SOD profiles of these organisms can be used to address the evolutionary history of these enzymes and vice-versa. Indeed, given their phylogenetic trajectory and the variability of trace metals in aquatic ecosystems (Kremling and Streu, 2001; Whitfield, 2001; Anbar and Knoll, 2002; Sanudo-Wilhelmy et al., 2002; Saito et al., 2003; Seyler and Boaventura, 2003), algae

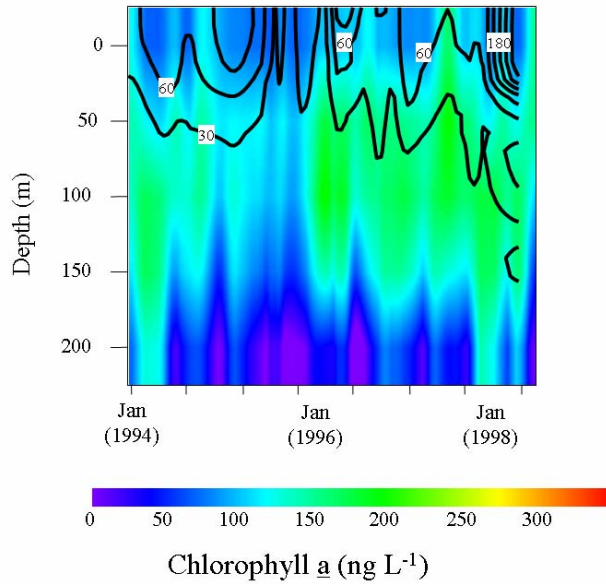


Figure 1.1: Seasonal hydrogen peroxide and chlorophyll at the Hawaii Ocean Times Series (HOT) station ALOHA. Data collected from Jan 1994 to Dec 1998 (Gasc et al., 2002). Color represents average chlorophyll in  $\text{ng}\cdot\text{L}^{-1}$  and contour lines are of equal hydrogen peroxide concentrations in nM. Within the water column algae are the most prominent source of ROS. Significant abiological ROS production would require the presence of free transition metals. At this location, the average trace metal concentrations are too low to produce (from Fenton reactions, see text) the level of ROS observed. Some work has suggested that in coastal and estuarine regions, CDOM may serve as both a source and a sink for ROS {Andrews, 2000 #432; Voelker, 2000 #431; Zepp, 1992 #430; Blough, 1995 #433}, Andrews et al. 2000, Voelker et al. 2000).

However, the low nutrient- low chlorophyll waters at the HOT station are unlikely to experience the same levels of CDOM and abiotically produced ROS.

serve as excellent models for understanding the environmental regulation of oxidative stress and the efficacy of SOD in preventing damage to cellular machinery.

### 1.1 Source and Sinks of Reactive Oxygen Species (ROS) in Algae

O<sub>2</sub> has a triplet ground state, making it an excellent oxidizing agent (and hence, terminal electron acceptor) in aqueous solutions (Halliwell, 1995). However, O<sub>2</sub> can be reduced to several intermediates besides H<sub>2</sub>O. The overall four-electron reduction of molecular oxygen is thermodynamically a highly favored reaction ( $E_o' = +0.815$  V vs. NHE @ pH 7.25) and occurs in mitochondria and aerobic, heterotrophic prokaryotes (Table 1.1). All intermediate levels of reduced O<sub>2</sub> are invariably deficient in hydrogen atoms and thermodynamically more reactive than H<sub>2</sub>O, and hence comprise a suite of ROS. They include the superoxide anion radical (O<sub>2</sub><sup>•-</sup>), hydrogen peroxide (H<sub>2</sub>O<sub>2</sub>), hydroperoxy radical (HO<sub>2</sub><sup>•</sup>), and the hydroxyl radical (HO<sup>•</sup>) (Gabig and Babior, 1982).

Virtually all ROS found in aquatic environments are the result of biological production through redox reactions with O<sub>2</sub> (Boveris and Cadenas, 1982; Han et al., 2001). O<sub>2</sub><sup>•-</sup> is formed by the following reaction:



which has a standard reduction potential ( $E_o'$  vs. NHE, pH 7) of -0.33 V (Table 1.1). Potential sources of ROS include Mehler (“pseudocyclic”) electron flow around PSI (Asada, 1999) and in the mitochondria between respiratory complexes II and III and cytochrome c oxidase (Dufour et al., 2000; Casteilla et al., 2001).

The most reactive ROS is the hydroxyl radical (HO<sup>•</sup>) which is generated by the Haber –Weiss reaction (Haber and Weiss, 1934; Weiss, 1935):

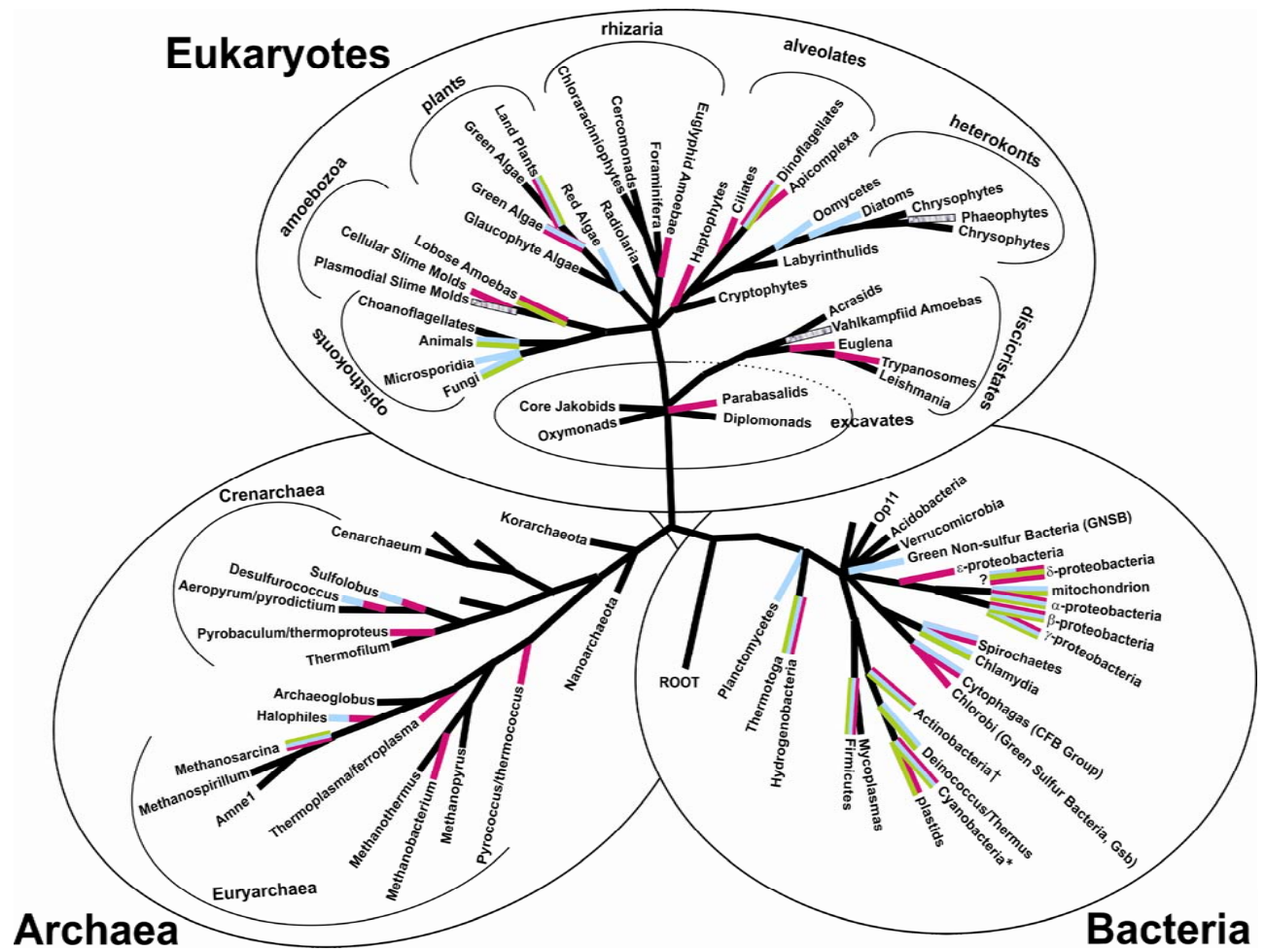


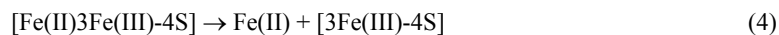
Figure 1.2: Synthetic distribution based on known evidence from biochemical and genetic data of the various superoxide dismutases over the tree of life (figure modified after (Baldauf et al., 2004). All the potential routes for genetic inheritance are evident in SOD genes. FeSOD is widely distributed between all major clades while specifically MnSOD is more prevalent in Bacteria and Eukaryota. Fe and MnSOD have contrasting potential evolutionary histories. In eukaryotic photosynthetic autotrophs, the ancestral origin of FeSOD may be from the GSB ancestor of PSI in cyanobacteria, while MnSOD has a variety of possible origins mainly the proteobacterial ancestor to PSII and mitochondria; both plastid metalloforms having been acquired through cyanobacteria. CuZnSOD demonstrates multiple lateral gene transfers. Furthermore, organisms often possess multiple copies of CuZnSOD in their genomes, which are in general significantly phylogenetically distant. Branches are colored according to known SODs: magenta- FeSOD, cyan- MnSOD, cyan/magenta- Fe/MnSOD (cambialistic), green- CuZnSOD, and grey- unknown form of SOD. \* NiSOD genes found in genomes of 4 cyanobacteria. CuZnSOD only found in *Gloeobacter* sp. †NiSOD and FeZnSOD found in *Streptomyces* spp.



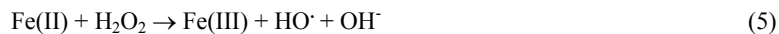
This reaction is further catalyzed by Fe released *in vivo* from Fe<sub>4</sub>S<sub>4</sub> clusters by O<sub>2</sub><sup>·-</sup> :



where Fe(II) is released:



This “free” Fe(II) either immediately reacts with H<sub>2</sub>O<sub>2</sub> to produce hydroxyl radicals through the Fenton reaction (Fenton and Jackson, 1899):



or is quickly oxidized:



and is then available to react with the superoxide anion radical and start the reaction again (Bielski and Cabelli, 1995). Due to the reactive nature of the hydroxyl radical, strong selective pressures favor cells that destroy the reactants (i.e. the superoxide anion radical and hydrogen peroxide) to benign products, ultimately H<sub>2</sub>O (Liochev and Fridovich, 1994, 1999).

The initial electron donation leading to the superoxide anion radical is unfavored and is the *main* factor limiting the reactivity of molecular oxygen (Table 1.1). Consequently, the oxidizing potential in O<sub>2</sub> cannot be accessed until after this first reduction and thus, molecular oxygen, can coexist with reducing agents without reacting rapidly (Ho et al., 1995a; Ho et al., 1995b). Although, the reaction is not thermodynamically favored, electron equivalents produced *in vivo* often form O<sub>2</sub><sup>·-</sup> if reducing agents, such as flavins and hydroquinones, are available. Once the initial electron donation produces superoxide anion radicals, the resulting molecule readily

propagates free radical oxidation in a variety of biological molecules such as leukoflavins, tetrahydropterins, and catecholamines (Fridovich, 1981), and inactivates iron–sulfur containing compounds (Fridovich, 1997). Once produced, these ROS attack lipids, nucleic acids, and damage most cellular machinery (Voet and Voet, 1990). Thus, despite the energetic advantage gained from using  $O_2$  as a terminal electron acceptor, cells are required to maintain an efficient defense system against its by-products.

### 1.1 The SOD Defense System

Three major enzyme systems have evolved in oxygenic photoautotrophs to deactivate ROS: the superoxide dismutases, catalases, and peroxidases (for review, see Asada 1999). Cells also maintain a suite of non-enzymatic antioxidants (including carotenoids and glutathione) but these will not be addressed here because their chemistry generally overlaps with the catalases and peroxidases (Halliwell, 1999; Mallick and Mohn, 2000).

Superoxide dismutases (SODs) are comprised of 150 to 220 amino acid residue subunits that form homo-dimeric or tetrameric protein complexes which coordinate specific metal cofactors. SOD catalyzes the dismutation of the superoxide anion radical into hydrogen peroxide and molecular oxygen according to (for scheme, see Table 1.2):



which can be analyzed as two reduction half reactions:



The redox mechanism toggles the active site metal between a reduced and oxidized form (i.e., either donating or accepting an electron). Thus, SOD is active whether the metal

center is oxidized or reduced. For example, if Fe(III) is present at the active site, then the enzyme acts as an oxidant and O<sub>2</sub> is produced. If Fe(II) is present, the enzyme acts as a reductant and produces H<sub>2</sub>O<sub>2</sub>. This basic redox bifunctionality has been verified for all metalloforms of SOD regardless of the metal cofactor. The perpetual cycling of the redox state of the active site metal cofactor explains why SOD catalysis proceeds at a near diffusion-limited rate of approximately  $10^9 \text{ M}^{-1}\bullet\text{s}^{-1}$ , which is four orders of magnitude faster than the spontaneous dismutation of the superoxide anion radical. Thus SOD removes superoxide and thereby precludes the development of Haber-Weiss and Fenton chemistries and therefore, the production of even more radicals. All SODs provide this efficient defensive capability despite major differences in their structures.

### *1.2.1 Iron and Manganese SODs*

Based on amino acid alignments, Fe and MnSOD are ~50% similar (Fridovich, 1998; Fink and Scandalios, 2002b) and appear to have evolved from a gene duplication event from a common ancestor. These two SOD types are typically homodimers or tetramers that contain one metal atom per 200 to 220 amino acid residue subunit with molecular masses between 14 to 30 kDa (Steinman, 1982a). Certain Archaea express a dual metal or cambialistic SOD; that is, they may have either Fe or Mn at the active site in the same protein. While, this may not be surprising based on structural similarity to both the obligate FeSOD and MnSOD, it is the exception rather than the rule (Edward et al., 1998). It is not known if there are cambialistic SODs in algae.

Although there is high degree of similarity between FeSOD and MnSOD, two specific amino acid residues differentiate them: residue 77 (Gln in FeSOD and Gly in

MnSOD) and 146 (Ala in FeSOD to either Gln or His in MnSOD) (Weatherburn, 2001). Based on structural studies, these amino acid residues are critical to the redox activity of the metal cofactor; thus, while it is possible to substitute Fe for Mn in the active site of MnSOD (or vice versa), the resulting complex exhibits little or no catalytic activity. The lack of activity is likely due to standard electrical potential differences ( $E_o'$  vs. NHE, pH 7) (Renault et al., 2000). These differences underlie the considerable distance between the redox potentials of the two metal centers. For example, the active site Fe redox potential,  $E_o'$ , is much lower for Fe when Fe is in the active site of the MnSOD protein than in FeSOD (Renault et al., 2000).  $E_o'$  is a thermodynamic parameter that indicates the energetically favored direction for a reaction. If  $E_o'$  is lowered, Fe(III) is stabilized when substituted in MnSOD and hence the ability of the metal to accept electrons is thermodynamically impeded (Batinic-Haberle, 2002; Batinic-Haberle et al., 2004). The substituted metal center (stabilized as an oxidized species) cannot then oxidize  $O_2^-$  to  $O_2$  (one of the two half reactions of  $O_2^-$  disproportionation; see previous section text). Thus, mutations in the binding site in SODs not only are critical for metal selectivity, but modulate or “tune” the  $E_o'$  to facilitate enzymatic activity.

An important difference between the Fe and MnSODs is their intracellular location (Fig. 1.3). FeSOD is typically localized in the chloroplasts and the cytoplasm (Kliebenstein et al., 1998; Fink and Scandalios, 2002b). In contrast, MnSOD is almost always found in mitochondria (Kitayama et al., 1999; Wu et al., 1999). This localization appears to have changed during the evolutionary radiations as some cyanobacteria, which have both Fe and MnSOD, have MnSOD in both periplasmic *and* thylakoid membranes (Herbert et al., 1992; Chen et al., 2001; Li et al., 2002). Importantly, in cyanobacteria,

the factor which determines the localization is an N terminal hydrophobic, transmembrane helix tail on the MnSOD (Atzenhofer et al., 2002; Regelsberger et al., 2002). Thus, the overall tertiary structure of Fe and MnSODs remains similar.

### *1.2.2 Copper-Zinc SODs*

CuZnSOD has different primary and tertiary structures than FeSOD and MnSOD, and almost certainly evolved independently. The CuZn enzymes have between 150 to 160 amino acid residues per subunit and are homo-dimeric; each monomer has a molecular weight between 31 to 33 kDa (Steinman, 1982a; Fridovich, 1998). For each subunit there is one Cu and one Zn atom, potentially allowing for two active sites per enzyme. This enzyme is stable with reports of the second-order rate constant ( $k_f$ ) maintaining stability in 8M urea for several hours at room temperature (Steinman, 1982a). It can also withstand multiple freeze/thaw cycles and prolonged refrigeration once purified. This stability may arise from the high glycine content (13-17%) which contributes to extensive  $\beta$ -pleated sheet conformation (Chen et al., 2001). CuZnSOD is typically localized in the chloroplasts of higher plants and/or free in the cytosol (Wu et al., 1999)(Fig. 1.3). However, in metazoans, <1% of total cellular CuZnSOD (if present) may be accounted for in the mitochondrial intermembrane space (Okado-Matsumoto and Fridovich, 2001; Inarrea, 2002) it is typically found soluble both within cell cytoplasm and also in extracellular spaces. The discovery of CuZnSOD in prokaryotes (Steinman, 1982b; Bannister and Parker, 1985; Steinman, 1985; Benov and Fridovich, 1994; Benov and Fridovich, 1996) ended the speculation that this metalloform of the enzyme evolved before the divergence of the three domains of life. In prokaryotes, CuZnSOD has been

found in the periplasm of  $\alpha$ ,  $\beta$ , and  $\gamma$  proteobacteria. There are very few data known regarding CuZnSOD in eukaryotic algae (Okamoto et al., 2001).

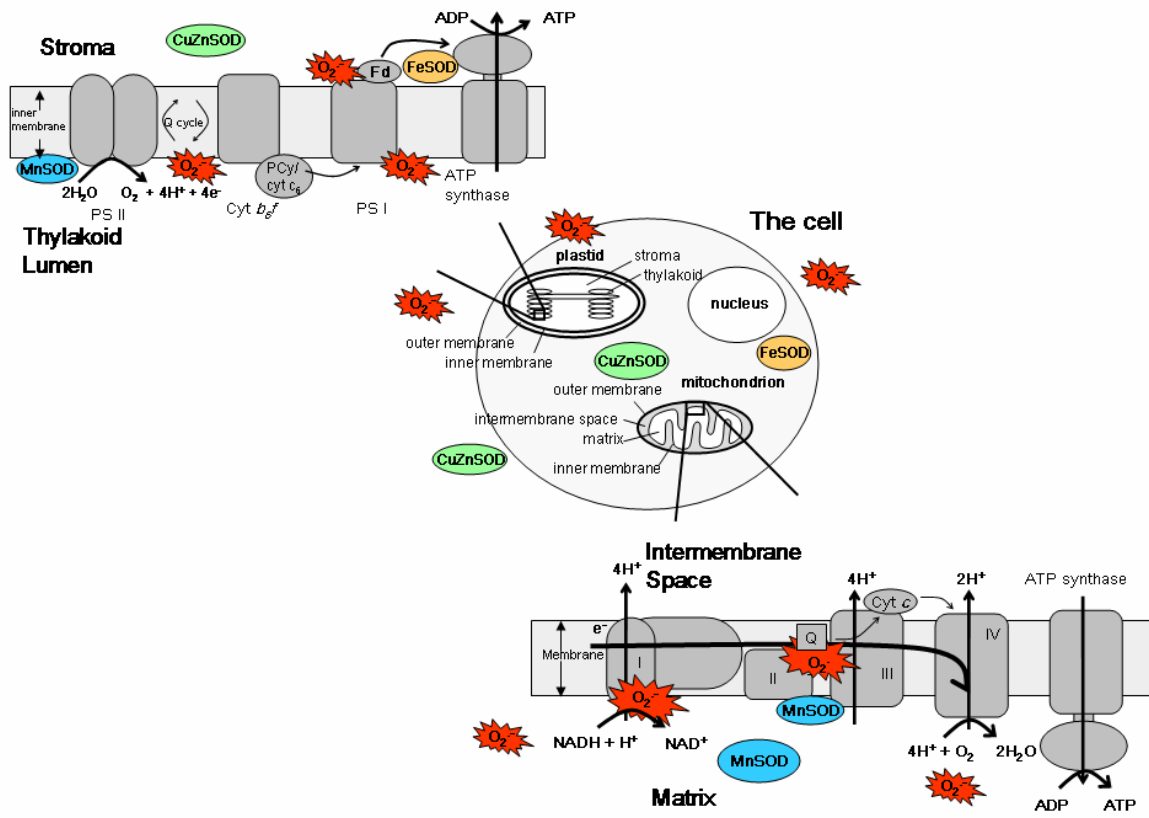


Figure 1.3: Subcellular localization of superoxide dismutases. This conceptual scheme summarizes all known locations of SODs within eukaryotic cells. An important attribute of SODs is that they are poised and ready at metabolic the site of superoxide production. Soluble forms of SOD found in the cytoplasm are typically CuZnSOD in embryophytes. Occasionally, FeSOD can be found soluble but, both cytoplasmic and extracellular SODs are characteristic of multicellular organisms that have cell signaling pathways through which ROS are exchanged. The chloroplast can be associated with Fe, Mn, and/or CuZnSOD. In diatoms, MnSOD can be found here, most likely associated with the lumen side of PSII (Wolfe-Simon unpublished). CuZnSOD and FeSOD may fill the same role on the stromal side of PSI, with the former dominantly found in embryophytes and charophytes and the latter in the cyanobacteria, chlorophytes, and dinoflagellates. Much research is still needed to completely understand the SODs with in other algal plastids. The mitochondria have MnSOD almost exclusively. No other SOD has been found associated with these organelles in photosynthetic autotrophs

### 1.2.3 Nickel SODs

The NiSOD has a completely different structure from either the Fe or MnSODs or the CuZnSODs; it was first discovered, cloned and characterized in the bacterial genus, *Streptomyces* (Youn et al., 1996; Barondeau et al., 2004; Wuerger et al., 2004).

Additionally, a survey of available genomes suggests this form of SOD may be active in prokaryotic algae as well (Fig. 1.4) (Palenik et al., 2003). Given that the most abundant cyanobacteria on Earth are *Prochlorococcus* sp. and *Synechococcus* sp., SOD may reveal a major global importance for nickel (Partensky et al., 1999; Palenik et al., 2003).

### 1.3 Objectives of dissertation research

SODs represent a paralogous group of identical functioning enzymes of which only two are evolutionarily related. The use biogeochemically important metals at the active site and are vital to the survival of life. Algae, specifically the secondary red plastid-containing lineages, are a relatively recently evolved group of organisms that have extremely diverse and flexible lifestyles. Algae and SODs are an ideal model system to probe a variety of profound physiological and evolutionary questions. Specifically, this dissertation will address the molecular ecology of this model system using a variety of molecular biology, biochemical and phylogenetic techniques. Chapter two reviews what is known about SODs in prokaryotic and eukaryotic photoautotrophs and will initiate an evolutionary discussion. Chapter three explores the physiological details of MnSOD in the diatom *Thalassiosira pseudonana*. And finally, Chapter four will focus on the molecular phylogeny of the Fe- and MnSOD family and expand on the evolutionary

discussion after the details of the molecular and biochemical nature of SODs has been explored.

In particular, this dissertation seeks to address the following questions:

**Question 1)** *What are the SOD enzymes expressed in diatoms and is there evidence for them conferring a selective advantage to diatoms?* Do diatoms have a unique SOD profile? Do diatom SODs reflect novel use of the biogeochemically metal cofactors in SODs? What organelles are diatom SODs directed towards? How does the environment affect SOD expression patterns in diatoms? I hypothesize that indeed marine diatoms will show unique patterns of SOD expression and that this expression has helped their ecological success.

**Question 2)** *Do SODs contribute to the historical rise and modern oceanic ecological success of the secondary red plastid-containing eukaryotes including diatoms?* What is the phylogenetic position of secondary red plastid-containing organisms with respect to SOD? Can we assess what extent the SOD cofactor metal biogeochemistry affects the evolution of these organisms? Is this important to secondary red algae? Does the subcellular localization of SOD in diatoms have implications for the molecular evolution of this group of algae? I hypothesize that the phylogenetic analyses of diatom and other secondary red-plastid containing organisms will show a unique and polyphyletic origin to the secondary red lineage of algae.

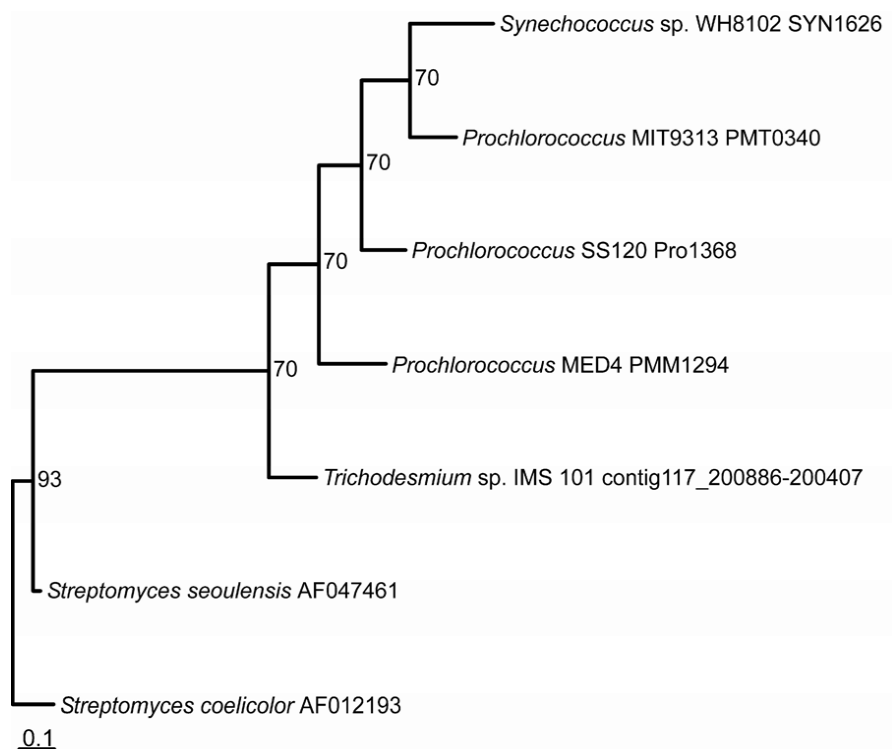


Figure 1.4: Phylogenetic tree of NiSOD genes. NiSODs have been biochemically characterized in the two *Streptomyces* sp. shown. The cyanobacteria sequences represented here are derived from genomic data, but no biochemical or physiological data are yet available for the activity of NiSODs in cyanobacteria. Interestingly, both *Prochlorococcus* sp. strains shown possess only the gene for NiSOD- they do not contain genetic information for any other known form of SOD. The evolutionary significance of NiSODs is not yet clear but, the increase in genomic data will help resolve this issue. This may prove to be a major sink for Ni in environments where these are the dominant organisms. This unrooted tree was generated using the Genetic Database Environment (GDE) sequence alignment editor (Smith et al., 1994) based on a DNA maximum

likelihood approach using fastDNAmI (Felsenstein, 1981; Olsen et al., 1994), the branching pattern is supported by bootstrap analysis (100 replicates). The tree has been modified for clarity. Accession numbers are given for the *Streptomyces* sp. and ORF identification numbers are give for all the cyanobacteria. Scale bar represents the number of substitutions per nucleotide site.

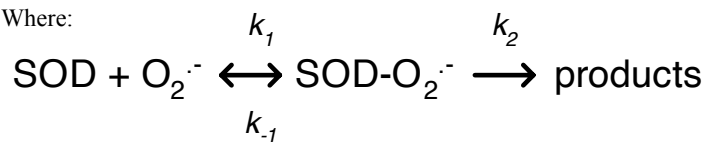
**Table 1.1: The four one-electron reactions for the reduction of O<sub>2</sub> to H<sub>2</sub>O in aqueous solution and the corresponding reduction potentials.**

	E°' (V vs. NHE, pH 7)
$\text{O}_2 + \text{e}^- \rightarrow \text{O}_2^-$	-0.33
$\text{O}_2^- + \text{e}^- + 2\text{H}^+ \rightarrow \text{H}_2\text{O}_2$	+0.89
$\text{H}_2\text{O}_2 + \text{e}^- + \text{H}^+ \rightarrow \text{H}_2\text{O} + \text{OH}$	+0.38
$\text{OH} + \text{e}^- + \text{H}^+ \rightarrow \text{H}_2\text{O}$	+2.31
From (Ho et al., 1995b)	

**Table 1.2. The basic superoxide dismutase ping-pong mechanism**  
(after Falconi et al., 2002)

---

Where:



$k_1$  = second-order association rate

$k_{-1}$  = first-order enzyme-substrate dissociation constant

$k_2$  = first-order catalytic rate constant

$$k_f = k_2 / K_m = k_1 k_2 / (k_{-1} + k_2)$$

where:

$k_f$  = second-order rate constant

$K_m$  = Michaelis-Menten constant

2<sup>nd</sup> order catalytic rate ( $k_{cat} / K_m$ )  $\approx 10^9 \text{ M}^{-1} \text{ sec}^{-1}$

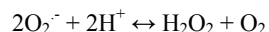
note: the catalytic process is diffusion limited; that is,  $k_f = k_1$  because  $k_2 \gg k_{-1}$

---

## 2.0 Review of SODs in Prokaryotic and Eukaryotic Algae

### Abstract

Superoxide dismutases (SOD) catalyze the disproportionation of the potentially destructive superoxide anion radical ( $O_2^-$ , a by-product of aerobic metabolism) to molecular oxygen and hydrogen peroxide:



Based on metal cofactors, four known metalloforms of SOD enzymes have been identified: they contain either Fe, Mn, Cu and Zn, or Ni. Orthologs of all metalloforms are present in oxygenic photoautotrophs. The expression of SOD is highly regulated, with specific metalloforms playing an inducible, protective role for specific cellular compartments. The various metalloforms of SOD are not distributed equally within either cyanobacteria or eukaryotic algae. Typically, cyanobacteria contain either a NiSOD alone, or combinations of Mn and Ni, or Fe and Mn metalloforms (CuZn is rare among the cyanobacteria). The bacillariophytes and rhodophytes retain an active MnSOD, while the chlorophytes, haptophytes, and embryophytes have either FeSOD, or multiple combinations of Fe, Mn, and CuZnSODs. NiSOD is a relatively novel SOD and has been generally excluded from evolutionary analyses. In both cyanobacteria and chlorophyte algae, the FeSOD metalloform appears to be associated with photosystem I (PSI), where its primary role is most likely to deactivate reactive oxygen produced by the Mehler reaction. The CuZnSOD also appears to be associated with the plastid, but is phylogenetically more restricted in its distribution. In eukaryotic algae, SODs are all nuclear encoded and, based on nucleotide sequence, protein structures, and phylogenetic distributions, appear to have unique evolutionary histories arising from the lateral gene

transfer of three distinct genes to the nucleus after the endosymbiotic acquisition of mitochondria and plastids. The varied phylogenetic histories and subcellular localizations suggest significantly different selection on these SOD metalloforms following the endosymbiont organelle-to-host gene transfer.

## **2.1 Environmental Regulation of SODs in Algae**

### *2.1.1 Visible Light Stress*

Although the biology of visible (400-700 nm) light stress has been an area of active research for vascular plant systems over the last two decades, the impact of high irradiance on the ecology of algae has been under-emphasized (Cullen and Lewis, 1995). Very few studies have been conducted on algal cultures grown at irradiance values greater than  $1000 \mu\text{mol}\cdot\text{m}^{-2}\cdot\text{s}^{-1}$  (for reference the maximum solar irradiance on Earth at local noon is  $2200 \mu\text{mol}\cdot\text{m}^{-2}\cdot\text{s}^{-1}$ ), which is unfortunate as the majority of the ocean photosynthetic carbon fixation often is light-saturated (Falkowski and Raven, 1997). These high light levels can suppress photosynthetic rates due to the photochemical production of ROS *in vivo*, which can damage the photosynthetic apparatus (Critchley, 1994; Nickelsen and Rochaix, 1994; Telfer and Barber, 1994).

Irradiance experiments showed that different metalloforms of SOD have selective inducible protective functions related to their subcellular distribution. As described above, in cyanobacteria, MnSOD is typically embedded in membranes while FeSOD is soluble. Studies using a variety of mutants, inhibitors, and light conditions have demonstrated that FeSOD is associated with the photoprotection of PSI (Herbert et al. 1992, Thomas et al. 1998). Field data also illustrated the selective protective functions

for the SODs, as FeSOD was largely associated with nitrogen-fixing heterocysts which only contain PSI (Canini et al., 1998). Specifically, cells exposed to higher irradiances showed a dramatic increase in SOD activity and content. Thus, different metalloforms of SOD protect different cellular proteins and can provide an *in vivo* tool to study cellular responses to oxidative stress (Lesser and Stochaj, 1990).

### 2.1.2 Ultraviolet Radiation

UV-B (280-320 nm) radiation inhibits PSII within the photosynthetic machinery (Iwanzik et al., 1983; Kulandaivelu and Noorundeen, 1983; Greenberg et al., 1989; Renger et al., 1989; Schofield et al., 1994) by degrading the D1/32 kDa protein complex (Greenberg et al., 1989; Richter et al., 1990; Melis et al., 1992; Jansen et al., 1993). Because the quinones, which are integral prosthetic components of PSII, absorb UV-B light (Greenberg et al., 1989; Melis et al., 1992; Jansen et al., 1993), it has been hypothesized that damage occurs beyond the photosynthetic reaction molecule, probably at the primary ( $Q_A$ ) and secondary ( $Q_B$ ) quinone electron acceptors in the reaction centers (Prasil et al., 1996).

In both green algae and diatoms, SODs exhibit a dose-dependent regulation in response to UV-B radiation (Malanga and Puntarulo, 1995; Malanga et al., 1997; Rijstenbil, 2002). Interestingly, the ROS produced with UV-A (UV-A, 320-400nm) do not stimulate a significant increase in SOD. Therefore, the differences in the protective response in non-enzymatic antioxidants and SOD probably reflect the specific and different target sites of the UV-A and UV-B damage (Rijstenbil, 2002, 2003).

### *2.1.3 Nutrient Stress*

Oxidative stress occurs under nutrient limitation as cellular metabolic rates are disrupted and the cellular scaffolding degrades. For example, photosynthetic machinery, which represents a significant fraction of the total cellular protein, is translationally impaired and cellular components are catabolized to maintain photosynthetic activity (Falkowski and Raven, 1997). Because certain key constituents of PSII reaction centers are destroyed, and instead of driving photosynthesis, absorbed light is dissipated via alternative pathways and frequently leads to the production of ROS. Additionally, under acute nutrient limitation, the respiratory degradation of cellular proteins and membranes can lead to the production of ROS species. In cyanobacteria, nitrogen limitation resulted in an increase in FeSOD expression exclusively associated with PSI in heterocysts, but no change in MnSOD (Liu et al., 2000; Li et al., 2002).

### *2.1.4 Metal Toxicity*

Excess free metal ions can initiate Fenton reactions (for review see Pinto et al., 2003). Many cyanobacteria have been shown to produce extracellular metal chelators that serve both as nutritive (to modulate the uptake of micronutrient trace metals) and antioxidant buffers (to prevent Fenton chemistry) (Ahner and Morel, 1995; Martinez et al., 2000). Although, intracellular chelation is a major preventive mechanism in many organisms, this phenomenon is poorly understood in algae. The most comprehensive group of metal toxicity studies examined various SOD responses under both acute and chronic metal conditions (Okamoto et al., 1996; Okamoto and Colepicolo, 1998; Okamoto et al., 2001; Okamoto et al., 2001). In dinoflagellates, lethal metal levels, most notably Cu, elicited a 53% increase in total SOD activity within hours of exposure and was mirrored by

increased lipid peroxidation. The specific response, however, varied depending on metal (Okamoto et al., 2001; Okomoto et al., 2001). Metal stress also initiated an increase in mRNA transcript levels of *sodB* (which encodes FeSOD), however, the translation of these transcripts appeared to be regulated by a circadian rhythm, so that conclusive evidence for the direct regulation of FeSOD by ROS has yet to be demonstrated. Responses to high metal concentrations have also been found in diatoms and green algae (Rijstenbil et al., 1994; Canini et al., 1998).

## 2.2 Algal SODs in an Evolutionary Context

There are three possible sources of the separate SOD genes in eukaryotic algae: 1) an archeozoon (i.e., the protoeukaryotic host that existed before the acquisition of organelles), 2) lateral gene transfer from the genome of the donors of organelles to the host cell, and 3) lateral gene transfer independent of organelle acquisition (Martin and Russell, 2003).

All mitochondria likely originated from a common eubacterial ancestor belonging to the  $\alpha$ -proteobacteria, which was acquired by an archeozoon through a single endosymbiotic event (Gray et al., 1999). In contrast, the origin of plastids is more diverse (Delwiche, 1999; Palmer, 2003). Primary plastids are derived from the endosymbiotic acquisition of cyanobacteria and found in chlorophytes, prasinophytes, rhodophytes, and embryophytes, while secondary plastids were acquired from primary plastid algae through a few endosymbiotic events involving several heterotrophic eukaryotic cells. Secondary plastid algal phyla, for which SOD genetic data are available, include a diatom (Bacillariophyceae, e.g. *Thalassiosira pseudonana*), a haptophyte (e.g. *Emiliania huxleyi*) and dinoflagellates (Dinophyceae, e.g. *Lingulodinium polyedrum*) (Okamoto and Colepicolo, 1998; Okamoto et al., 2001; Okomoto et al., 2001; Armbrust et al., 2004).

As part of endosymbiotic processes, gene transfers occurred from the endosymbiont genome(s) to the host nucleus including genes encoding for SOD.

Figure 1.2 shows all known SODs superimposed over the tree of life. FeSODs dominate the Archaea including a few cambialistic enzymes that change depending on environmental conditions. The MnSOD gene, *sodA*, is more widely distributed in the bacteria and eukaryota. Most organisms that possess MnSOD also have either FeSOD, CuZnSOD, or all three. Important exceptions to this are the green non-sulfur bacteria (GNSB), rhodophytes and diatoms. CuZnSODs are widely present over the entire tree. We first consider the dispersal of the Fe and MnSOD genes based on available genetic and biochemical data.

Phylogenetic trees suggest that Fe and MnSOD are derived from a common ancestor via a gene duplication event (Fig. 2.1). The FeSOD cluster contains the basal eukaryotic group, parabasalids, which do not appear to have mitochondria. This cluster then divides into a strongly supported group containing green plants exclusively and a diverse group containing cyanobacteria, the green sulfur bacterium (GSB)

*Chlorobium tepidum*, proteobacteria and eukaryotes (*E. huxleyi*, alveolates).

Interestingly, dinoflagellate and other alveolate SODs appear, in this context, to have been derived from proteobacteria. A similar situation is found in most dinoflagellates which contain the type 2 Rubisco, apparently acquired from  $\alpha$ -proteobacteria by lateral gene transfer (Delwiche and Palmer, 1996). This differs from other plastid targeted proteins, such as glyceraldehyde-3-phosphate dehydrogenase (GAPDH), where

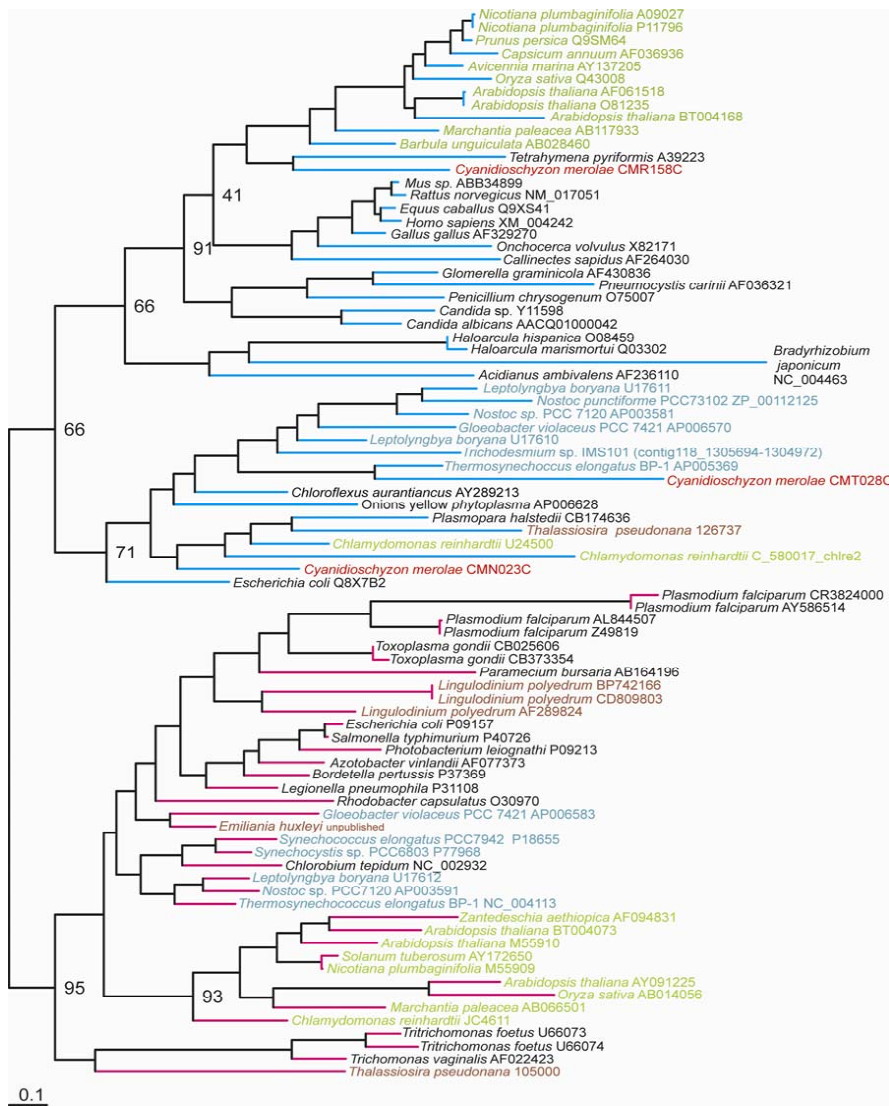


Figure 2.1: Unrooted phylogenetic tree for iron and manganese superoxide dismutase proteins. The phylogenetic clusters reflect the evolutionary history of these nuclear encoded genes. The MnSOD branches follow a mitochondrial origin while the FeSOD patterns are likely due to originating from the plastid symbiont. FeSOD likely derived

from the ancestral progenitors of PSI in cyanobacteria, the GSB. Interestingly, MnSOD may have originated from the proteobacterial source of PSII, which is also associated with the origin of mitochondria. See text for full discussion. SOD amino acid sequences were aligned using CLUSTALX (Thompson et al., 1994; Thompson et al., 1997) and the Genetic Data Environment (GDE) (Smith et al., 1994) multiple sequence editor. A maximum-likelihood tree was constructed using PHYML (Guindon and Gascuel, 2003) employing an empirical model of evolution (Whelan and Goldman, 2001) and the branching pattern is supported by bootstrap analysis (100 replicates). The scale represents the expected number of substitutions per amino acid position. The tree has been modified for clarity. FeSOD representatives are indicated with magenta branches while MnSOD representatives are in cyan. Species text color key: green – chlorophytes and higher plants, red – rhodophytes, aqua – cyanobacteria, brown – chromophyte algae. Accession numbers of the sequences are next to each taxa.

phylogenies suggest all secondary plastid targeted genes have a common primary plastid origin (Takishita et al., 2004).

The MnSOD cluster divides into two moderately supported sister groups (Fig. 2.1). The first branches into two sister clusters, one containing Euryarcheota and the  $\alpha$ -proteobacterium, *Bradyrhizobium*, and the second includes eukaryotic groups (Metazoa, fungi, higher plants, green and red algae, and ciliates). Accordingly, and in agreement with the mitochondrial localization of MnSOD, this cluster is consistent with a mitochondrial inheritance of MnSOD. The second main MnSOD cluster divides into a group mostly represented by cyanobacteria, and a diverse group including bacteria and eukaryotes. This latter group contains green and red algae, and two stramenopile sequences including *T. pseudonana*.

One interpretation of this phylogenetic analysis is that Mn and FeSODs are very ancient molecules that were selected prior to the oxidation of Earth, approximately 2.3 billion years ago (Bekker et al. 2004), when these two metals were relatively abundant in the ocean. The retention of these two proteins in eukaryotes reflects the history of the endosymbiotic appropriation of mitochondria and the two photosystems in oxygenic plastids. MnSOD appears to have been inherited by eukaryotic algae through proteobacteria, whose ancestors were the progenitors of both mitochondria and PSII (Michel and Deisenhofer, 1988; Martin and Russell, 2003) which eukaryotic algae inherited by organelle acquisition. In contrast, the biochemical association of FeSOD with PSI in extant plastids and phylogenetic distribution of the protein suggest that it was acquired through GSB, the closest extant relative to the progenitors of PS I in cyanobacteria (Baymann et al., 2001). Functional *sodB* may have been lost during the

evolution, leading to its absence in the bacillariophytes and rhodophytes (Matsuzaki et al., 2004). Genomic analysis suggests that diatoms have retained two pseudogenes for FeSOD (Armbrust et al., 2004). But, evidence for the sole use of the MnSOD metalloform (apparently in a variety of post-translationally modified forms) has been shown biochemically in the diatom *Thalassiosira pseudonana* and *T. oceanica* (Peers and Price, 2004, Wolfe unpublished). Further biochemical and molecular genetic data are needed to confirm this phenomenon.

The wide distribution of CuZnSOD suggests multiple lateral gene transfers between evolutionarily diverse organisms. For example, there are typically multiple copies of the genes for CuZnSOD in higher plants (Jesus et al., 1989; Grace, 1990; Fink and Scandalios, 2002b). There are generally two types of CuZnSODs in organisms that contain this enzyme: in higher plants they can be cytoplasmic or chloroplastic forms while metazoa have cytoplasmic and extra-cellular forms. These forms are all phylogenetically related to the bacterial forms (Fink and Scandalios, 2002b). Moreover, the gene encoding CuZnSOD (*sodC*) is found in a myriad of dsDNA virus genomes, further suggesting that it is readily transferred between prokaryotic and eukaryotic hosts. This could also account for the apparently recent acquisition of *sodC* in the euryarchaeon *Methanosarcina acetivorans* (Fig. 1.2; Galagan et al. 2002). A few studies have linked presence of CuZnSOD or FeSOD as proof of the endosymbiotic origins of plastids and mitochondria (Jesus et al., 1989; Grace, 1990), however given the frequent occurrence of lateral gene transfer of *sodC*, such an interpretation may not be valid.

### 2.3 Conclusions and Future Directions

In summary, examples of the four known metalloforms of SOD, which are distinguished by their metal cofactor: Fe, Mn, CuZn, and Ni, have been identified in eukaryotic and prokaryotic algae. However, very little is known regarding the location, regulation, and the cause of this metalloform diversity. From an evolutionary perspective, phylogenetic relationships among the various SODs provide key insight into the history of organelles. Specifically, eukaryotic algae show a spectrum of SODs whose nuclear-encoded genes are derived from endosymbiotic events. Altogether, Mn and FeSOD address several issues regarding the evolution of photoautotrophic eukaryotes related to the inheritance of proteins directly from organelles and specifically plastid history. A group of MnSODs seems to have remained closely related among diverse algal phyla. In contrast, FeSOD may reflect dramatic evolutionary changes related to plastid endosymbiosis. It highlights the early divergence between the green and red plastid lineages (Grzebyk et al., 2003). It also suggests different evolutionary history of acquisition of plastids between the diatoms, haptophytes, and dinoflagellates, which may challenge the hypothesis of a single endosymbiotic acquisition of secondary plastids (Cavalier-Smith, 1999; Palmer, 2003; Falkowski et al., 2004a; Grzebyk et al., 2004).

For algae, SODs are a window into past events and the importance of the genetic transfers that occurred. Efforts should focus on using the SODs' homologous origins and multiple metal employments to further understand the success of different algal forms in contrasting environments. The regulation of specific metalloforms of SOD by light, nutrients and other environmental pressures may also help to determine the necessity through evolutionary time of particular trace metal requirements for organelles and the

whole cell. We need a better understanding of SOD as representative of the first in line of the enzymatic antioxidant arsenal. The importance of lateral gene transfers in algae should be further explored as a tool to understand the extant biodiversity. Algal SODs may provide key information to help understand this stochastic evolutionary process. Finally, we may then be able to relate these data back to the evolutionary history of algae, and begin to understand why these organisms are so drastically diverse and different between the ocean and land.

### 3.0 Localization and Role of Manganese Superoxide Dismutase in a Marine Diatom

#### Abstract

Superoxide dismutase (SOD) catalyzes the transformation of superoxide to molecular oxygen and hydrogen peroxide. Of the four known SOD isoforms, distinguished by their metal cofactor (Fe, Mn, Cu/Zn, Ni), MnSOD is the dominant form in the diatom *Thalassiosira pseudonana* (Bacillariophyceae). We cloned the MnSOD gene, *sodA*, using the expression vector pBAD, over expressed the product in *Escherichia coli* and purified the mature protein (TpMnSOD). This recombinant enzyme was then used to generate a polyclonal antibody in rabbit that recognizes MnSOD in *T. pseudonana*. *In vivo* concentrations of TpMnSOD are approximately 0.9 amols per cell based on a quantitative immunoblot technique using the recombinant protein as a standard. Immunogold staining indicates that TpMnSOD is localized in the chloroplasts, which is in contrast to most other eukaryotic algae (including chlorophytes and embryophytes) where MnSOD is localized exclusively in the mitochondria. Cellular Mn budgets, based on the photosynthetic Mn complex in photosystem II, cannot account for 50-80% of measured Mn within diatom cells. Chloroplastic MnSOD accounts for 10-20% of cellular Mn, depending on incident light intensity and cellular growth rate. While MnSOD accounts for a significant fraction of the cellular Mn, TpMnSOD accounts for less than 2% of the total protein in the cell. The TpMnSOD has a rapid turnover rate with an apparent half-life of 6-8 hours when grown under continuous light. TpMnSOD concentrations increase relative to chlorophyll, with an increase in incident light intensity in order to minimize photosynthetic oxidative stress. The employment of a manganese-based SOD, linked to

photosynthetic stress in *T. pseudonana*, may contribute to its continued success in the low iron regions of the modern ocean.

### 3.1 Introduction

All aerobic organisms produce intracellular and extracellular reactive oxygen species (ROS) as metabolic byproducts (Haliwell 1982, Asada 1999, Apel and Hirt 2005). Photoautotrophs also produce ROS through photosynthesis (Falkowski and Raven, 1997; Anderson et al., 1999; Wolfe-Simon et al., 2005). The ROS byproducts include superoxide ( $O_2^{\cdot-}$ ), hydrogen peroxide ( $H_2O_2$ ), and hydroxyl radical ( $HO^{\cdot}$ ) (Haliwell 1982).  $O_2^{\cdot-}$  is particularly destructive because it cannot diffuse across cell membranes, and therefore, must be destroyed at the site of production. Superoxide dismutases (SODs) are a polyphyletic family of enzymes that protect cells from  $O_2^{\cdot-}$ . SODs come in four isoforms, recognized by their metal center cofactors (Fe, Mn, Cu/Zn, and Ni), and catalyze the destruction of  $O_2^{\cdot-}$  to  $H_2O_2$  and  $O_2$ . This key antioxidant has been well studied in many eukaryotic systems, including metazoa and plants (Bowler et al., 1992; Scandalios, 1993; Fridovich, 1995; Raychaudhuri and Deng, 2000; Zelko et al., 2002). However, few studies on the intracellular regulation of SOD in eukaryotic red algae are available, which is unfortunate as these algae dominate the ocean (Falkowski et al., 2004b).

One of the dominant photoautotrophs in the ocean are the Bacillariophyta (e.g. diatoms) which appear to rely primarily on the manganese form of SOD (MnSOD) (Peers and Price, 2004); therefore, understanding the regulation of MnSOD in diatoms is important, as this enzyme must be critical to the cell's ability to cope with oxidative

stress. The regulation and subcellular localization of MnSOD varies significantly among algal taxa (Wolfe-Simon et al., 2005). In cyanobacteria, MnSOD is found in the periplasm and is associated with the thylakoid membranes (Herbert et al., 1992; Chen et al., 2001; Li et al., 2002). In contrast, MnSOD is found in the mitochondria of embryophytes, chlorophytes, and dinoflagellates (Kliebenstein et al., 1998; Kitayama et al., 1999; Wu et al., 1999; Okamoto et al., 2001; Okamoto et al., 2001; Fink and Scandalios, 2002b). No information on the subcellular localization of MnSOD and the associated kinetics in diatoms is available.

Given our lack of understanding of MnSOD in diatoms despite their global significance, we examined the expression and preliminary regulation of MnSOD in the bloom forming diatom *Thalassiosira pseudonana* CCMP1335 (Ziemann et al., 1991; Levasseur et al., 1992; Zigone et al., 1995; Cabecadas et al., 1999). Our results demonstrate that MnSOD has a rapid turnover rate mediated by incident light levels and is localized in the chloroplast, which allows for close coupling to photosynthetic activity.

## 3.2 Materials and Methods

### 3.2.1 Organisms, culture conditions, and standard protocols

Axenic cultures of *Thalassiosira pseudonana* CCMP1335 cells were used for all manipulations, including nucleic acid isolation and physiological studies. Cells were maintained in f/2+Si medium (Guillard and Ryther, 1962; Guillard, 1975) at 35 psu (practical salinity units) and 20°C with aeration under fluorescent cool white lamps with an incident light intensity of 120  $\mu\text{mol}\cdot\text{m}^{-2}\cdot\text{s}^{-1}$  unless otherwise stated. Chlorophyll a was analyzed using standard 90% acetone extractions from glass fiber filtered culture (Jeffrey and Humphrey, 1975) measured on a spectrophotometer (Agilent 8453E, Agilent Technologies Inc.). Variable fluorescence (fv/fm) was acquired using a fast repetition rate fluorometer (Kolber et al., 1998). Total carbon (inorganic and organic, subset of samples acidified to remove inorganic carbon) and nitrogen content of cultures were measured with a Carlo Erba NA-1500 elemental analyzer.

### 3.2.2 Cloning and purification of recombinant TpMnSOD

Total nucleic acids from mid log growth *Thalassiosira pseudonana* cells were extracted and treated with DNA-free (Ambion, Inc. Austin, TX, catalog no. 1906) to remove DNA. First strand cDNA was synthesized with total RNA using M-MLV Reverse Transcriptase (Invitrogen Corp., Carlsbad, CA, catalog no. 28025-013). The cDNA was then used as a template for PCR to amplify sodA with the specific primers 5'ATGAAAATCCATCATGATAAGCAT3' and 5'TCCTCGCACGGGGACTCCTG3' which were designed based on the publicly available genome sequence of *T. pseudonana*. The full copy of the gene was then cloned into the pBAD vector (Invitrogen Corp.,

Carlsbad, CA, catalog no. K4300-40) and transformed into *Escherichia coli* for overexpression. The expression of the protein was controlled by varying the concentration of arabinose to achieve ideal expressed product. The vector contains a poly his-tag as well as a V5 epitope region. Thus, the recombinant protein was purified using Ni-NTA resin (Qiagen, Valencia, CA, catalog nos. 30230 and 30410) using both gravity chromatography and FPLC.

### *3.2.3 Antibody production against TpMnSOD*

For the initial immunization, equal volumes of recombinant TpMnSOD protein in a 2mg/ml concentration and Freund's Complete adjuvant were emulsified using a micro-emulsifying needle. 0.8 ml of the emulsified protein and adjuvant were injected subcutaneously into two New Zealand White rabbits in four sites (max 0.2 ml per site). A subsequent injection was given 30 days later and was prepared using equal volumes of the provided antigen in a 1mg/ml concentration and Freund's incomplete adjuvant. The emulsified protein and adjuvant were injected subcutaneously, with a maximum of 0.2 ml/site. Subsequent injections were given at 30-35 day intervals. Blood draws from the central ear artery were performed between 10-20 days after each subsequent injection. The maximum blood withdrawn did not exceed the standard recommendation of blood amount withdrawn of 15% of total blood volume, or 1% of body weight.

### *3.2.4 Immunoblot analyses*

Protein was extracted from cell pellets in 2% SDS, 0.05M sodium carbonate, 7.5% glycerol, 0.025% bromothymol blue, 5mM PMSF, and 0.1M DTT. Sample protein

concentration was quantified using either the bicinchoninic acid method (Pierce Biotechnology, Inc. Rockford, IL, cat no. 23227) or a fluorescent method (Invitrogen Corp., Eugene, OR, cat. no. R33200). Samples were then run on either 12, 15, or 18% (w/v) polyacrylamide gels and then blotted onto polyvinylidene fluoride (PVDF) membrane (Towbin et al., 1979). The blots were then probed with anti-TpMnSOD, the antibody raised against the recombinant MnSOD in *Thalassiosira pseudonana*. An HRP conjugated secondary antibody (BioRad Laboratories, Inc. Hercules, CA, catalog no. 172-1019) was used according to instructions and the blots were visualized with a chemiluminescent substrate system on film (Pierce Biotechnology, Inc. Rockford, IL catalog no. 34080). For quantitative immunoblot, known concentrations of both cells (total number) and protein (total  $\mu\text{g}$ ) were run on gels and then compared to unknown samples using densitometry (N=3).

### *3.2.5 Immunogold staining*

After fixation for 3 hr in a modified EM Fixative (3% Sodium Chloride, 0.1M Sodium Cacodylate, 2.5% Glutaraldehyde, pH 7.4), cell pellets were rinsed three times in Eppendorf tubes (2 x 15 min and 1x overnight) in 3% Sodium Chloride, 0.1M Sodium Cacodylate, pH 7.4 (Cells for TEM imaging only were also post-fixed for 2 hr in 1% buffered Osmium Tetroxide.). After the washes the cells were then dehydrated through a graded series of Ethanol washes, starting with 50% Ethanol to 100% Ethanol. The pellets were then embedded in Dr. Spurr's Low Viscosity Embedding Media within the Eppendorf tubes.

Sections were cut using a LKB 2088 ultramicrotome (LKB-Produkter, S-161 25 Bromma, Sweden), collected on 300-mesh gold grids and immunostained. Briefly, each grid was incubated for 1 hr. in Tris-buffered saline-tween + 0.5% BSA (TBS-t: 0.02M Tris, 0.15M NaCl, 0.1% Tween-20), pH 7.6. The grids were then transferred to primary antibody diluted in TBS-t (50µl drops). The grids were then incubated overnight in humidified chamber at 4°C. The next morning, the grids and solutions were left to come to room temperature and then the grids were washed 10 times, 1 min each time. Then the grids were transferred to the appropriate gold-labeled secondary antibody (1:20 or 1:15, Sigma-Aldrich Co., St. Louis, Mo, catalog no. G7402) diluted in TBS-t. They were incubated in the secondary antibody for 1hr at room temperature. The grids were washed 10 times, 1 minute each in TBS-t, then the same amount of times in ultra pure water. The grids were then counter-stained with Uranyl Acetate and Lead Citrate and photographed in a JEM-100CXII Electron Microscope (JEOL LTD., Tokyo, Japan) at 80 kV.

### 3.3 Results

#### 3.3.1 Native molecular mass and western analyses

Western blots from denaturing polyacrylamide gel electrophoresis (PAGE) of crude cell extract (Fig. 3.1) probed with anti-TpMnSOD reveal a major band of approximately 23 kDa which corresponds well with the predicted subunit molecular mass of 22.8 kDa for MnSOD. The anti-TpMnSOD cross reacted with other diatom species, and weakly recognized MnSOD in several dinoflagellates (Table 3.1). Interestingly, there was no anti-TpMnSOD cross-reactivity with two other heterokonts: the Eustigmatophyceae and Raphidophyceae. No reactivity was observed in the chlorophytes, cyanobacteria, prymnesiophytes, cryptophytes, and rhodophytes.

#### 3.3.2 MnSOD and the cellular manganese budget in diatoms

Based on quantitative immuno-analyses of MnSOD in nutrient replete exponentially growing cultures of *T. pseudonana*, this marine diatom maintains 0.91 amol MnSOD per cell when grown at moderate light levels. This quantity of MnSOD accounts for 1.4% of the total cellular protein (Table 3.2). This pool turns over rapidly as TpMnSOD is undetectable after 16 h under continuous light when protein synthesis is blocked (Fig. 3.2) corresponding to a 5-8 hour half-life. The turnover was mediated by light as TpMnSOD was detectable even after 27 h when cells were kept in darkness regardless of whether protein synthesis was inhibited.

The total Mn associated with TpMnSOD ranges between 10-20% of the total cellular Mn (Fig. 3.3, see legend for calculation details). Raven (1990) estimated that between 2 to 4  $\mu\text{mol Mn mol C}^{-1}$  are needed to support the Mn requirement of PSII in *T.*

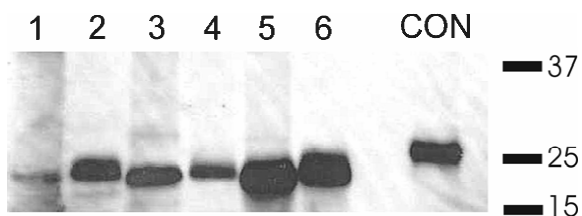


Figure 3.1: Immunoblot of Selected Diatom Species. Immunoblots showing the anti-TpMnSOD antibody we produced cross-reacted with multiple diatom species. The phylum specificity of this antibody suggests that all diatoms have an MnSOD with similar structure. All lanes loaded with 30 $\mu$ g total protein (except control loaded with 10ng pure recombinant TpMnSOD): lane 1, *Ditylum brightwellii* CCMP358; lane 2, *Navicula incerta* CCMP542; lane 3, *Nitzschia brevistriata* CCMP551; lane 4, *Stephanopyxis turris* CCMP815; lane 5, *Thalassiosira pseudonana* CCMP1010; lane 6, *Skeletonema costatum* CCMP1332; con, control protein overexpressed and purified recombinant TpMnSOD. Note: *T. pseudonana* strain used in this immunoblot is CCMP1010 and different than CCMP1335, which is the one used for cloning and over-expression of *sodA*. Marker indicates molecular weight standards in kDa.

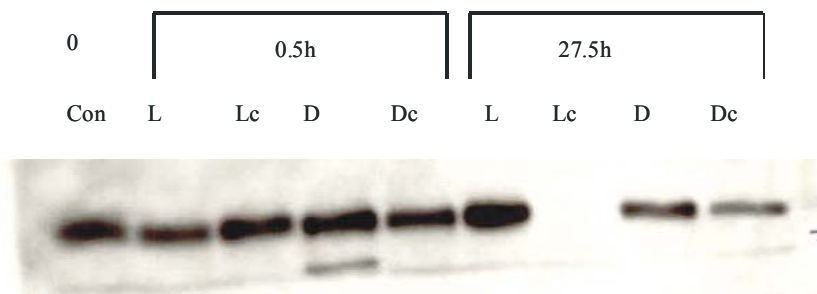


Figure 3.2: Immunoblot of *Thalassiosira pseudonana* CCMP1335 cells and cells treated with cycloheximide (Lc, Dc) to inhibit protein synthesis. After 27 hours the protein is below detection in the cells grown under light with protein synthesis inhibited. This suggests that the turnover of TpMnSOD is related to processes that occur when cells are exposed to light. Conversely, cells exposed to continuous darkness show evidence of TpMnSOD through out the experiment. Each lane is loaded with 8 $\mu$ g of total protein extracts. Antibody was specifically raised against recombinant protein in control lane.

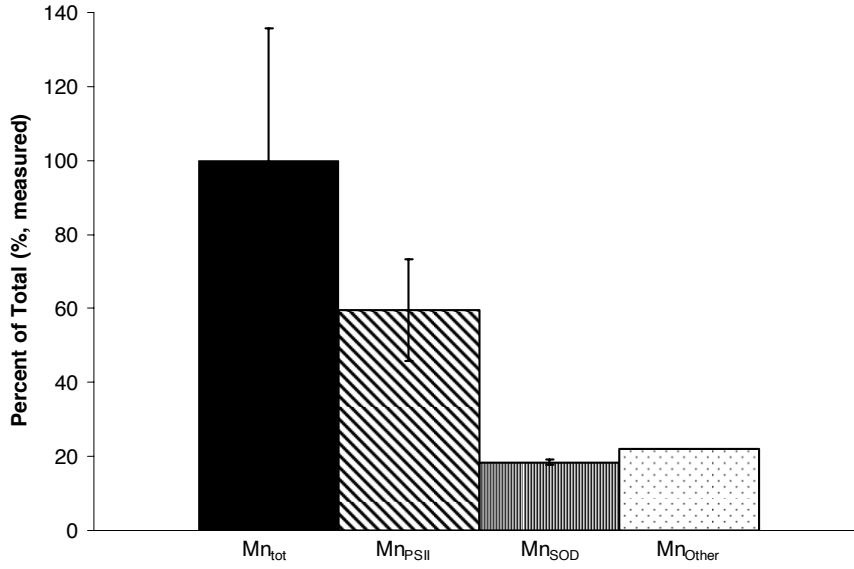


Figure 3.3: Intracellular Distribution of Manganese for *Thalassiosira pseudonana*

CCMP1335. Total cellular Mn ( $Mn_{tot}$ ) was estimated from the  $C_{org}$ -specific Mn quotas ( $\mu\text{mol Mn mol C}^{-1}$ ) of Sunda and Huntsman (1998, Fig. 7 and high light, low Mn Table 2) and the  $C_{org}$  content of mid-log exponentially growing cells ( $0.89 \text{ pmols } C_{org} \text{ cell}^{-1}$ ). Mn in photosystem II ( $Mn_{PSII}$ ) is that modeled by Raven (1990). Mn in SOD was estimated as the average measured MnSOD concentration using the quantitative immunotechnique ( $\text{mols of MnSOD cell}^{-1}$ , Table 3.2). Note that as  $C_{org}$  decreases in cells as light increases while moles of MnSOD  $\text{cell}^{-1}$  stays constant across light levels, the percent of Mn in MnSOD may increase with irradiance (see also Fig. 3.5).

*pseudonana*. Approximately 60% of total Mn within a cell can be accounted for by the PSII Mn-complex (Sunda and Huntsman, 1986; Raven, 1990; Sunda and Huntsman, 1998). Based on immuno- quantitative analyses, MnSOD accounts for another 18% of the Mn budget. Thus, ~80% of the total Mn budget is associated with MnSOD and PSII.

### 3.3.3 Immunolocalization of MnSOD in plastids

Immunogold labeling measurements suggest that MnSOD is mainly confined to the chloroplast (Fig. 3.4). The gold label is predominantly associated with thylakoid membranes and the pyrenoid. It is not associated with the cytosol or the mitochondria. Since the chloroplast localized MnSOD is regulated by the nuclear-encoded *sodA* gene, plastid/endoplasmic reticulum transit peptides must be present, but they have not yet been identified .

### 3.3.4 Impact of light on *TpMnSOD* expression

When acclimated to a range of irradiance levels (25, 50, 120, 350, 800  $\mu\text{mol m}^{-2} \text{s}^{-1}$ ), *T. pseudonana* cells show a 73% increase in growth rate (Fig. 3.5). Total chlorophyll *a* cell<sup>-1</sup> is constant at low light levels (25 to 50  $\mu\text{mol m}^{-2} \text{s}^{-1}$ ), but decreases by 63% as the incident light intensity increases from 50 to 800  $\mu\text{mol m}^{-2} \text{s}^{-1}$ . (note: Cells were kept optically thin in semi-continuous batch cultures to avoid cell concentration concerns like self shading.) Over this range of irradiances, the amount of *TpMnSOD* per unit chlorophyll increased by 60% (Fig. 3.5) reflecting changes in the chlorophyll

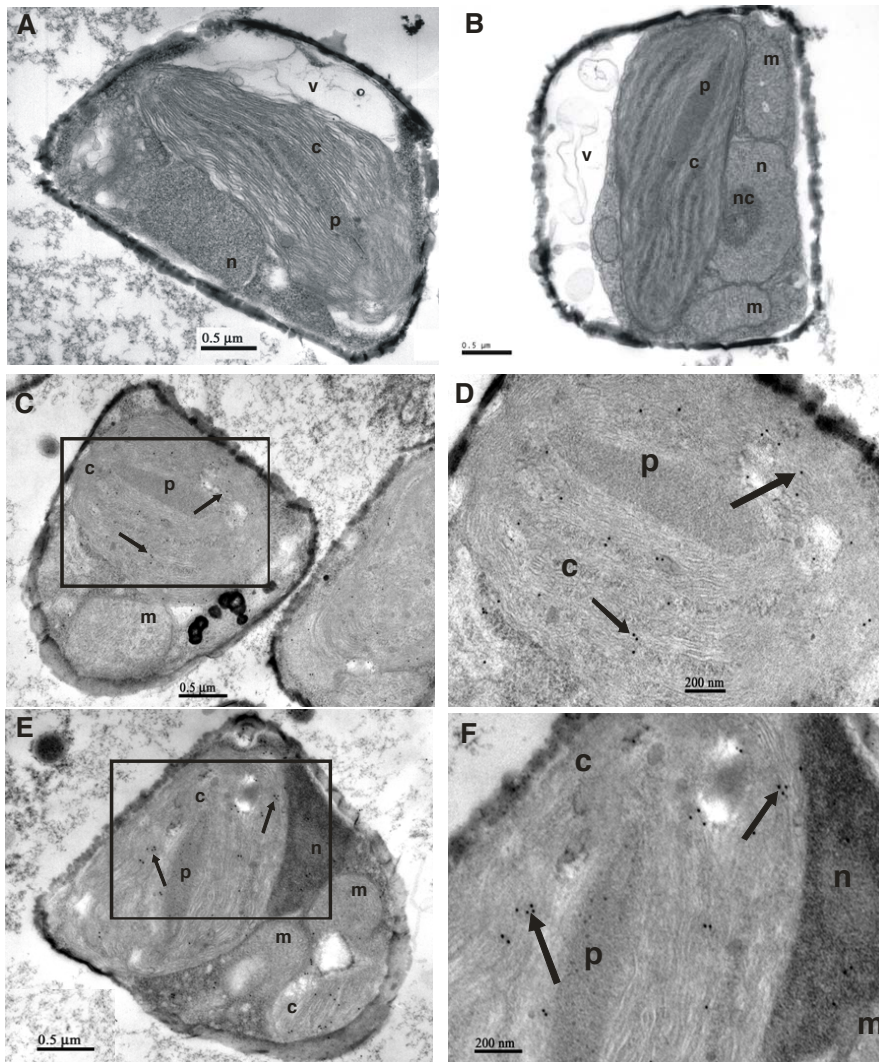


Figure 3.4: Immunogold localization of MnSOD in *Thalassiosira pseudonana*

CCMP1335. A, Osmium tetroxide stained electron micrograph of whole cell. B, Second different view of Osmium tetroxide stained cell. C, Immunogold labeling of the chloroplast with the anti-TpMnSOD antibody. D, Magnified view of delineated area in

B. E, Immunogold labeling of the chloroplast in another cell of *T. pseudonana*. F, Magnified view of delineated area in E. Note the absence of labeling of mitochondrial and cytosolic regions. Key: c, chloroplast; p, pyrenoid; m, mitochondrion; n, nucleus; nc, nucleolus; v, vacuole. Arrows indicate black, electron dense gold label corresponding to TpMnSOD. Scale bars = length as indicated. Note, granules apparent in the pyrenoid of F are crystalline RUBISCO, clearly not as electron dense as the gold particles.

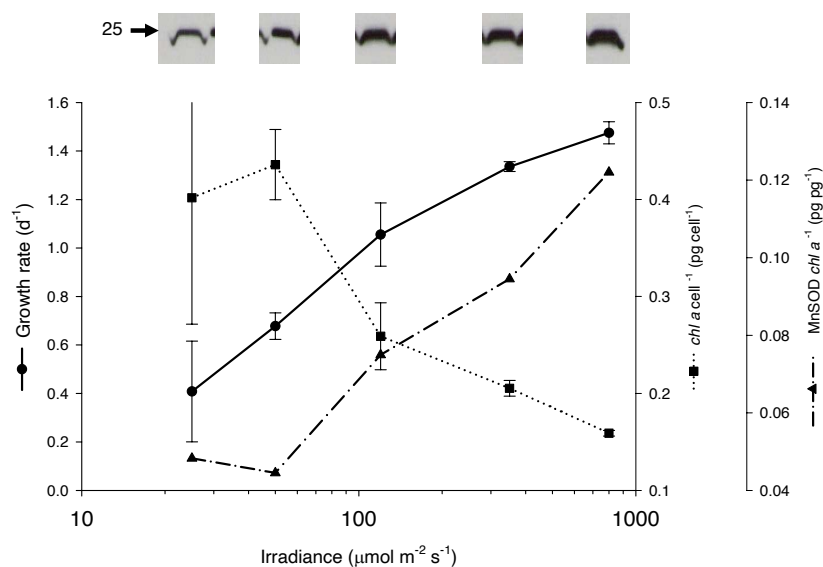


Figure 3.5: Comparison of growth rate, total cellular chlorophyll, and MnSOD per unit chlorophyll of *Thalassiosira pseudonana* CCMP1335 cells grown at different continuous light intensities. Western blot images above the graph are of protein samples loaded according to equal chlorophyll. Growth rate (solid black circles and solid line) increases by two-fold over these light levels. Concurrently, cellular chlorophyll (solid black squares, dotted line) decreases. Although MnSOD is constant per unit protein (data not shown), MnSOD per unit chlorophyll (solid black triangles, dashed and dotted line; and western blot above image) increases. This supports the strong association of the relative contribution of MnSOD to protecting the photosynthetic machinery; especially as the light harvesting pigments decrease.

concentration not MnSOD. Although the chlorophyll *a*-normalized MnSOD content of *T. pseudonana* increased with increasing light, the amount of MnSOD per total cellular protein was constant (data not shown). Thus the demand for MnSOD per cell in these cells appears to be constant over these light levels despite declining chlorophyll. A similar relationship between light intensity, SOD, and chlorosis was also seen for the chloroplastic CuZnSOD in bean and other higher plants (Gonzalez et al., 1998 and references therein).

To further examine the relationship between light and MnSOD, the time course of TpMnSOD expression was followed over 30 h in cells acclimated to a 12/12 hr photoperiod. TpMnSOD expression did not vary significantly over photoperiod when grown at  $120 \mu\text{mol m}^{-2} \text{s}^{-1}$  incident light (control), but increased by 40% within 24h and after one dark period when transferred to high light ( $>800 \mu\text{mol m}^{-2} \text{s}^{-1}$ ) (Fig. 3.6A-B).

The maximum photosynthetic quantum yield (Fv/Fm, Kolber et al., 1998) initially decreased by 50% under high light, but recovered and exceeded the control within 24 hours (Fig. 3.6A-B). After a period of recovery (the dark cycle) to reorganize their metabolic profile, the cells then effectively cope with the high light stress with increased MnSOD expression. The increase in MnSOD expression per unit protein in the high light treatment (12:12 L:D) is significant ( $p=0.0007$ ) and is not exhibited by cells exposed to continuous high light. Protein normalized MnSOD expression doubled in *T. pseudonana* cells acclimated to continuous light after transfer from culture under a diel light cycle at both  $120$  and  $800 \mu\text{mol m}^{-2} \text{s}^{-1}$  (data not shown). Thus, continuous light apparently results in greater oxidative stress in diatoms than does a diel light cycle.

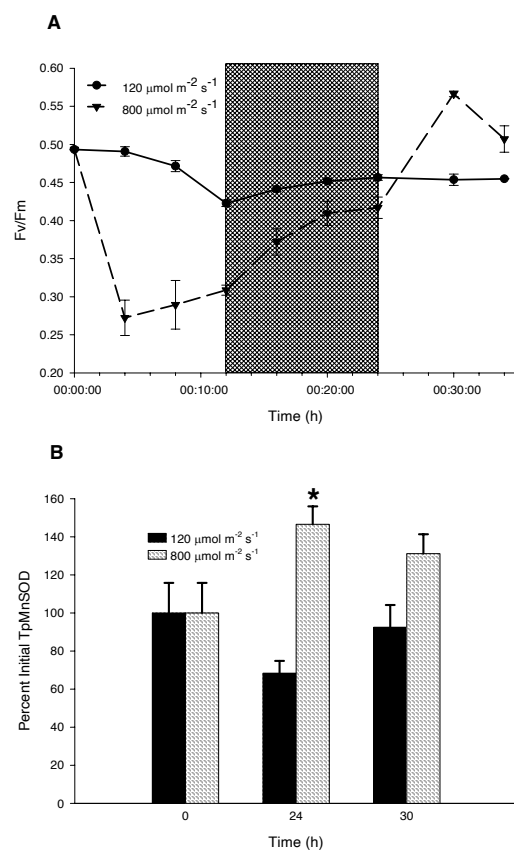


Figure 3.6. Diel expression of MnSOD in *Thalassiosira pseudonana* CCMP1335. Here is the quantum yield, A, of cells exposed to 12:12 L:D cycle under high light (800  $\mu\text{mol m}^{-2} \text{s}^{-1}$ , solid black triangles and dashed line) and control light (120  $\mu\text{mol m}^{-2} \text{s}^{-1}$ , solid black circles solid line) over time (x-axis). Fv/Fm decreases in the high light over the first 12 h when compared to the control and then recovered during and after the dark period. The dark period is represented by the shaded area. Immunoblot densitometric analysis, B, shows significant recovery after the dark period of TpMnSOD in the high

light (hatched bars) treatment with as compared to the expression of TpMnSOD in the control light (solid bars) cultures (values are means,  $n=2 \pm \text{SD}$ ). Asterisks denote significant differences between treatments ( $p = 0.0105$ )

### 3.4 Discussion

MnSOD is localized in the chloroplasts for the diatom *Thalassiosira pseudonana*. This subcellular location is in contrast with all other cellular MnSOD distributions in eukaryotic photoautotrophs, where MnSOD is found exclusively in the mitochondria (Grace, 1990; Moller, 2001; del Rio et al., 2003). The presence of MnSOD in the chloroplast results in cells having a high cellular Mn requirement, given the substantial turnover of photosynthetic machinery. For example, the D1 protein (PsbA) has a turnover rate of approximately 30 minutes, one of the fastest turnover protein rates on Earth (Kim et al., 1993; Sundby et al., 1993; Andersson and Aro, 1997; Neidhardt et al., 1998), due to the high activity photosystem II (PSII) (Mattoo et al., 1984). Chloroplast specific SODs influence the D1 protein turn over due to their role in catalyzing the destruction of ROS in the chloroplast (Barber and Andersson, 1992; Aro et al., 1993; Andersson and Aro, 1997).

If diatoms use MnSOD to suppress oxidative stress associated with photosynthesis in the chloroplast, we would expect diatoms to have higher Mn requirements than other classes of phytoplankton. Thus, not surprisingly, diatoms have high Mn requirements compared to other eukaryotic algae (Raven, 1990; Raven et al., 1999; Ho et al., 2003; Quigg et al., 2003). Given the potentially large Mn requirement associated with photosynthesis, a great deal of effort has been focused on determining the cellular Mn budget. Current cellular Mn budgets for diatoms have been based solely on the Mn associated with PSII (Raven, 1990). These budgets significantly underestimate measured cellular Mn concentrations (Sunda and Huntsman, 1986; Sunda and Huntsman, 1998; Peers and Price, 2004); however, including MnSOD (10-20% of total cellular Mn),

up to 80% of the total cellular Mn can be accounted for, all of which is in the chloroplasts (Sunda and Huntsman, 1986; Raven, 1990; Sunda and Huntsman, 1998; Peers and Price, 2004).

Manganese is not often bio-limiting in the oceans. Concentration profiles from numerous ocean basins show that Mn is often at biologically useful concentrations while Fe is typically undetectable in surface waters (Li, 1991; Shiller, 1997; Nozaki et al., 1998; Whitfield, 2001). Measured values for Mn in the Atlantic basin range from about  $25 \text{ nmol} \cdot \text{kg}^{-1}$  in coastal regions to between 2 to  $5 \text{ nmol} \cdot \text{kg}^{-1}$  at open ocean stations (Shiller, 1997). Using average values of chlorophyll as a proxy for biomass:  $5 \text{ } \mu\text{g} \cdot \text{kg}^{-1}$  and  $1 \text{ } \mu\text{g} \cdot \text{kg}^{-1}$  for coastal and oceanic regions, respectively (Falkowski and Raven, 1997), and an average of  $77 \text{ } \mu\text{g MnSOD} \cdot \text{mg chl } a^{-1}$  (based on our measurements, see fig. 3.5), we calculated that oceanic Mn concentrations support more than 1000 turnovers of Mn in diatoms assuming growth rate between 1 to  $2 \text{ d}^{-1}$ . Mn could thus serve as a possible metal replacement for iron and other bio-limiting metals in marine algae (Whitfield, 2001; Peers and Price, 2004).

The high Mn requirement of diatoms is significant to the ecology of these eukaryotic algae, as the role of trace metals has been shown to structure oceanic phytoplankton productivity and community composition in many regions (Saito et al., 2003; Coale et al., 2004). A major focus of research has been on iron, which limits productivity and is only present in sub nM concentrations in most of the world's oceans (Boyd et al., 2000; Coale et al., 2004). Therefore, it is not surprising that some photoautotrophs have evolved mechanisms to compensate for low Fe availability. For example, diatoms can use flavodoxin, instead of the Fe-requiring ferredoxin, under low

Fe conditions to support electron transport in PSI (LaRoche et al., 1993; McKay et al., 1999). Similarly, some cyanobacteria and chlorophytes substitute the Cu-containing plastocyanin for the Fe-heme cytochrome  $c_6$  in PSI to transfer electrons between the cytochrome  $b_6f$  complex and  $P700^+$  (Quinn and Merchant, 1999). This strategy is based on substituting the most limiting element with biochemistry that utilizes a non-limiting element.

This strategic biochemical substitution suggests that phytoplankton living in chronically Fe-limited waters may gain a competitive advantage if they can use alternative metals. Cyanobacteria from oligotrophic areas contain either NiSOD alone or both Ni and MnSOD instead of FeSOD found in freshwater species (Partensky et al., 1999; Palenik et al., 2003; Wolfe-Simon et al., 2005). Thus, two of the most successful groups of marine phytoplankton (diatoms and cyanobacteria, Falkowski et al., 2004a; Falkowski et al., 2004b) use non-Fe SODs to cope with oxidative stress in the Fe-poor regions of the modern ocean. Modern chlorophytes, including embryophytes, do not use Fe enzyme replacements. Therefore, it is not surprising that these taxa are not dominant in the oceans and are found primarily in terrestrial, freshwater, and estuarine systems that have abundant Fe concentrations (Sternner et al., 2004, and others). Thus, utilization of MnSODs may be one more mechanism underlying the dominance of red alga taxa over the last 275 Ma (Falkowski et al., 2004a; Falkowski et al., 2004b).

Chlorophytes (as well as some embryophytes) typically utilize FeSOD isoforms in the chloroplast (Sakurai et al., 1993; Chen et al., 1996; Kitayama et al., 1999). Consequently, the use of MnSOD in the chloroplast should lower a cell's iron demand because there is less FeSOD in use. These proteomic differences are reflected in the

metal quotas of various marine phytoplankton taxa as diatoms have significantly lower Fe requirements than chlorophytes (Ho et al., 2003; Quigg et al., 2003). This biochemical difference may reflect the environments under which the diverse photosynthetic taxa evolved (Williams, 2001). The ancient aquatic ecosystem is thought to have been chemically reduced, which would have made iron abundantly available to evolving organisms (Brocks et al., 1999; Anbar and Knoll, 2002). As oxygen increased and oxidized most of the Fe to an insoluble oxide form, organisms were forced to evolve alternative options for biochemical pathways. Thus, the nutritional difference between chlorophytes and diatoms may contribute to the success of the diatoms in the low Fe modern marine environment (Falkowski et al., 2004a).

## TABLES

**Table 3.1. Antibody Cross Reactivity.** We reverse transcribed, amplified and cloned the gene for MnSOD from freshly extracted *Thalassiosira pseudonana* mRNA. We then raised an antibody in rabbits to the recombinant protein and tested the antibody against a wide range of whole cell protein extractions from cyanobacteria, primary green, primary red and secondary red algae. Here we present data showing the specificity of this antibody. It primarily recognizes only diatoms and only weakly some dinoflagellates. It did not cross react with any other phylum or class of algae. All algae were grown in pure culture at optimal conditions as recommended by the Culture Collection of Marine Phytoplankton\* ([www.bigelow.org](http://www.bigelow.org)).

TAXA IDENTIFICATION	CCMP*	RECOGNITION
BACILLARYOPHYTA		
<i>Ditylum brightwellii</i>	358	+
<i>Navicula incerta</i>	542	+
<i>Nitzschia brevistriata</i>	551	+
<i>Stephanopyxis turris</i>	815	+
<i>Thalassiosira pseudonana</i>	1010	+
<i>Skeletonema costatum</i>	1332	+
DINOPHYCEAE		
<i>Karlodinium micrum</i>	415	~
<i>Heterocapsa triquetra</i>	449	~
<i>Amphidinium carterae</i>	1314	~
<i>Prorocentrum minimum</i>	1329	~
EUSTIGMATOPHYCEAE		
<i>Nannochloropsis oculata</i>	525	-
RAPHIDOPHYCEAE		
<i>Heterosigma akashiwo</i>	1680	-
CHLOROPHYTA		
<i>Dunaliella tertiolecta</i>	1320	-
<i>Pyramimonas parkeae</i>	724	-
<i>Nannochloris atomus</i>	509	-
<i>Pycnococcus provasolii</i>	1203	-
<i>Tetraselmis marina</i>	898	-
PRYMNESIOPHYTA		
<i>Isochrysis galbana</i>	1323	-
<i>Emiliana huxleyi</i>	373	-
CRYPTOPHYCEAE		
<i>Rhodomonas salina</i>	1319	-
RHODOPHYTA		
<i>Porphyridium</i> sp.	X	-
CYANOBACTERIA		
<i>Trichodesmium</i> sp. IMS101	X	-
<i>Synechocystis</i> sp.	PCC6803	-

**Table 3.2. Statistics for MnSOD in *Thalassiosira pseudonana* CCMP1335.** These data show the cell specific MnSOD budget based on quantitative immuno-analyses (see methods section). Although MnSOD accounts for a small percentage of the total protein, it is an important pool of manganese in the cell. Cells grown under continuous light, 120  $\mu\text{mol m}^{-2}\text{s}^{-1}$ , 20°C.

Protein mass per cell	19.8 $\pm$ 3 fg MnSOD cell <sup>-1</sup>
Molecules per cell	5.5 $\pm$ 0.9 $\times 10^5$ MnSOD cell <sup>-1</sup> <sup>1</sup>
Molecules per cell	2.7 $\pm$ 0.5 $\times 10^5$ HOLO- MnSOD cell <sup>-1</sup> <sup>2</sup>
Moles per cell	0.9 $\pm$ 0.2 amol cell <sup>-1</sup>
Cell volume	19.6 $\pm$ 0.8 fL <sup>3</sup>
Percent of total protein	1.4 $\pm$ 0.2 %

<sup>1</sup> based on M.W. of 21.798 kDa

<sup>2</sup> Based on hypothetical homodimer with a M.W. of 43.696 kDa

<sup>3</sup> Based on scanning electron micrography (SEM)

## 4.0 The Molecular Evolution of Iron and Manganese Superoxide Dismutases in

### Secondary Red Algae

#### Abstract

Secondary endosymbiosis of red plastids in eukaryotic algae is an area of heated debate. There are two extant lineages of plastid containing organisms: green and red lineages. The primary endosymbiosis occurred as a single event leading to both when a mitochondrion containing heterotrophic eukaryote engulfed a cyanobacterium-like prokaryote. The secondary endosymbiotic event(s) then occurred when one or more heterotrophic eukaryote(s) appropriated a primary plastid containing eukaryote. The timing and nature of the second event(s) is unclear. During each endosymbiotic event, genes were transferred to the new host's nucleus. One such enzyme family, superoxide dismutases (SODs), are all nuclear encoded genes whose products are directed either towards the plastid, mitochondrion, or cytosol. Our phylogenetic analyses of the homologous Fe/MnSOD family expose complex evolutionary histories. All eukaryotic photosynthetic autotrophs (including the aplastidic euglenozoa and apicomplexa) share cyanobacteria as the common ancestor for FeSOD. Thus, FeSODs were inherited from the primary endosymbiont in both red and green secondary plastid-containing eukaryotes including euglenozoa, alveolates, haptophytes, and heterokonts. MnSOD is present the nucleus of only a few secondary red-plastid derived eukaryotes namely the stramenopiles (heterokonts and oomycetes) and secondary green-plastid containing eukaryotes. This suggests the inheritance of MnSOD from the primary endosymbiont's nucleus and its loss by most other plastid-derived eukaryotes. The secondary red-plastid host had a preference for retaining the MnSOD gene. Since secondary red-plastid containing

eukaryotes dominate the modern marine environment and Fe is much less abundant than Mn in the ocean, the preference for a Mn enzyme over an Fe based one suggests that the secondary red-plastid containing eukaryotes had a selective advantage over the primary and secondary green plastid containing eukaryotes.

#### 4.1 Introduction

Photosynthetic eukaryotes evolved from the endosymbiotic appropriation of plastids from other, preexisting, photosynthetic organisms (Delwiche, 1999; Palmer, 2003). Unique to photoautotrophs, at least two endosymbiotic events have been documented. The primary endosymbiosis involved a heterotrophic eukaryotic host cell which engulfed a cyanobacterium-like prokaryote. This “primary” event led to the evolution of modern plastids in most green algae and all higher plants in which the plastid is bound by two envelope membranes, one derived from the cyanobacterium and the second from the invagination of the host cell (Bhattacharya and Medlin, 1995; Delwiche, 1999; McFadden, 2001). Secondary endosymbiosis occurred when another eukaryotic host cell engulfed a primary photosynthetic eukaryote, leading to a plastid bound by three or four membranes (Delwiche, 1999). Whereas primary endosymbionts are thought to derive from a single event, these organisms subsequently diverged and led to primary green and red plastid-containing lineages (Falkowski et al., 2004a). The phylogenetic relationships between secondary photosynthetic eukaryotes are more ambiguous (Nozaki et al., 2003a; Nozaki et al., 2003b; Nozaki et al., 2004). How many secondary events were there? When did it/they occur? And what were the selection pressures that led to their occurrence and subsequent long-term, ecological success?

Based on nuclear, plastid, and mitochondrial genome analyses, secondary endosymbionts contain a plastid derived originally from either a red or green primary eukaryote or alga. Substantial gene transfers to the secondary nucleus have occurred, with genes originating from both the primary plastid and the primary host nucleus.

Numerous studies have evaluated many of these genes and have yet to unambiguously resolve the position of secondary red-plastid containing eukaryotes.

Superoxide dismutases (SODs) are a nuclear encoded polyphyletic family of enzymes that likely originated from either the plastid or mitochondrial genomes based on their phylogenetic position and their current subcellular localization in extant eukaryotic photoautotrophs (Grace, 1990; Smith and Doolittle, 1992). Based on the metal center cofactors, four known extant isoforms of SODs are recognized: Fe, Mn, Cu/Zn, and Ni. These enzymes all catalyze the destruction of  $O_2^{\cdot -}$  to  $H_2O_2$  and  $O_2$ . Superoxide,  $O_2^{\cdot -}$ , is particularly destructive because it cannot diffuse across cell membranes, and therefore, must be destroyed at the site of production. This key antioxidant has been well studied in many eukaryotic systems, including metazoa and plants (Bowler et al., 1992; Scandalios, 1993; Fink and Scandalios, 2002b; Zelko et al., 2002) and is shown to be localized mainly in either the mitochondria or plastids.

Diatoms are members of the secondary red plastid-containing group called stramenopiles and are extraordinarily successful in the ocean. The stramenopiles are a polyphyletic group of organisms and are relatively understudied in terms of the phylogenetic position with respect to Fe- and MnSODs. Due to the informative subcellular localization of the SODs, their phylogeny in secondary red-plastid containing algae may help resolve the number of endosymbiotic events leading to the current mitochondria and plastids and the environmental pressure under which these events took place.

In this paper, we examine the evolutionary history of the Fe- and MnSOD proteins in photoautotrophs, specifically the secondary red-plastid containing algal lineages

(chlorophyll a/c containing algae). Using Bayesian and maximum likelihood analyses of the FeSODs, we found a large monophyletic SOD clade which includes cyanobacteria, primary green algae, secondary green algae, alveolates and green plants. This corresponds to a single primary endosymbiosis and the primary plastid as the source for the FeSOD gene. In contrast, MnSODs in photoautotrophs appears to reveal a bifurcated phylogeny. One group contains primary green algae basal to a cluster of primary and secondary red-plastid containing eukaryotes (stramenopiles: diatoms and oomycetes). The second is dominated by green plants and cyanobacteria. These results suggest that the MnSOD genes were inherited from the primary host for red and green algae and from the primary plastid in green plants. Thus, MnSODs diverged in photosynthetic organisms after the divergence of green plants from the primary green algae.

## 4.2 Materials and Methods

All SOD amino acid sequences integrated into this analysis were derived from the GeneBank/EMBL and SWISS-PROT databases (Table 4.1). We calculated similarity indices based on the BLOSUM62 matrix (Henikoff and Henikoff 1992). The evolutionary relationship of the Mn and FeSODs was determined by both Bayesian inference and maximum likelihood (ML) methods. Molecules were collected and initially aligned using the software package VectorNTI 8 (Invitrogen Corp., Carlsbad, CA, 2002). Alignments were also constructed using the CLUSTALX program (Thompson et al., 1994) and manually adjusted using BioEdit (Hall, 1999) and are available from F. W.-S. upon request. Similarity indices were calculated also using software package VectorNTI 8 (Invitrogen Corp., Carlsbad, CA, 2002). Trees were inferred with Bayesian inference and the maximum likelihood methods generated using the Mr Bayes package and PHYML (Huelsenbeck and Ronquist, 2001; Guindon and Gascuel, 2003; Ronquist and Huelsenbeck, 2003; Guindon et al., 2004). In the Bayesian inference we employed a mixed fixed rate estimator and the final model used was the WAG model (Whelan and Goldman, 2001). We also employed the WAG model for the PHYML analysis. Metropolis-coupled Markov chain Monte Carlo from a random starting tree was initiated and run for at least  $1 \times 10^6$  generations (see figure legends). Trees were sampled each 100<sup>th</sup> cycle. Multiple chains were run (see figure legends) with n-1 chains heated and one cold with the first 25% of the samples discarded (burnin). Stabilization of the log likelihoods was monitored to verify convergence by the end of the run (average of the split frequency of chains was approximately 0.01). A consensus tree was made with the remaining phylogenies (again discarding the first 25%) to determine

the posterior probabilities at the different nodes. The PHYML program was used to generate bootstrap supported trees (100 replicates) also employing the WAG model. The trees were viewed and modified using TREEVIEW (Page, 1996) and TreeExplorer ([http://evolgen.biol.metro-u.ac.jp/TE/TE\\_man.html](http://evolgen.biol.metro-u.ac.jp/TE/TE_man.html)). To examine the phylogenetic history specifically of photoautotrophs a subset of the data set was prepared and submitted to the same Bayesian analyses. Null hypotheses to confirm the most likely tree and convergence were tested by running full analyses repeatedly as well as forcing monophyly of known polyphyletic groups to observe if the data can surmount incorrect prior choices.

### 4.3 Results

To infer the evolutionary histories of the Fe and MnSOD proteins, amino acid sequences were aligned with homologs from other organisms, and phylogenetic analyses were performed. Because this gene family is a result of a duplication event, we also assessed the level of similarity between groups of proteins to examine which region of the protein has had less free mutational changes (Table 4.2). In general, the Mn enzymes are overall more similar to each other and within clades. Furthermore, the highest level of similarity is dominated by the C-terminal region. Bayesian ML trees were inferred, and posterior probabilities were calculated for each node. The analysis of algal Mn and Fe superoxide dismutases has been made using 20 eukaryotic MnSOD sequences (Table 3) and 11 FeSOD sequences compared with 108 other sequences ranging from the Archaea to opisthokonts and green plants (Table 4.1). Algal sequences include both eukaryotic (primary and secondary) and prokaryotic representatives.

The average length of the sequences is 218 amino acids (AA) but ranges from 192 to 286 AA with the full length alignment containing 399 positions (data not shown, for excerpts see Fig. 4.1). The phylogenetic trees were constructed using the composite alignment including both Mn and FeSOD forms to examine the phylogenetic relationship between the origins of the SOD gene in the algae. Alignment excerpts of three key areas showed the high degree of similarity as well as the subtle primary sequence differences between the Fe and MnSODs (Fig. 4.1). These three regions contain amino acids identified as contributing to the metal binding site (Vance and Miller, 1998; Weatherburn, 2001; Maliekal et al., 2002). The sites are identical with the metal cofactor





[illegible]

Figure 4.1: Excerpts of amino acid sequence alignment of the Fe and MnSODs used in this study. The asterisks denote primary and secondary sphere amino acids involved in either binding or coordination of the metal site. See text for discussion. A) N-terminal excerpt, B) Middle excerpt, C) C-terminal excerpt.

coordinated in a trigonal bipyramid by three histidines (H138, H195, H315) and an aspartate (D311) residue plus a solvent molecule (positions refer to alignment excerpts Figure 4.1, for *Escherichia coli* number see Lah et al., 1995; Borgstahl et al., 2000). The major primary conserved *difference* between Fe and MnSODs is also evident in the position of glutamine residues. The FeSOD active site is secondarily influenced by Q191 while the Mn form relies on Q290. This results in a subtle change in the second sphere electrical tuning of the protein and has consequences for the metal specificity of the holo-protein (Edwards et al., 2001).

Overall, major differences between the larger Fe and Mn clades involve the rate and extent of diversification. The Mn lineage is evolving faster (longer branch lengths) than the FeSODs. Furthermore, the MnSOD sequences are more diverse (Table 4.3) and form more sub-clades than FeSODs. Archaeal sequences, although well supported and firmly placed within the Mn clade, are all non-metal specific or *cambialistic* proteins. This means that they can use either Mn or Fe in the active site of the SOD protein. Specifically, at the key second sphere glutamine residue mentioned above, all these sequences have a glycine residue insertion.

#### 4.3.1 FeSOD clade

The Fe clade in both the Bayesian and ML trees divides into two main groups: Fe-1 and Fe-2 (Fig. 4.2 and Fig. 4.3). Fe-1 is dominated by anaerobic photosynthetic  $\alpha$ -proteobacteria and eukaryotic parasites (Euglenozoa and Parabasilids). Fe-2 splits into 2 groups one characterized by cyanobacteria, green sulfur bacteria (GSB), primary green plastid containing algae and green plants and the other cluster is composed of proteobacteria, alveolates, and Euglenozoa. The Bayesian analyses show a moderately

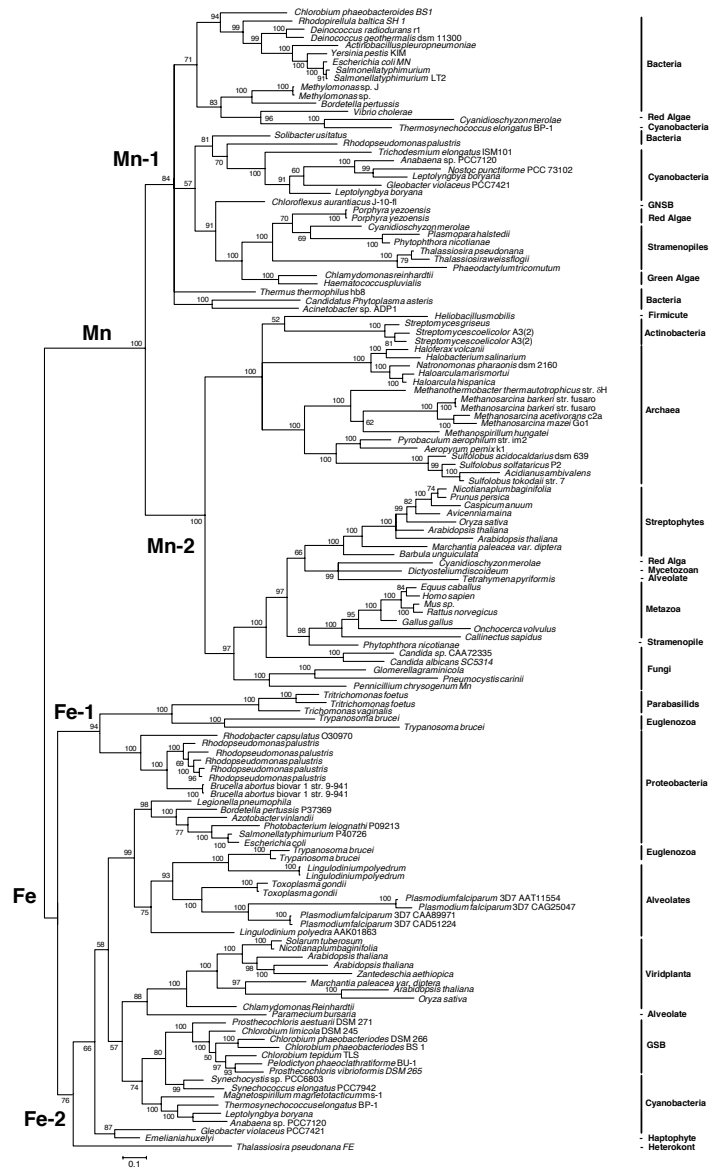


Figure 4.2: Bayesian based evolutionary relationship among the Fe/MnSOD family of proteins. Phylogeny representing all major taxa was inferred from a Bayesian analysis

based on amino acid sequences. The tree elucidates the endosymbiotic origin of this family of SODs in eukaryotes. The Fe clade shows a clear primary photosynthetic endosymbiotic origin evolving from the cyanobacteria and green sulfur bacteria (GSB). The MnSOD clade shows a few different photosynthetic clusters most notably a separation of the single celled primary green and primary and secondary red plastid containing eukaryotes from the green plants. The monophyletic relationship of the MnSODs in red-plastid algae is congruent with other estimated relationships. The basal primary green plastid alga to this cluster suggests a common origin for these sequences. Fe and Mn sequences were aligned using CLUSTALX (Thompson et al., 1997) and edited with BioEdit (Hall, 1999). This is the tree of highest likelihood identified in the Bayesian tree pool using the fixed rate WAG model ( $\text{Ln likelihood} = -37193.92$ ) and run for  $2.5 \times 10^6$  generations. Numbers at the nodes represent posterior probabilities. Scale bar represents the number of substitutions per amino acid site.

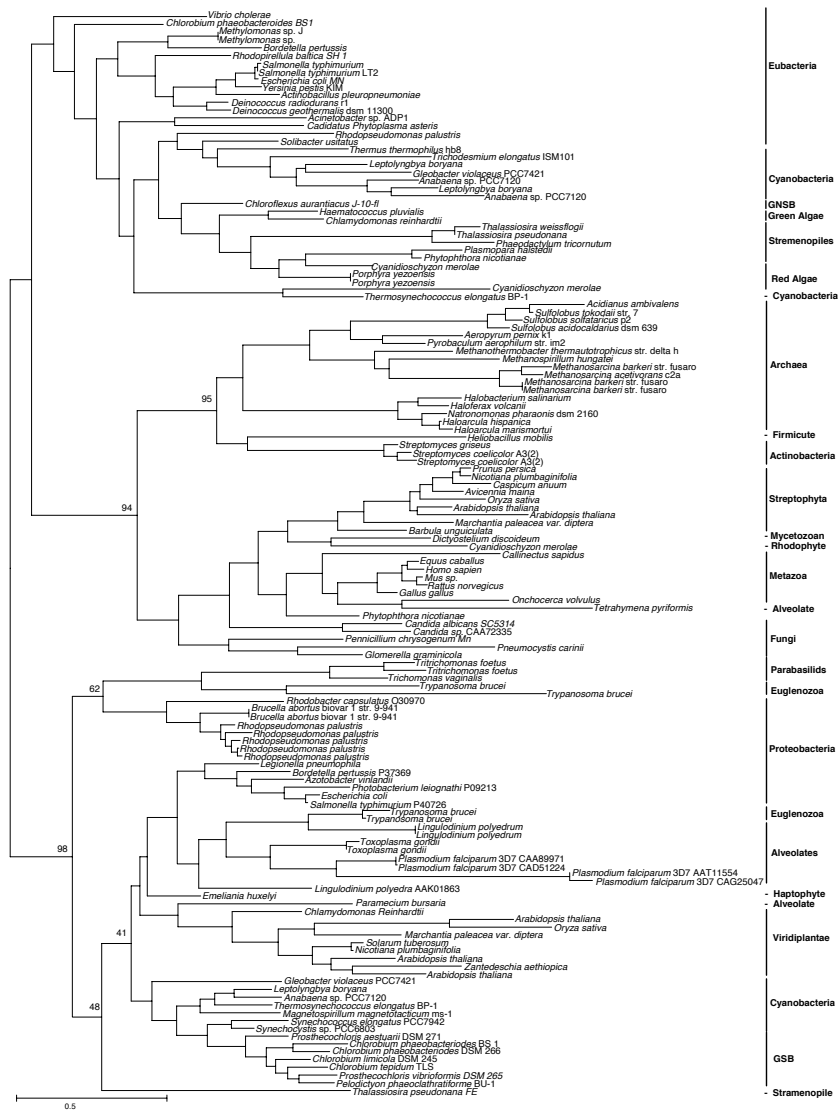


Figure 4.3: Maximum likelihood based evolutionary relationship among the Fe/MnSOD family of proteins. This tree agrees to a large extent with the Bayesian inferred tree. Important regions of difference are the clustering of the green plants in the FeSOD clade.

Bootstrap support is weak for many of the internal nodes which are resolved in the Bayesian tree. However, this tree validates many of the same hypotheses in agreement with the Bayesian tree. Sequences were aligned as in Figure 1. A maximum likelihood tree was constructed using PHYML ([http://evolgen.biol.metro-u.ac.jp/TE/TE\\_man.html](http://evolgen.biol.metro-u.ac.jp/TE/TE_man.html)) employing the WAG empirical fixed rate model of evolution (Whelan and Goldman, 2001). The scale bar represents the expected number of substitutions per amino acid position

supported (74%) posterior probability for a common ancestor for all the cyanobacteria FeSOD clustered with the GSB.

The second half of Fe-2 shows a cluster of alveolates and euglenozoa together with a variety of proteobacteria. Except for *Tetrahymena pyriformis*, all alveolates sequences known are FeSODs. This includes three sequences from the dinoflagellate *Lingulodinium polyedra* (Okamoto and Colepicolo, 1998; Okamoto et al., 2001; Okamoto et al., 2001). Furthermore, many organisms in this sub-clade are either obligate or facultative anaerobes. These all share a common ancestor with the photosynthetic taxa cluster. The ML tree describes a slightly different phylogeny of these organisms with green plants more closely related to the alveolates and proteobacteria while the cyanobacteria and GSB form their own monophyletic group. However, this branching pattern is not well supported (<50%).

#### 4.3.2 MnSOD clade

The MnSOD clade describes a contrasting phylogenetic history. Both the Bayesian and ML trees show two main clusters. Mn-1 is characterized by Eubacteria and eukaryotic primary and secondary plastid containing eukaryotes while Mn-2 is dominated by a split between Archaea and green plants/opisthokonts. The Bayesian analyses show a trifurcation at the root of Mn-1 group, which is better resolved in the ML and phototroph trees (Figs. 4.3 and 4.4). The cyanobacteria share a recent common ancestor with primary green and red, and secondary red-plastid containing eukaryotes (stramenopiles consisting of diatoms and the oomycetes).

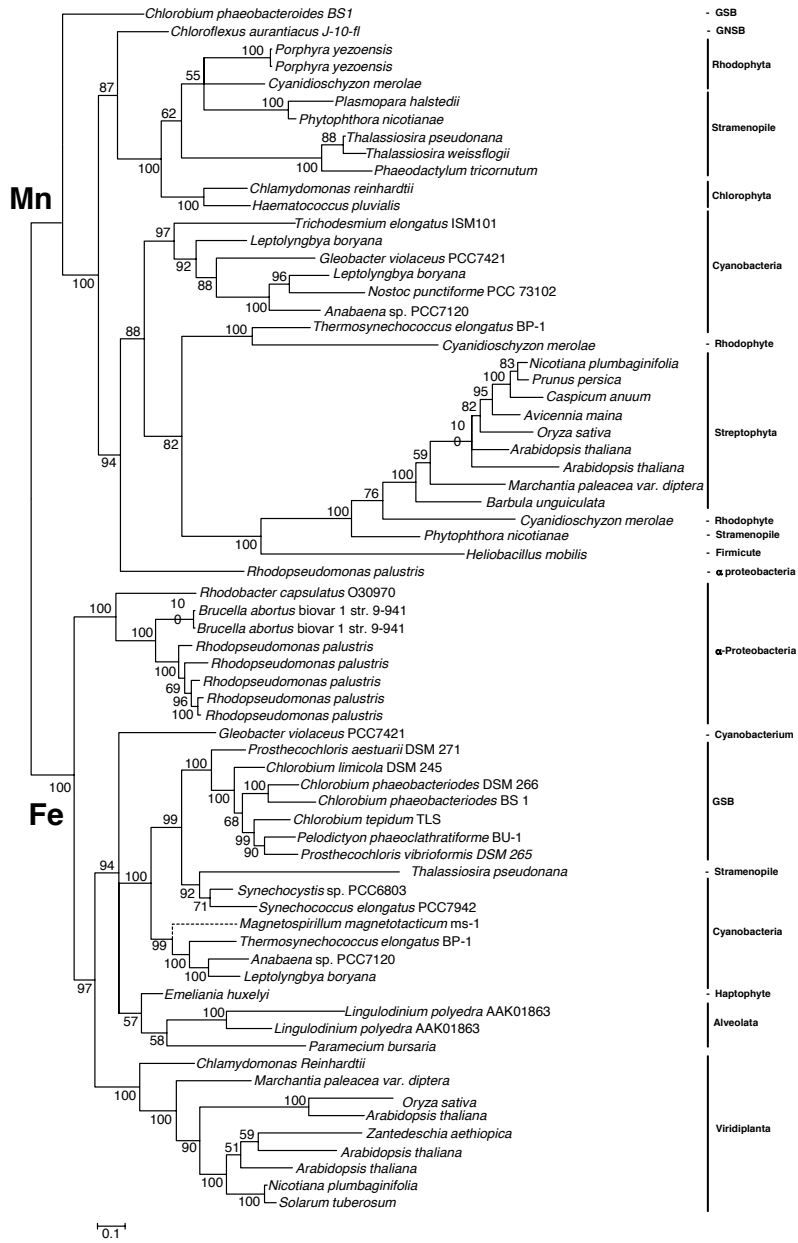


Figure 4.4: Bayesian based tree constructed as in Figure 1 based on plastid related organisms (analyses run for  $2 \times 10^6$  generations). Here the monophyly of plastid related eukaryotes to the cyanobacteria is better resolved for FeSOD. In the MnSOD clade, the cyanobacteria and green plants form a monophyletic cluster excluding primary green, and primary and secondary red algae. This is in contrast to the full trees including all organisms. The high posterior probability support (100%) for the divergence of these two groups before the inheritance of MnSOD suggests a closer, primary host relationship between the primary green, and primary and secondary red algae. Furthermore, this strongly supports the relationship between MnSODs of plants and cyanobacteria. Scale bar represents the expected number of substitutions per amino acid site.

The Mn-2 clade shows an unambiguous well supported (Bayesian posterior probability 100%/ML bootstrap 94%) divergence between Archaea and crown eukaryotes. The Archeal group forms the expected Crenarchaeota and Euryarchaeota clusters. Interestingly, four Eubacterial sequences always fall in the Archaea MnSOD clade. These sequences are the photosynthetic firmicute *Heliobacillus mobilis* and three Actinobacterial *Streptomyces* sp. representatives. The other half of Mn-2 characterizes the divergence of opisthokonts and green plants. Here also a few curious species fall into this group in both the Bayesian and ML analyses. First, a second copy of Mn SOD in the stramenopile *Phytophthora nicotianae* always clusters with the opisthokonts. Of further interest the alveolate *Tetrahymena pyriformis*, the mycetozoan *Dictyostelium discoideum*, and a third copy of MnSOD from the rhodophyte *Cyanidioschyzon merolae* share a recent common ancestor with the green plants. Mycetozoan phylogeny has been thoroughly explored and typically show them clustering at the base of the opisthokonts (Baldauf 1997). Together with the other two polyphyletic sequences here may suggest an enigmatic origin for second and third copies of the MnSOD gene in green plants.

#### 4.3.3 Phototrophic SOD phylogeny

A subset of 69 sequences was also analyzed which represent all the photosynthetic organisms in this data set. This Bayesian tree clarifies many of the same and some different phylogenetic relationships evident in the other trees with stronger statistical support. In the Fe clade the  $\alpha$ -proteobacteria cluster early and separately from the other taxa. This tree also shows the monophyletic relationship between the FeSOD sequences of green plants, primary green algae, alveolates, cyanobacteria, and secondary red plastid containing eukaryotes. In this analysis the cyanobacteria share a recent common ancestor

with the only stramenopile representative for FeSOD (*Thalassiosira pseudonana*). In contrast, the haptophyte *Emiliana huxleyi* and the dinoflagellate *Lingulodinium polyedra*, cluster with the alveolates.

The primary and secondary red-plastid containing organisms (including stramenopiles) share a common ancestor with the primary green algae for MnSOD. Separately, the green plants form a monophyletic group with the cyanobacteria and again diverge from three distant species: primary red alga *Cyanidioschyzon merolae*, stramenopile *Phytophthora nicotianae*, and firmicute bacteria *Heliobacillus mobilis*.

## 4.4 Discussion

### 4.4.1 Position of primary and secondary plastid-containing eukaryotes

Primary plastid-containing eukaryotes are all the result of a single endosymbiotic event and include the primary red plastid-containing algae and the primary green containing algae. Our analyses of FeSOD sequences show a large monophyletic relationship between primary green algae, green plants, cyanobacteria, alveolates and just a few representative of secondary red algae. This suggest a primary plastid origin to for this gene. This is corroborated by the plastid directed localization of this protein in extant taxa (Kliebenstein et al., 1998; Kitayama et al., 1999; Wu et al., 1999; Okamoto et al., 2001; Okomoto et al., 2001; Fink and Scandalios, 2002a).

Secondary plastid-containing eukaryotes (including the red lineage: stramenopiles, alveolates, haptophytes and the green lineage: euglenozoa) evolved when a secondary endosymbiosis between host cell engulfed an already photosynthetic eukaryotic cell. There are four genetic sources of SOD genes in secondary plastid-containing eukaryotes. These are the primary endosymbiont plastid and nucleus, the secondary host's mitochondria and/or the secondary host cell's genome. As is shown in our data, secondary green-plastid containing organisms (i.e. Euglenozoa and alveolates) have only FeSOD while secondary red-plastid eukaryotes can have either MnSOD or FeSOD or both. In the FeSOD clade, these organisms form a monophyletic cluster with the cyanobacteria and the green plants. A single primary endosymbiotic event is the accepted hypothesis thus, the last common ancestor for this gene in this diverse group of organisms is the primary endosymbiont plastid. Congruent with the primary plastid

origin of this gene, these proteins are all directed to the modern plastid in extant photosynthetic eukaryotes.

MnSOD is curiously absent among the secondary green plastid-containing eukaryotes but is present in the primary green algae (*Chlamydomonas reinhardtii* and *Hematococcus pulvairs*). The secondary green plastid groups are all parasites that have adapted to an aerobic lifestyle. The use of FeSOD is common among anaerobic organisms and there is a selective pressure to use FeSOD instead of MnSOD among obligate anaerobes because of the greater biological availability of Fe in anaerobic environments (Saito et al., 2003). Thus, these organisms secondarily lost the genes for MnSOD.

The opposite is true for the red plastid organisms. Among the diverse red lineage, primary red-plastid eukaryotes do not contain FeSODs. Furthermore, MnSODs are known only in stramenopiles. This suggests that the primary red algae either lost the gene following the divergence of secondary red plastid organisms (which all seem to retain a copy of FeSOD) or, the secondary red line acquired a copy from the secondary host. The general red lineage preference for MnSOD over the FeSODs is evidence by the multiple copies present in both the primary and secondary red plastid-containing taxa. The relatively recently evolved diatoms are the only red lineage group that theoretically has a copy of both Fe- and MnSOD. The abandonment of FeSOD in red plastid eukaryotes will be discussed below as related to the subcellular localization of the gene products.

In the analysis of just the photosynthetic taxa, the MnSOD clade including green plants and cyanobacteria are separate from a monophyletic clade with primary green-

plastid eukaryotes basal to a group of primary and secondary red-plastid containing eukaryotes. The monophyletic cluster of red derived eukaryotes has a robust posterior probability (100) and suggests that secondarily derived eukaryotes all share a common origin for this gene. Because they also share an ancestor with the primary green alga, we would expect MnSOD to be originally from the primary endosymbiont nucleus. In the full data set analyses, the cluster of cyanobacteria with the primary and secondary red and green alga has a weak posterior probability (57). This suggests, that the origin for MnSOD in green plants is likely the primary endosymbiont plastid while in the primary green alga and red (primary and secondary) algae it may be from the primary endosymbiont host nucleus.

#### *4.4.2 The secondary red-plastid puzzle*

There are two current hypotheses for the evolution of secondary red-plastid containing eukaryotes. The chromoalveolate hypothesis states that there was a single endosymbiotic event leading to all secondary red-plastid eukaryotes and thus secondary heterotrophic host would be identical (Cavalier-Smith, 1999). Because there is ample evidence for a single primary endosymbiotic event, this hypothesis would suggest a consistent monophyletic relationship between all diverse secondary red algae for genes that were vertically inherited. Most data which support this hypothesis are only weakly supported and the proponents of this theory suggest that multiple concatenated nuclear-encoded protein coding genes will be required to substantially show this relationship with high support (Harper and Keeling, 2003). The most popular gene family used to demonstrate this hypothesis is the nuclear encoded glyceraldehyde-3-phosphate dehydrogenase (GAPDH) which has multiple forms and can be localized in either the

mitochondrion, plastid or cytoplasm. The extant dispersion of GAPDH is a result of gene duplication of the cytosolic form and the replacement of the cyanobacterial plastid targeted GAPDH by one of these duplicated copies (Fast et al., 2001). The convoluted nature of GAPDH complicates the molecular history. For example, TPI-GAPDH fusion protein originated as a mitochondrial gene but, after transfer to the nucleus, it is not reimported into the mitochondria (Liaud et al., 2000). Gene redirections such as this can obscure the molecular phylogenetic significance of a nuclear encoded, organelle targeted gene.

The close relationship shown for GAPDH between alveolates and haptophytes is not surprising as dinoflagellates (alveolates) have been shown to have multiple endosymbiotic relationships with haptophytes (Yoon et al., 2004). It has also been suggested that the only way to explain the red plastid ancestor to the apicomplexa is that they have to share this GAPDH gene replacement event. But, new evidence for substantial eukaryotic lateral gene transfer could accomplish the same phylogenetic results (Andersson et al., 2003).

The second hypothesis suggests that secondary red-plastid eukaryotes evolved from different secondary hosts. The vast genetic and morphological diversity among the secondary reds has been shown by numerous authors. The phylogenetic evolution of Fe- and MnSODs also supports this diverse origin. To explain the dispersion of secondary red plastid-containing eukaryotes in the trees present here, there is a subtle hypothesis that would incorporate both of the previous ideas. Perhaps there was a single origin for the secondary red plastid algal host but before the second endosymbiotic event this host diverged. Our data for the SOD suggest that this may be another possibility.

Many studies have focused on understanding the phylogenetic position of secondary red alga. In our data two separate evolutionary histories are evident. The photosynthetic eukaryotes in the FeSOD mainly utilize this protein in the plastid. If the chromalvelate hypothesis holds, then we should see a monophyly of these organisms supporting the single origin for their plastids. However, FeSOD is curiously absent from primary red algae, which would be the ancestors to the secondary red algae; which included in our analyses represent all three of the major “chomist” groups. Instead we showed their distribution throughout, and *not* monophyly, in the FeSOD clade.

#### *4.4.3 Evidence for LGT beyond endosymbiosis*

The Fe/MnSOD family is well suited to point out evidence of lateral gene transfer (LGT) because they are found in all three domains of life, derive from an ancient gene duplication and are all nuclear encoded in eukaryotes; thus, their evolution is not influenced by the difference in evolutionary rates between nuclear and plastid or mitochondrial genomes (refs). Furthermore, they are highly conserved making them suitable for studying relationships over large evolutionary distances. Our data suggests evidence of LGT in a few instances.

Four Eubacterial sequences (firmicutes and actinobacteria) cluster with the Archaea in the MnSOD clade. This is evidence for LGT but the identity of the donor lineage is ambiguous due to uncertainty in the phylogenetic position of the bacteria. The eubacteria might be the out group to the larger Archaea cluster which would suggest that the Archaea acquired this gene from the bacterial ancestors. This would be consisted with the deeply branching nature of these bacterial representatives.

#### *4.4.4 Correlative relationship between the molecular evolution of Photosystems I and II and the Fe/MnSOD family*

The cyanobacterium-like prokaryote that became the primary plastid evolved from the fusion of two anaerobic photosynthetic prokaryotes each contributing to half of the mechanism for oxygenic photosynthesis (Gupta et al., 1999; Baymann et al., 2001). Oxygenic photosynthesis is a combination of photosystem (PS) I and PSII which splits water (Blankenship and Hartman, 1998). The ancestor to PSI has been shown to resemble the extant green sulfur bacteria (GSB) while the ancestor to PSII was an  $\alpha$ -proteobacterium. Concurrently, the ancestor to mitochondria was also an  $\alpha$ -proteobacterium (Esser et al., 2004). SOD proteins are physically involved with protecting of both photosynthetic and respiratory processes and are thus found even in the anaerobic photosynthetic GSB and an  $\alpha$ -proteobacterium. Our data suggests that FeSODs in oxygenic photoautotrophs evolved from the GSB ancestor to PSI because of the strongly supported (Bayesian posterior probability 100) cluster of GSB with cyanobacteria deep in the larger monophyletic group of photosynthetic eukaryotes. Moreover, physiological evidence also supports this origin. Heterocystous cyanobacteria express only FeSOD along side PSI in the formation of anaerobic heterocysts (Liu et al., 2000; Li et al., 2002). Photosynthetic eukaryotes express this protein almost exclusively in the chloroplast.

In contrast, the source for MnSOD in plastid containing eukaryotes is less clear. Green plants and primary green algae express MnSOD exclusively in the mitochondria which would suggest an  $\alpha$ -proteobacterial origin for this protein. In fact, the basal group to the green plant cluster in the MnSOD clade is the  $\alpha$ -proteobacteria

*Rhodopseudomonas plalustris* and thus this gene may have originated from the mitochondrial genome. However, for the primary green and primary and secondary red lines this may not be the case. Although, it is not clear from our data what might be the source.

## 4.5 Conclusions

The origin of the eukaryotic algal superoxide dismutases gene seems to correlate with the hypothesized scheme for their development (Knoll, 1992). Red and green phytoplankton (both using chlorophyll a, but either c or b as an accessory, respectively) are believed to have diverged early in their history at approximately 800 to 1000 Ma. After this divergence, green phytoplankton dominated the biota until approximately 250 Ma at the dawn of the Mesozoic Era. Hypotheses suggesting multiple endosymbioses conferring genetic advantages for red phytoplankton may help to clarify their dominance and continued success in today's ocean (Grzebyk et al., 2003; Grzebyk et al., 2004). That is, instead of just one endosymbiotic event for the acquisition of a plastid, there have been multiple secondary or even tertiary events.

Iron and manganese superoxide dismutases are typically specific in eukaryotes for either mitochondrion or plastid. These organelles also possess many other metabolic processes that require significant amounts of metal cofactors. In aerobic environments the availability of Fe is greatly reduced (Williams and Silva, 1996; Williams, 2001). But the Earth has not always been subjected to the sizable oxygen concentrations that exist today (Anbar and Knoll, 2002). Fe is more abundant than Mn under the reducing conditions of early earth and the extant anaerobic organisms that evolved under these conditions still possess FeSOD today. In fact organisms with low-potential metabolisms would experience much less pressure to develop alternative enzymes (Vance and Miller, 2001). The ability to use a homologous enzyme that did not require Fe would confer a selective advantage on a lineage. Archaea are most often extremeophiles living in conditions not suited to many other organisms (Kirschvink et al., 2000). These

organisms' possess the cambilistic Fe/MnSOD that are distinct among this protein family but more closely related to the MnSODs. These evolved mid way between the two fixed forms of Fe- and MnSOD.

The wide distribution of the Fe- and MnSODs among all groups of life suggest they evolved very early. Algal evolution occurred during most of Earth history and the most recently evolved secondary red plastid-containing eukaryotes rose to prominence in the Mesozoic (approx. 250 million years ago) and continue to dominate the modern ocean (Katz ref). The shift to MnSOD may correspond to the periodic shifts in redox conditions of the ocean as evident by the drastic changes in the geologic record and algal diversification. These drastic changes involved major shifts in the biological availability of different metal cofactors. As oxygen concentrations fluctuated, so did the amount of Fe that was accessible to life; increased oxygen in the atmosphere lead to decreasing soluble Fe in aquatic systems. There are a number of documented examples of metal substitutions in metalloenzymes either directly into the original protein or convergent evolution of a new protein that could use a more bioavailable metal (La Roche et al., 1999; McKay et al., 1999; Quinn and Merchant, 1999). Secondary red algae dominate the Fe-poor modern ocean along with cyanobacteria who possess either MnSODs or an alternative NiSOD (Wolfe-Simon et al., 2005). The Fe/MnSOD family may thus serve as a reliable evolutionary signature to help understand how geologic events influenced genetic composition.

Table 4.1 All Fe- and MnSOD amino acid sequences used in analyses and their ID

Group	OTU	Metal	GenBank accession number or URL
alveolate	<i>Lingulodinium polyedrum</i>	Fe	BP742166
alveolate	<i>Toxoplasma gondii</i>	Fe	CB373354
alveolate	<i>Toxoplasma gondii</i>	Fe	CB025606
alveolate	<i>Lingulodinium polyedrum</i>	Fe	AAK01863
alveolate	<i>Paramecium bursaria</i>	Fe	BAD11813
alveolate	<i>Plasmodium falciparum</i> 3d7 (2)	Fe	CAG25047
alveolate	<i>Plasmodium falciparum</i> 3d7 (3)	Fe	AAT11554
alveolate	<i>Plasmodium falciparum</i> 3d7 (4)	Fe	CAA89971
alveolate	<i>Plasmodium falciparum</i> 3d7	Fe	CAD51224
cyano	<i>Gloeobacter violaceus</i> PCC 7421	Fe	BAC92268
cyano	<i>Leptolyngbya boryana</i>	Fe	AAA69954
cyano	<i>Nostoc</i> sp. PCC 7120	Fe	BAB74637
cyano	<i>Synechococcus elongatus</i> PCC 7942	Fe	P18655
cyano	<i>Synechocystis</i> sp. PCC 6803	Fe	P77968
cyano	<i>Thermosynechococcus elongatus</i> BP-1	Fe	NP_682309
euglenozoa	<i>Trypanosoma brucei</i>	Fe	EAN80527
euglenozoa	<i>Trypanosoma brucei</i>	Fe	EAN80536
euglenozoa	<i>Trypanosoma brucei</i>	Fe	AAZ11448
euglenozoa	<i>Trypanosoma brucei</i>	Fe	EAN80448
green	<i>Chlamydomonas reinhardtii</i>	Fe	AAB04944
gsb	<i>Prosthecochloris vibrioformis</i> DSM 265	Fe	EAO16013
gsb	<i>Pelodictyon phaeoclathratiforme</i> BU-1	Fe	EAN26037
gsb	<i>Chlorobium tepidum</i> TLS	Fe	AAM72443
gsb	<i>Prosthecochloris aestuarii</i> DSM 271	Fe	EAN22564
gsb	<i>Chlorobium phaeobacteroides</i> DSM 266	Fe	EAM35831
gsb	<i>Chlorobium phaeobacteroides</i> BS1	Fe	EAM63850
gsb	<i>Chlorobium limicola</i> DSM 245	Fe	EAM42875
haptophyte	<i>emeliana huxleyi</i>	Fe	
parabasilid	<i>Tritrichomonas foetus</i>	Fe	AAC47734
parabasilid	<i>Tritrichomonas foetus</i>	Fe	AAC47735
parabasilid	<i>Trichomonas vaginalis</i>	Fe	AAC48291
plant	<i>Arabidopsis thaliana</i>	Fe	AAO42100
plant	<i>Arabidopsis thaliana</i>	Fe	AAM14164
plant	<i>Marchantia paleacea</i> var. <i>diptera</i>	Fe	BAC66948
plant	<i>Arabidopsis thaliana</i>	Fe	AAA32791
plant	<i>Nicotiana glauca</i>	Fe	P11796
plant	<i>Oryza sativa</i>	Fe	BAA37131
plant	<i>Solanum tuberosum</i>	Fe	AAO16563
plant	<i>zantedeschia aethiopica</i>	Fe	
proteobacteria	<i>Rhodospseudomonas palustris</i> BisB18	Fe	ZP_00846288
proteobacteria	<i>Magnetospirillum magnetotacticum</i> MS-1	Fe	ZP_00054068

proteobacteria	<i>Rhodopseudomonas palustris</i> BisB5	Fe	ZP_00805469
proteobacteria	<i>Brucella abortus</i> biovar 1 str. 9-941	Fe	YP_221327
proteobacteria	<i>Rhodopseudomonas palustris</i> CGA009	Fe	CAE27134
proteobacteria	<i>Rhodopseudomonas palustris</i> BisA53	Fe	ZP_00810096
proteobacteria	<i>Rhodopseudomonas palustris</i> HaA2	Fe	ZP_00840210
proteobacteria	<i>Azotobacter vinelandii</i> AvOP	Fe	ZP_00417890
proteobacteria	<i>Bordetella pertussis</i>	Fe	P37369
proteobacteria	<i>Brucella abortus</i> biovar 1 str. 9-941	Fe	AAX73966
proteobacteria	<i>Escherichia coli</i>	Fe	P09157
proteobacteria	<i>Legionella pneumophila</i>	Fe	P31108
proteobacteria	<i>Photobacterium leiognathi</i>	Fe	P09213
proteobacteria	<i>Rhodobacter capsulatus</i>	Fe	O30970
proteobacteria	<i>Salmonella typhimurium</i>	Fe	P40726
stramenopile	<i>Thalassiosira pseudonana</i>	Fe	
Actinobacteria	<i>Streptomyces griseus</i>	Mn (Fe-Zn)	AAD30139
Actinobacteria	<i>Streptomyces coelicolor</i> A3(2)	Mn (Fe)	AAD33128
Actinobacteria	<i>Streptomyces coelicolor</i> A3(2)	Mn	NP_625295
alveolate	<i>Tetrahymena pyriformis</i>	Mn (Fe)	A39223
archaea	<i>Methanosarcina barkeri</i> str. fusaro	Mn	YP_307037
archaea	<i>Haloferax volcanii</i> DS2	Mn	AAA73375
archaea	<i>Sulfolobus acidocaldarius</i> DSM 639	Mn	YP_254907
archaea	<i>Methanothermobacter thermautotrophicus</i> str. Delta H	Mn	NP_275303
archaea	<i>Methanospirillum hungatei</i> JF-1	Mn	ZP_00867623
archaea	<i>Sulfolobus solfataricus</i> P2	Mn (Fe)	NP_341862
archaea	<i>Methanosarcina acetivorans</i> C2A	Mn	NP_616507
archaea	<i>Natronomonas pharaonis</i> DSM 2160	Mn	CAI50111
archaea	<i>Methanosarcina mazei</i> Go1	Mn	NP_634447
archaea	<i>Sulfolobus tokodaii</i> str. 7	Mn	NP_378284
archaea	<i>Halobacterium salinarum</i>	Mn	P09737
archaea	<i>Methanosarcina barkeri</i> str. fusaro	Mn	ZP_00543823
archaea	<i>Pyrobaculum aerophilum</i> str. IM2	Mn	NP_558493
archaea	<i>Aeropyrum pernix</i> K1	Mn	NP_147461
archaea	<i>Acidianus ambivalens</i>	Mn	AAF36989
archaea	<i>Haloarcula hispanica</i>	Mn	O08459
archaea	<i>Haloarcula marismortui</i>	Mn	Q03302
cyano	<i>Nostoc</i> sp. PCC 7120	Mn	BAB77594
cyano	<i>Gloeobacter violaceus</i> PCC 7421	Mn	BAC88623
cyano	<i>Leptolyngbya boryana</i>	Mn	AAA69952
cyano	<i>Leptolyngbya boryana</i>	Mn	AAA69953
cyano	<i>Nostoc punctiforme</i> PCC 73102	Mn	ZP_00112125
cyano	<i>Thermosynechococcus elongatus</i> BP-1	Mn	BAC07589
cyano	<i>trichodesmium</i> ims101 soda1	Mn	
Deinococcus-Thermus	<i>Deinococcus geothermalis</i> DSM 11300	Mn	ZP_00397917
Deinococcus-Thermus	<i>Deinococcus radiodurans</i> R1	Mn	NP_295003
Deinococcus-Thermus	<i>Thermus thermophilus</i> HB8	Mn	YP_143823

Fibrobacteres/	<i>Solibacter usitatus</i> Ellin6076	Mn	ZP_00523034
Firmicutes	<i>Candidatus Phytoplasma asteris</i>	Mn	BAD04527
Firmicutes	<i>heliobacillus</i>	Mn	
fungi	<i>Candida albicans</i> SC5314	Mn	EAK99231
fungi	<i>Candida</i> sp. HN95	Mn	CAA72335
fungi	<i>Glomerella graminicola</i>	Mn	AAL27457
fungi	<i>Penicillium chrysogenum</i>	Mn	O75007
fungi	<i>Pneumocystis carinii</i>	Mn	AAC24764
gnsb	<i>Chloroflexus aurantiacus</i> J-10-fl	Mn	AAP41921
green	<i>Chlamydomonas reinhardtii</i>	Mn	AAA80639
green	<i>Haematococcus pluvialis</i>	Mn	AAW69292
gsb	<i>Chlorobium phaeobacteroides</i> BS1	Mn	EAM61711
metazoa	<i>Callinectes sapidus</i>	Mn	AF264030
metazoa	<i>Equus caballus</i>	Mn	Q9XS41
metazoa	<i>Gallus gallus</i>	Mn	AAG46055
metazoa	<i>Homo sapiens</i>	Mn	XP_004242
metazoa	<i>Mus</i> sp.	Mn	AAB34899
metazoa	<i>Onchocerca volvulus</i>	Mn	CAA57657
metazoa	<i>Rattus norvegicus</i>	Mn	NP_058747
mycetozoa	<i>Dictyostelium discoideum</i>	Mn	EAL71885
Planctomycetes	<i>Rhodopirellula baltica</i> SH 1	Mn	CAD74947
plant	<i>Arabidopsis thaliana</i>	Mn	AAO42188
plant	<i>Marchantia paleacea</i> var. diptera	Mn	BAD13494
plant	<i>Prunus persica</i>	Mn	Q9SM64
plant	<i>Nicotiana glauca</i>	Mn	CAA00824
plant	<i>Arabidopsis thaliana</i>	Mn	O81235
plant	<i>Avicennia marina</i>	Mn	AAN15216
plant	<i>Barbula unguiculata</i>	Mn	BAA86881
plant	<i>Capsicum annuum</i>	Mn	AAB88870
plant	<i>Oryza sativa</i>	Mn	Q43008
proteobacteria	<i>Bordetella pertussis</i>	Mn	CAA59267
proteobacteria	<i>Salmonella typhimurium</i>	Mn	AAC43331
proteobacteria	<i>Actinobacillus pleuropneumoniae</i>	Mn	AAB03279
proteobacteria	<i>Methylobacter</i> sp. J	Mn	P23744
proteobacteria	<i>Methylobacter</i> sp.	Mn	A38461
proteobacteria	<i>Vibrio cholerae</i>	Mn	AAK53547
proteobacteria	<i>Rhodopseudomonas palustris</i> HaA2	Mn	ZP_00843005
proteobacteria	<i>Salmonella typhimurium</i> LT2	Mn	AAL22895
proteobacteria	<i>Acinetobacter</i> sp. ADP1	Mn	CAA86923
proteobacteria	<i>Escherichia coli</i> O157:H7	Mn	Q8X7B2
proteobacteria	<i>Yersinia pestis</i> KIM	Mn	AE014009
Rhodophyte	<i>Porphyra yezoensis</i>	Mn	AAZ75664
Rhodophyte	<i>Porphyra yezoensis</i>	Mn	AAZ75665
Rhodophyte	<i>Cyanidioschyzon merolae</i>	Mn	cmn023c
Rhodophyte	<i>Cyanidioschyzon merolae</i>	Mn	cmr158c

Rhodophyte	<i>Cyanidioschyzon merolae</i>	Mn	cmt028c
stramenopile	<i>Plasmopara halstedii</i> SSH	Mn	CB174636
stramenopile	<i>Phytophthora nicotianae</i>	Mn	AAV57576
stramenopile	<i>Phytophthora nicotianae</i>	Mn	AAV57577
stramenopile	<i>Thalassiosira weissflogii</i>	Mn	AAQ04679
stramenopile	<i>Phaeodactylum tricornutum</i>	Mn	PtMnSOD_assem
stramenopile	<i>Thalassiosira pseudonana</i>	Mn	

Table 4.2. Averages of Similarity Indices of Fe and Mn Superoxide Dismutases

Fe					Mn						
	Bacteria	Alveolates	Cyanobacteria	Plants		Opisthokonts	Bacteria	Archaea	Cyanobacteria	Plants	Red (1° +2°)
	[18]	[9]	[5]	[8]		[10]	[18]	[X]	[7]	[10]	[9]
N-terminus					N-terminus						
C-terminus					C-terminus						
Total	76.3	63.3	78.2	61.5	Total	65.1	58.9	68.2	78.2	78.4	54.9

Table 4.3. Prokaryotic and eukaryotic plastid-related sequences used in analyses

Isozyme		Taxa	Asseccion #
Mn	Cyanobacteria	<i>Trichodesmium elongatus</i> ISM101	
		<i>Gleobacter violaceus</i> PCC7421	BAC88623
		<i>Leptolyngbya boryana</i>	AAA69952, AAA69953
		<i>Thermosynechococcus elongatus</i> BP-1	BAC07589
		<i>Nostoc punctiforme</i> PCC 73102	ZP_00112125
		<i>Anabaena</i> sp. PCC7120	BAB77594
	Rhodophytes	<i>Prophyra yezoensis</i>	AAZ75664, AAZ75665
		<i>Cyanidioschyzon merolae</i> (3)	
	Stramenopile	<i>Phaeodactylum tricomutum</i>	
		<i>Thalassiosira pseudonana</i> CCMP1335	
		<i>Thalassiosira weissflogii</i>	
		<i>Plasmopara halstedii</i>	CB174636
	Chlorophytes	<i>Phytophthora nicotianae</i>	AAY57576, AAY57577
		<i>Haematococcus pluvialis</i>	AAW69292
		<i>Chlamydomonas reinhardtii</i>	AAA80639
Fe	Cyanobacteria	<i>Gleobacter violaceus</i> PCC7421	BAC92268
		<i>Synechococcus elongatus</i> PCC7942	P18655
		<i>Synechocystis</i> sp. PCC6803	P77968
		<i>Thermosynechococcus elongatus</i> BP-1	NP_682309
		<i>Leptolyngbya boryana</i>	AAA69954
		<i>Anabaena</i> sp. PCC7120	BAB74637
	Alveolate	<i>Lingulodinium polyedra</i>	BP742166, AAK01863
	Stramenopile	<i>Thalassiosira pseudonana</i> CCMP1335	
	Haptophyte	<i>Emeliana hux</i>	
	Chlorophytes	<i>Chlamydomonas reinhardtii</i>	AAB04944

## References

- Ahner BA, Morel FMM** (1995) Phytochelatin production in marine algae: II. induction by various metals. *Limnology & Oceanography* **40**: 658-665
- Amanatidou A, Bennik MH, Gorris LG, Smid EJ** (2001) Superoxide dismutase plays an important role in the survival of *Lactobacillus sake* upon exposure to elevated oxygen. *Archives of Microbiology* **176**: 79-88
- Anbar AD, Knoll AH** (2002) Proterozoic ocean chemistry and evolution: a bioinorganic bridge? *Science* **297**: 1137-1142
- Anderson JM, Park Y-I, Chow WS** (1999) Unifying model for the photoinactivation of Photosystem II *in vivo* under steady-state photosynthesis. *Photosynthesis Research* **56**: 1-13
- Andersson B, Aro EM** (1997) Proteolytic activities and proteases of plant chloroplasts. *Physiologia Plantarum* **100**: 780-793
- Andersson JO, Sjogren AM, Davis LA, Embley TM, Roger AJ** (2003) Phylogenetic analyses of diplomonad genes reveal frequent lateral gene transfers affecting eukaryotes. *Current Biology* **13**: 94-104
- Apel K, Hirt H** (2004) REACTIVE OXYGEN SPECIES: Metabolism, oxidative stress, and signal transduction. *Annual Review of Plant Biology* **55**: 373-399
- Armbrust EV, Berges JA, Bowler C, Green BR, Martinez D, Putnam NH, Zhou S, Allen AE, Apt KE, Bechner M, Brzezinski MA, Chaal BK, Chiovitti A, Davis AK, Demarest MS, Detter JC, Glavina T, Goodstein D, Hadi MZ, Hellsten U, Hildebrand M, Jenkins BD, Jurka J, Kapitonov VV, Kroger N, Lau WW, Lane TW, Larimer FW, Lippmeier JC, Lucas S, Medina M, Montsant A, Obornik M, Parker MS, Palenik B, Pazour GJ, Richardson PM, Rynearson TA, Saito MA, Schwartz DC, Thamtrakoln K, Valentin K, Vardi A, Wilkerson FP, Rokhsar DS** (2004) The genome of the diatom *Thalassiosira pseudonana*: ecology, evolution, and metabolism. *Science* **306**: 79-86
- Aro EM, Virgin I, Andersson B** (1993) Photoinhibition of Photosystem II. Inactivation, protein damage and turnover. *Biochimica et Biophysica Acta* **1143**: 113-134
- Asada K** (1999) The water-water cycle as alternative photon and electron sinks. *Philosophical Transactions of the Royal Society of London B Biological Sciences* **355**: 1419-1431
- Atzenhofer W, Regelsberger G, Jacob U, Peschek G, Furtmuller P, Huber R, Obinger C** (2002) The 2.0 Å resolution structure of the catalytic portion of a cyanobacterial membrane-bound manganese superoxide dismutase. *J Mol Biol* **321**: 479-489

- Baldauf SL** (2003) The deep roots of eukaryotes. *Science* **300**: 1703-1706
- Baldauf SL, Bhattacharya D, Cockrill P, Hugenholtz P, Pawlowski J, Simpson AGB** (2004) The origin and radiation of life on earth. In J Cracraft, MJ Donoghue, eds, *Assembling the tree of life*. Oxford University Press, New York
- Bannister JV, Parker MW** (1985) The presence of a copper/zinc superoxide dismutase in the bacterium *Photobacterium leiognathi*: a likely case of gene transfer from eukaryotes to prokaryotes. *Proceedings of the National Academy of Sciences of the United States of America* **82**: 149-152
- Barber J, Andersson B** (1992) Too much of a good thing: light can be bad for photosynthesis. *Trends in Biochemical Sciences* **17**: 61-66
- Barondeau DP, Kassmann CJ, Bruns CK, Tainer JA, Getzoff ED** (2004) Nickel superoxide dismutase structure and mechanism. *Biochemistry* **43**: 8038-8047
- Batinic-Haberle I** (2002) Manganese porphyrins and related compounds as mimics of superoxide dismutase. In L Packer, ed, *Superoxide Dismutase*, Vol 349. Academic Press, New York, pp 223-233
- Batinic-Haberle I, Spasojevic I, Stevens R, Hambright P, Neta P, Okado-Matsumoto A, Fridovich I** (2004) New class of potent catalysts of  $O_2^-$  dismutation. Mn (III) *ortho*-methoxyethylpyridyl- and di-*ortho*-methoxyethyl-imidazolylporphyrins. *Dalton Transactions* **11**: 1696-1702
- Baymann F, Brugna M, Muhlenhoff U, Nitschke W** (2001) Daddy, where did (PS)I come from? *Biochimica et Biophysica Acta* **1507**: 291-310
- Benov L, Fridovich I** (1996) Functional significance of the Cu,ZnSOD in *Escherichia coli*. *Archives of Biochemistry & Biophysics* **327**: 249-253
- Benov LT, Fridovich I** (1994) *Escherichia coli* expresses a copper- and zinc-containing superoxide dismutase. *Journal of Biological Chemistry* **269**: 25310-25314
- Bhattacharya D, Medlin L** (1995) The phylogeny of plastids: A review based on comparisons of small subunit ribosomal RNA coding regions. *Journal of Phycology* **31**: 489-498
- Blankenship RE, Hartman H** (1998) The origin and evolution of oxygenic photosynthesis. *Trends in Biochemical Sciences* **23**: 94-97
- Blough NV, Zepp RG** (1995) Reactive oxygen species in natural waters. In CS Foote, JS Valentine, A Greenberg, JF Liebman, eds, *Active oxygen in chemistry*, Vol 2. Blackie Academic & Professional, New York, pp 280-333

- Borgstahl GE, Pokross M, Chehab R, Sekher A, Snell EH** (2000) Cryo-trapping the six-coordinate, distorted-octahedral active site of manganese superoxide dismutase. *J Mol Biol* **296**: 951-959
- Boveris A, Cadenas E** (1982) Production of superoxide radicals and hydrogen peroxide in mitochondria. *In* LW Oberley, ed, *Superoxide Dismutase*, Vol II. CRC Press, Inc., Boca Raton, pp 15-30
- Bowler C, Montagu MV, Inze D** (1992) Superoxide dismutase and stress tolerance. *Annual Review of Plant Physiology and Plant Molecular Biology* **43**: 83-116
- Boyd PW, Watson AJ, Law CS, Abraham ER, Trull T, Murdoch R, Bakker DC, Bowie AR, Buesseler KO, Chang H, Charette M, Croot P, Downing K, Frew R, Gall M, Hadfield M, Hall J, Harvey M, Jameson G, LaRoche J, Liddicoat M, Ling R, Maldonado MT, McKay RM, Nodder S, Pickmere S, Pridmore R, Rintoul S, Safi K, Sutton P, Strzepek R, Tanneberger K, Turner S, Waite A, Zeldis J** (2000) A mesoscale phytoplankton bloom in the polar Southern Ocean stimulated by iron fertilization.[see comment]. *Nature* **407**: 695-702
- Brocks JJ, Logan GA, Buick R, Summons RE** (1999) Archean molecular fossils and the early rise of eukaryotes. *Science* **285**: 1033-1036
- Cabecadas I, Brogueira MJ, Cabecadas G** (1999) Phytoplankton spring bloom in the Targus coastal waters: hydrological and chemical conditions. *Aquatic Ecology* **33**: 243-250
- Canini A, Albertano P, Caiola MG** (1998) Localization of Fe-containing superoxide dismutase in cyanobacteria from the Baltic Sea: depth and light dependency. *New Phytologist* **139**: 247-254
- Casteilla L, Rigoulet M, Penicaud L** (2001) Mitochondrial ROS metabolism: modulation by uncoupling proteins. *IUBMB Life* **52**: 181-188
- Cavalier-Smith T** (1999) Principles of protein and lipid targeting in secondary endosymbiosis: euglenoid, dinoflagellate, and sporozoan plastid origins and the eukaryote family tree. *Journal of Eukaryotic Microbiology* **46**: 347-366
- Chen H, Romo-Leroux PA, Salin ML** (1996) The iron-containing superoxide dismutase-encoding gene from *Chlamydomonas reinhardtii* obtained by direct and inverse PCR. *Gene* **168**: 113-116
- Chen J, Liao C, Mao SJ, Chen T, Weng C** (2001) A simple technique for the simultaneous determination of molecular weight and activity of superoxide dismutase using SDS-PAGE. *Journal of Biochemical & Biophysical Methods* **47**: 233-237
- Coale KH, Johnson KS, Chavez FP, Buesseler KO, Barber RT, Brzezinski MA, Cochlan WP, Millero FJ, Falkowski PG, Bauer JE, Wanninkhof RH, Kudela**

- RM, Altabet MA, Hales BE, Takahashi T, Landry MR, Bidigare RR, Wang X, Chase Z, Strutton PG, Friederich GE, Gorbunov MY, Lance VP, Hiltling AK, Hiscock MR, Demarest M, Hiscock WT, Sullivan KF, Tanner SJ, Gordon RM, Hunter CN, Elrod VA, Fitzwater SE, Jones JL, Tozzi S, Koblizek M, Roberts AE, Herndon J, Brewster J, Ladizinsky N, Smith G, Cooper D, Timothy D, Brown SL, Selph KE, Sheridan CC, Twining BS, Johnson ZI** (2004) Southern Ocean Iron Enrichment Experiment: Carbon Cycling in High- and Low-Si Waters. *Science* **304**: 408-414
- Critchley C** (1994) D1 protein turnover: response to photodamage or mechanism? *In* N Baker, JR Bowyer, eds, Photoinhibition of photosynthesis from molecular mechanisms to the field. BIOS Scientific Publ., Oxford, pp 195-201
- Cullen JJ, Lewis MR** (1995) Biological processes and optical measurements near the sea-surface: some issues relevant to remote sensing. *Journal of Geophysical Research* **100**: 13255-13266
- del Rio LA, Sandalio LM, Altomare DA, Zilinskas BA** (2003) Mitochondrial and peroxisomal manganese superoxide dismutase: differential expression during leaf senescence. *J Exp Bot* **54**: 923-933
- Delwiche CF** (1999) Tracing the thread of plastid diversity through the tapestry of life. *American Naturalist* **154**: S164-177
- Delwiche CF, Palmer JD** (1996) Rampant horizontal transfer and duplication of rubisco genes in eubacteria and plastids. *Molecular Biology and Evolution* **13**: 873-882
- Dismukes GC, Klimov VV, Baranov SV, Kozlov YN, DasGupta J, Tyryshkin A** (2001) The origin of atmospheric oxygen on Earth: The innovation of oxygenic photosynthesis. *Proceedings of the National Academy of Sciences of the United States of America* **98**: 2170-2175
- Dufour E, Boulay J, Rincheval V, Sainsard-Chanet A** (2000) A casual link between respiration and senescence in *Podospora anserina*. *Proceedings of the National Academy of Sciences of the United States of America* **97**: 4138-4143
- Edward RA, Whittaker MM, Whittaker JW, Jameson GB, Baker EN** (1998) Distinct metal environment in Fe-substituted manganese superoxide dismutase provides a structural basis of metal specificity. *Journal of the American Chemical Society* **120**: 9684-9685
- Edwards RA, Whittaker MM, Whittaker JW, Baker EN, Jameson GB** (2001) Outer sphere mutations perturb metal reactivity in manganese superoxide dismutase. *Biochemistry* **40**: 15-27
- Esser C, Ahmadinejad N, Wiegand C, Rotte C, Sebastiani F, Gelius-Dietrich G, Henze K, Kretschmann E, Richly E, Leister D, Bryant D, Steel MA, Lockhart PJ, Penny D, Martin W** (2004) A genome phylogeny for

mitochondria among alpha-proteobacteria and a predominantly eubacterial ancestry of yeast nuclear genes. *Molecular Biology & Evolution* **21**: 1643-1660

**Falconi M, O'Neill P, Stroppolo ME, Desideri A** (2002) Superoxide dismutase kinetics. *Methods in Enzymology* **349**: 38-49

**Falkowski PG, Katz ME, Knoll AH, Quigg A, Raven JA, Schofield O, Taylor FJR** (2004a) The evolution of modern eukaryotic phytoplankton. *Science* **305**: 354-360

**Falkowski PG, Raven JA** (1997) *Aquatic Photosynthesis*. Blackwell Science, Ltd., Malden

**Falkowski PG, Schofield O, Katz ME, Schoothbrugge Bvd, Knoll A** (2004b) Why is the land green and the ocean red? *In* H Thierstein, J Young, eds, *Coccolithophorids*. Springer-Verlag, Berlin

**Fast NM, Kissinger JC, Roos DS, Keeling PJ** (2001) Nuclear-encoded, plastid-targeted genes suggest a single common origin for apicomplexan and dinoflagellate plastids.[see comment]. *Molecular Biology & Evolution* **18**: 418-426

**Fee JA** (1991) Regulation of sod genes in *Escherichia coli*: relevance to superoxide dismutase function. *Molecular Microbiology* **5**: 2599-2610

**Felsenstein J** (1981) Evolutionary trees from DNA sequences: a maximum likelihood approach. *Journal of Molecular Evolution* **17**: 368-376

**Fenton HJH, Jackson H** (1899) The oxidation of polyhydric alcohols in presence of iron. *Journal of the Chemical Society B* **75**: 1-11

**Fink RC, Scandalios JG** (2002a) Molecular evolution and structure-function relationships of the superoxide dismutase gene families in angiosperms and their relationship to other eukaryotic and prokaryotic superoxide dismutases. *Archives of Biochemistry & Biophysics* **399**: 19-36

**Fink RC, Scandalios JG** (2002b) Molecular evolution and structure-function relationships of the superoxide dismutase gene families in angiosperms and their relationship to other eukaryotic and prokaryotic superoxide dismutases. *Archives of Biochemistry & Biophysics* **399**: 19-36

**Fridovich I**, ed (1981) *The biology of superoxide and of superoxide dismutases*- In brief. Academic Press, New York

**Fridovich I** (1995) Superoxide radical and superoxide dismutase. *Annual Review of Biochemistry* **64**: 97-112

**Fridovich I** (1997) Superoxide anion radical ( $O_2^-$ ), superoxide dismutases, and related matters. *Journal of Biological Chemistry* **272**: 18515-18517

- Fridovich I** (1998) Oxygen toxicity: a radical explanation. *Journal of Experimental Biology* **201**: 1203-1209
- Gabig TG, Babior BM** (1982) Oxygen-dependent microbial killing by neutrophils. *In* LW Oberley, ed, *Superoxide Dismutase*, Vol II. CRC Press, Inc., Boca Raton, pp 1-14
- Gasc AM, Morris PJ, Karl DM** (2002) Sources and sinks of hydrogen peroxide at Station ALOHA. *In*. AGU Ocean Sciences Meeting, Honolulu, HI
- Gonzalez A, Steffen KL, Lynch JP** (1998) Light and excess manganese. *Plant Physiology* **118**: 493-504
- Grace SC** (1990) Phylogenetic distribution of superoxide dismutase supports an endosymbiotic origin for chloroplasts and mitochondria. *Life Sciences* **47**: 1875-1886
- Gray MW, Burger G, Lang BF** (1999) Mitochondrial evolution. *Science* **283**: 1476-1481
- Greenberg B, Gaba V, Canacini O, Malkin S, Mattoo A, Edelman M** (1989) Separate photosensitizers mediate degradation of the 32-kDa photosystem II reaction center protein in the visible and UV spectral regions. *Proceedings of the National Academy of Sciences of the United States of America* **86**: 6617-6620
- Grzebyk D, Katz ME, Knoll AH, Quigg A, Raven JA, Schofield O, Taylor FJR, Falkowski PG** (2004) The evolution of secondary symbionts: Are red plastids more portable? Response to Keeling et al. *Science* **306**: 2191
- Grzebyk D, Schofield O, Vetriani C, Falkowski PG** (2003) The mesozoic radiation of eukaryotic algae: the portable plastid hypothesis. *Journal of Phycology* **39**: 259-267
- Guillard RRL**, ed (1975) *Culture of phytoplankton for feeding marine invertebrates*. Plenum Press, New York
- Guillard RRL, Ryther JH** (1962) Studies of marine planktonic diatoms. I. *Cyclotella nana* Hustedt and *Detonula confervacea* Cleve. *Canadian Journal of Microbiology* **8**: 229-239
- Guindon S, Gascuel O** (2003) A simple, fast, and accurate algorithm to estimate large phylogenies by maximum likelihood. *Systematic Biology* **52**: 696-704
- Guindon S, Rodrigo AG, Dyer KA, Huelsenbeck JP** (2004) Modeling the site-specific variation of selection patterns along lineages. *Proceedings of the National Academy of Sciences of the United States of America* **101**: 12957-12962

- Gupta RS, Mukhtar T, Singh B** (1999) Evolutionary relationships among photosynthetic prokaryotes (*Heliobacterium chlorum*, *Chloroflexus aurantiacus*, cyanobacteria, *Chlorobium tepidum* and proteobacteria): implications regarding the origin of photosynthesis. *In* Molecular Microbiology, Vol 32. Blackwell Publishing Limited, p 893
- Haber F, Weiss J** (1934) The catalytic decomposition of hydrogen peroxide by iron salts. *Proceedings of the Royal Society of London* **147A**: 332-351
- Hall TA** (1999) BioEdit: a user-friendly biological sequence alignment editor and analysis program for Windows 95/98/NT. *Nucleic Acid Symposium Series* **41**: 95-98
- Halliwell B** (1982) The toxic effects of oxygen on plant tissues. *In* LW Oberley, ed, Superoxide Dismutase, Vol I. CRC Press, Inc., Boca Raton, pp 89-124
- Halliwell B** (1995) The biological significance of oxygen-derived species. *In* JS Valentine, CS Foote, A Greenberg, JF Liebman, eds, Active Oxygen in Biochemistry. Blackie Academic and Professional, New York, pp 313-335
- Halliwell B** (1999) Antioxidant defence mechanisms: From the beginning to the end (of the beginning). *Free Radical Research* **31**: 261-272
- Han D, Williams E, Cadenas E** (2001) Mitochondrial respiratory chain-dependent generation of superoxide anion and its release into the intermembrane space. *Biochemical Journal* **353**: 411-416
- Harper JT, Keeling PJ** (2003) Nucleus-Encoded, Plastid-Targeted Glyceraldehyde-3-Phosphate Dehydrogenase (GAPDH) Indicates a Single Origin for Chromalveolate Plastids *Mol Biol Evol* **20**: 1730-1735
- Herbert SK, Samson G, Fork DC, Laudenbach DE** (1992) Characterization of damage to photosystems I and II in a cyanobacterium lacking detectable iron superoxide dismutase activity. *Proc Natl Acad Sci U S A* **89**: 8716-8720
- Ho RYN, Liebman JF, Valentine JS** (1995a) Biological Reactions of Dioxygen: An Introduction. *In* JS Valentine, CS Foote, A Greenberg, JF Liebman, eds, Active Oxygen in Biochemistry. Blackie Academic and Professional, New York, pp 1-36
- Ho RYN, Liebman JF, Valentine JS** (1995b) Overview of energetics and reactivity of oxygen. *In* CS Foote, JS Valentine, A Greenberg, JF Liebman, eds, Active Oxygen in Chemistry, Ed 1 Vol 2. Blackie Academic and Professional, New York, pp 1-23
- Ho T-Y, Quigg A, Finkel ZV, Mulligan A, Wyman K, Falkowski PG, Morel FMM** (2003) On the elemental composition of some marine phytoplankton. *Journal of Phycology* **39**: 1145-1159

- Huelsenbeck JP, Ronquist F** (2001) MRBAYES: Bayesian inference of phylogeny. *Bioinformatics* **17**: 754-755
- Inarrea P** (2002) Purification and determination of activity of mitochondrial cyanide-sensitive superoxide dismutase in rat tissue extract. *In* L Packer, ed, *Superoxide Dismutase*, Vol 349. Academic Press, New York, pp 106-114
- Iwanzik W, Tevini M, Dohut G, Vots M, Weiss W, Graber P, Renger G** (1983) Action of UV-B on photosynthetic primary reactions in spinach chloroplasts. *Physiologia Plantarum* **58**: 401-407
- Jansen M, Gaba V, Greenberg B, Mattoo A, Elderman M** (1993) UV-B driven degradation of the D1 reaction-center protein of photosystem II proceeds via plastosemiquinone. *In* H Yamamoto, C Smith, eds, *Photosynthetic Responses to the Environment*. American Society of Plant Physiologists, Rockville, MD, pp 142-149
- Jeffrey SW, Humphrey GF** (1975) New spectrophotometric equations for determining chlorophylls a, b, c1 and c2 in higher plants, algae, and natural phytoplankton. *Biochem Physiol Pflanz* **167**: 191-194
- Jesus MDD, F T, Chapman DJ** (1989) Taxonomic distribution of copper-zinc superoxide dismutase in green algae and its phylogenetic importance. *Journal of Phycology* **25**: 767-772
- Joint I, Tait K, Callow ME, Callow JA, Milton D, Williams P, Camara M** (2002) Cell-to-cell communication across the prokaryote-eukaryote boundary. *Science* **298**: 1207
- Kim CS, Lee SG, Lee CK, Kim HG, Jung J** (1999a) Reactive oxygen species as causative agents in the ichthyotoxicity of the red tide dinoflagellate *Cochlodinium polykrikoides*. *Journal of Plankton Research* **21**: 2105-2115
- Kim D, Nakamura A, Okamoto T, Komatsu N, Oda T, Ishimatsu A, Muramatsu T** (1999b) Toxic potential of the raphidophyte *Olisthodiscus luteus*: mediation by reactive oxygen species. *Journal of Plankton Research* **21**: 1017-1027
- Kim JH, Nemson JA, Melis A** (1993) Photosystem II reaction center damage and repair in *Dunaliella salina* (green alga): analysis under physiological and irradiance-stress conditions. *Plant Physiology* **103**: 181-189
- Kirschvink JL, Gaidos EJ, Bertani LE, Beukes NJ, Gutzmer J, Maepa LN, Steinberger RE** (2000) Paleoproterozoic snowball Earth: Extreme climatic and geochemical global change and its biological consequences. *Proceedings of the National Academy of Sciences of the United States of America* **97**: 1400-1405

- Kitayama K, Kitayama M, Osafune T, Togasaki RK** (1999) Subcellular localization of iron and manganese superoxide dismutase in *Chlamydomonas reinhardtii* (Chlorophyceae). *Journal of Phycology* **35**: 136-142
- Kliebenstein DJ, Monde RA, Last RL** (1998) Superoxide dismutase in *Arabidopsis*: an eclectic enzyme family with disparate regulation and protein localization. *Plant Physiology* **118**: 637-650
- Knoll A** (2003) Life on a young planet: the first three billion years of evolution on earth. Princeton University Press, Princeton
- Knoll AH** (1992) The early evolution of eukaryotes: a geological perspective. *Science*. **256**: 622-627
- Kolber ZS, Prasil O, Falkowski PG** (1998) Measurement of variable chlorophyll fluorescence using fast repetition rate techniques: defining methodology and experimental protocols. *Biochimica et Biophysica Acta* **1367**: 88-106
- Koppenol WH** (1988) The paradox of oxygen: thermodynamics *versus* toxicity. In TE King, HS Manson, M Morrison, eds, *Oxidases and Related Redox Systems*, Vol 274. Alan R. Liss, Inc., New York, pp 93-109
- Kremling K, Streu P** (2001) The behaviour of dissolved Cd, Co, Zn, and Pb in North Atlantic near-surface waters (30 degrees N/60 degrees W-60 degrees N/2 degrees W). *Deep-Sea Research Part I Oceanographic Research Papers* **48**: 2541-2567
- Kulandaivelu G, Noorundeen A** (1983) Comparative study of the action of ultraviolet-C and ultraviolet-B radiation on photosynthetic electron transport. *Physiologia Plantarum* **58**: 389-394
- La Roche J, McKay RML, Boyd P** (1999) Immunological and molecular probes to detect phytoplankton responses to environmental stress in nature. *Hydrobiologia* **401**: 177-198
- Lah MS, Dixon MM, Pattridge KA, Stallings WC, Fee JA, Ludwig ML** (1995) Structure-function in *Escherichia coli* iron superoxide dismutase: comparisons with the manganese enzyme from *Thermus thermophilus*. *Biochemistry* **34**: 1646-1660
- LaRoche J, Geider RJ, Graziano LM, Murray H, Lewis K** (1993) Induction of specific proteins in eukaryotic algae grown under iron-, phosphorus-, or nitrogen-deficient conditions. *Journal of Phycology* **29**: 767-777
- Lesser MP, Stochaj WR** (1990) Photoadaptation and protection against active forms of oxygen in the symbiotic prokaryote *Prochloron* sp. and its ascidian host. *Applied & Environmental Microbiology* **56**: 1530-1535

- Levasseur M, Fortier L, Therriault J-C, Harrison PJ** (1992) Phytoplankton dynamics in a coastal jet frontal region. *Marine Ecology Progress Series* **86**: 283-295
- Li T, Huang X, Zhou R, Liu Y, Li B, Nomura C, Zhao J** (2002) Differential expression and localization of Mn and Fe superoxide dismutases in the heterocystous cyanobacterium *Anabaena* sp. strain PCC 7120. *J Bacteriol* **184**: 5096-5103
- Li Y-H** (1991) Distribution patterns of the elements in the ocean: A synthesis. *Geochimica et Cosmochimica Acta* **55**: 3223-3240
- Liaud M-F, Lichtl C, Apt K, Martin W, Cerff R** (2000) Compartment-Specific Isoforms of TPI and GAPDH are Imported into Diatom Mitochondria as a Fusion Protein: Evidence in Favor of a Mitochondrial Origin of the Eukaryotic Glycolytic Pathway  
*Mol Biol Evol* **17**: 213-223
- Liochev SI, Fridovich I** (1994) The role of  $O_2^{\cdot -}$  in the production of  $HO^{\cdot}$ : *in vitro* and *in vivo*. *Free Radical Biology and Medicine* **16**: 29-33
- Liochev SI, Fridovich I** (1999) Superoxide and iron: Partners in Crime. *IUBMB Life* **48**: 157-161
- Liu Y, Zhou R, Zhao J** (2000) Molecular cloning and sequencing of the *sodB* gene from a heterocystous cyanobacterium *Anabaena* sp. PCC 7120. *Biochimica et Biophysica Acta* **1491**: 248-252
- Malanga G, Calmanovici G, Puntarulo S** (1997) Oxidative damage to the chloroplasts from *Chlorella vulgaris* exposed to ultraviolet-B radiation. *Physiologia Plantarum* **101**: 455-462
- Malanga G, Puntarulo S** (1995) Oxidative stress and antioxidant content in *Chlorella vulgaris* after exposure to Ultraviolet-B radiation. *Physiologia Plantarum* **94**: 672-679
- Maliekal J, Karapetian A, Vance C, Yikilmaz E, Wu Q, Jackson T, Brunold TC, Spiro TG, Miller AF** (2002) Comparison and contrasts between the active site PKs of Mn-superoxide dismutase and those of Fe-superoxide dismutase. *Journal of the American Chemical Society* **124**: 15064-15075
- Mallick N, Mohn FH** (2000) Reactive oxygen species: response of algal cells. *Journal of Plant Physiology* **157**: 183-193
- Martin W, Russell MJ** (2003) On the origins of cells: a hypothesis for the evolutionary transitions from abiotic geochemistry to chemoautotrophic prokaryotes, and from prokaryotes to nucleated cells. *Phil. Trans. R. Soc. Lond. B* **358**: 59-85

- Martinez JS, Zhang GP, Holt PD, Jung H-T, Carrano CJ, Haygood MG, Butler A** (2000) Self-assembling amphiphilic siderophores from marine bacteria. *Science* **287**: 1245-1247
- Matsuzaki M, Misumi O, Shin IT, Maruyama S, Takahara M, Miyagishima SY, Mori T, Nishida K, Yagisawa F, Yoshida Y, Nishimura Y, Nakao S, Kobayashi T, Momoyama Y, Higashiyama T, Minoda A, Sano M, Nomoto H, Oishi K, Hayashi H, Ohta F, Nishizaka S, Haga S, Miura S, Morishita T, Kabeya Y, Terasawa K, Suzuki Y, Ishii Y, Asakawa S, Takano H, Ohta N, Kuroiwa H, Tanaka K, Shimizu N, Sugano S, Sato N, Nozaki H, Ogasawara N, Kohara Y, Kuroiwa T** (2004) Genome sequence of the ultrasmall unicellular red alga *Cyanidioschyzon merolae* 10D. *Nature* **428**: 653-657
- Mattoo AK, Hoffman-Falk H, Marder JB, Edelman M** (1984) Regulation of protein metabolism: coupling of photosynthetic electron transport to in vivo degradation of the rapidly metabolized 32-kilodalton protein of the chloroplast membranes. *Proceedings of the National Academy of Sciences* **81**: 1380-1384
- McFadden GI** (2001) Chloroplast origin and integration. *Plant Physiology* **125**: 50-53
- McKay RM, Roche JL, Yakunin AF, Durnford DG, Geider RJ** (1999) Accumulation of ferredoxin and flavodoxin in a marine diatom in response to Fe. *Journal of Phycology* **35**: 510-519
- Melis A, Nemson J, Harrison M** (1992) Damage to functional components and partial degradation of photosystem II reaction center proteins upon chloroplast exposure to ultraviolet-B radiation. *Biochimica et Biophysica Acta* **1100**: 312-320
- Michel H, Deisenhofer J** (1988) Relevance of the photosynthetic reaction center from purple bacteria to the structure of photosystem II. *Biochemistry* **27**: 1-7
- Moller IM** (2001) Plant mitochondria and oxidative stress: electron transport, NADPH turnover, and metabolism of reactive oxygen species. *Annual Review of Plant Physiology and Plant Molecular Biology* **52**: 561-591
- Neidhardt J, Benemann JR, Zhang L, Melis A** (1998) Photosystem-II repair and chloroplast recovery from irradiance stress: Relationship between chronic photoinhibition, light-harvesting chlorophyll antenna size and photosynthetic productivity in *Dunaliella salina* (green algae). *Photosynthesis Research* **56**: 175-184
- Nickelsen J, Rochaix JD** (1994) Regulation of synthesis of D1 and D2 proteins of photosystems II. In N Baker, JR Bowyer, eds, *Photoinhibition of photosynthesis from molecular mechanisms to the field*. BIOS Scientific Publ., Oxford, pp 179-190
- Nozaki H, Matsuzaki M, Misumi O, Kuroiwa H, Hasegawa M, Higashiyama T, Shin IT, Kohara Y, Ogasawara N, Kuroiwa T** (2004) Cyanobacterial genes

transmitted to the nucleus before divergence of red algae in the Chromista.  
*Journal of Molecular Evolution* **59**: 103-113

- Nozaki H, Matsuzaki M, Takahara M, Misumi O, Kuroiwa H, Hasegawa M, Shin-i T, Kohara Y, Ogasawara N, Kuroiwa T** (2003a) The phylogenetic position of red algae revealed by multiple nuclear genes from mitochondria-containing eukaryotes and an alternative hypothesis on the origin of plastids. *Journal of Molecular Evolution* **56**: 485-497
- Nozaki H, Ohta N, Matsuzaki M, Misumi O, Kuroiwa T** (2003b) Phylogeny of plastids based on cladistic analysis of gene loss inferred from complete plastid genome sequences. *Journal of Molecular Evolution* **57**: 377-382
- Nozaki Y, Yamada M, Nakanishi T, Nagaya Y, Nakamura K, Shitashima K, Tsubota H** (1998) The distribution of radionuclides and some trace metals in the water columns of the Japan and Bonin trenches. *Oceanologica Acta* **21**: 469-484
- Oda T, Akaike T, Sato K, Ishimatsu A, Takeshita S, Muramatsu T, Maeda H** (1992) Hydroxyl radical generation by red tide algae. *Archives of Biochemistry and biophysics* **294**: 38-43
- Oda T, Nakamura A, Shikayama M, Kawano I, Ishimatsu A, Muramatsu T** (1997) Generation of reactive oxygen species by raphidophycean phytoplankton. *Bioscience Biotechnology & Biochemistry* **61**: 1658-1662
- Okado-Matsumoto A, Fridovich I** (2001) Subcellular distribution of superoxide dismutases in rat liver: Cu,Zn-SOD in mitochondria. *Journal of Biological Chemistry* **276**: 38388-38393
- Okamoto OK, Asano CS, Aidar E, Colepicolo P** (1996) Effects of cadmium on growth and superoxide dismutase activity of the marine microalga *Tetraselmis gracilis* (Prasinophyceae). *Journal of Phycology* **32**: 74-79
- Okamoto OK, Colepicolo P** (1998) Response of superoxide dismutase to pollutant metal stress in the marine dinoflagellate *Gonyaulax polyedra*. *Comparative Biochemistry and Physiology, Part C: Toxicology & Pharmacology* **119**: 67-73
- Okamoto OK, Robertson DL, Fagan TF, Hastings JW, Colepicolo P** (2001) Different regulatory mechanisms modulate the expression of a dinoflagellate iron-superoxide dismutase. *Journal of Biological Chemistry* **276**: 19989-19993
- Okamoto OK, Pinto E, Latorre LR, Bechara EJH, Colepicolo P** (2001) Antioxidant modulation in response to metal-induced oxidative stress in algal chloroplasts. *Arch. Environ. Contam. Toxicol* **40**: 18-24
- Olsen GJ, Matsuda H, Hagstrom R, Overbeek R** (1994) fastDNAm1: A tool for construction of phylogenetic trees of DNA sequences using maximum likelihood. *Comput. Appl. Biosci.* **10**: 41-48

- Page RD** (1996) TreeView: an application to display phylogenetic trees on personal computers. *Computer Applications in the Biological Sciences* **12**: 357-358
- Palenik B, Brahamsha B, Larimer FW, Land M, Hauser L, Chain P, Lamerdin J, Regala W, Allen EE, McCarren J, Paulsen I, Dufresne A, Partensky F, Webb EA, Waterbury J** (2003) The genome of a motile marine *Synechococcus*. *Nature* **424**: 1037-1042
- Palmer JD** (2003) The symbiotic birth and spread of plastids: How many times and whodunit? *Journal of Phycology* **39**: 4-11
- Partensky F, Hess WR, Vaulot D** (1999) *Prochlorococcus*, a marine photosynthetic prokaryote of global significance. *Microbiol. Mol. Biol. Rev.* **63**: 106-127
- Peers G, Price NM** (2004) A role for manganese in superoxide dismutases and growth of iron-deficient diatoms. *Limnology and Oceanography* **49**: 1774-1783
- Pinto E, Sigaud-kutner TCS, Leitao M, Okamoto O, Morse D, Colepicolo P** (2003) Heavy metal-induced oxidative stress in algae. *Journal of Phycology* **39**: 1008-1018
- Prasil O, Kolber Z, Berry JA, Falkowski P** (1996) Cyclic electron flow around photosystem II in vivo. *Photosynthesis Research* **48**: 395-410
- Quigg A, Finkel ZV, Irwin AJ, Reinfelder JR, Rosenthal Y, Ho T-Y, Schofield O, Rosenthal FMM, Falkowski PG** (2003) The evolutionary inheritance of elemental stoichiometry in marine phytoplankton. *Nature* **425**: 291-294
- Quinn JM, Merchant S** (1999) Adaptation of *Senedesmus obliquus* (Chlorophyceae) to copper-deficiency: Transcriptional regulation of *PcyI* but not *CpxI*. *Journal of Phycology* **35**: 1253-1263
- Raven JA** (1990) Predictions of Mn and Fe use efficiencies of phototrophic growth as a function of light availability for growth and of C assimilation pathway. *New Phytologist* **116**: 1-18
- Raven JA, Evans MCW, Korb RE** (1999) The role of trace metals in photosynthetic electron transport in O<sub>2</sub>-evolving organisms. *Photosynthesis Research* **60**: 111-149
- Raychaudhuri SS, Deng XW** (2000) The role of superoxide dismutase in combating oxidative stress in higher plants. *The Botanical Review* **66**: 89-98
- Regelsberger G, Atzenhofer W, Ruker F, Peschek GA, Jakopitsch C, Paumann M, Furtmuller PG, Obinger C** (2002) Biochemical characterization of a membrane-bound manganese-containing superoxide dismutase from the cyanobacterium *Anabaena* PCC7120. *Journal of Biological Chemistry* **277**: 43615-43622

- Renault JP, Verchere-Beaur C, Morgenstern-Badarau I, Yamakura F, Gerloch M** (2000) EPR and ligand field studies of iron superoxide dismutases and iron-substituted manganese superoxide dismutases: relationships between electronic structure of the active site and activity. *Inorganic Chemistry* **39**: 2666-2675
- Renger G, Volker M, Eckert H, Fromme R, Hom-Veit S, Graber P** (1989) On the mechanism of photosystem II deterioration by UV-B irradiation. *Photochemistry and Photobiology* **49**: 97-105
- Richter M, Ruhle W, Wild A** (1990) On the mechanism of photosystem II photoinhibition I. A two-step degradation of D1-protein. *Photosynthesis Research* **24**: 229-235
- Rijstenbil JW** (2002) Assessment of oxidative stress in the planktonic diatom *Thalassiosira pseudonana* in response to UVA and UVB radiation. *Journal of Plankton Research* **24**: 1277-1288
- Rijstenbil JW** (2003) Effects of UVB radiation and salt stress on growth, pigments and antioxidative defence of the marine diatom *Cylindrotheca closterium*. *Marine Ecology Progress Series* **254**: 37-47
- Rijstenbil JW, Derksen JWM, Gerringa LJA, Poortvliet TCW, Sandee A, Van Den Berg M, Van Drie J, Wijnholds JA** (1994) Oxidative stress induced by copper: defense and damage in the marine planktonic diatom *Ditylum brightwellii*, grown in continuous cultures with high and low zinc levels. *Marine Biology* **119**: 583-590
- Ronquist F, Huelsenbeck JP** (2003) MRBAYES 3: Bayesian phylogenetic inference under mixed models. *Bioinformatics* **19**: 1572-1574
- Saito MA, Sigman DM, Morel FMM** (2003) The bioinorganic chemistry of the ancient ocean: the co-evolution of cyanobacterial metal requirements and biogeochemical cycles at the Archean-Proterozoic boundary? *Inorganica Chimica Acta* **356**: 308-318
- Sakurai H, Kusumoto N, Kitayama K, Togasaki RK** (1993) Isozymes of superoxide dismutase in *Chlamydomonas* and purification of one of the major isozymes containing Fe. *Plant & Cell Physiology* **34**: 1133-1137
- Sanudo-Wilhelmy SA, Olsen KA, Scelfo JM, Foster TD, Flegal AR** (2002) Trace metal distributions off the Antarctic Peninsula in the Weddell Sea. *Marine Chemistry* **77**: 157-170
- Scandalios JG** (1993) Oxygen stress and superoxide dismutases. *Plant Physiology* **101**: 7-12

- Schofield O, Moline MA, Prezelin BB** (1994) Palmer LTER: Photoadaptation in a coastal phytoplankton bloom and impact on the radiation utilization efficiency for carbon fixation. *Antarctic Journal of the United States* **29**: 214-216
- Seyler PT, Boaventura GR** (2003) Distribution and partition of trace metals in the Amazon basin. *Hydrological Processes* **17**: 1345-1361
- Shiller AM** (1997) Manganese in surface waters of the Atlantic Ocean. *Geophysical Research Letters* **24**: 1495-1498
- Smith MW, Doolittle RF** (1992) A comparison of evolutionary rates of the two major kinds of superoxide dismutase. *Journal of Molecular Evolution* **34**: 175-184
- Smith SW, Overbeek R, Woese CR, Gilbert W, Gillevet PM** (1994) The genetic data environment: an expandable GUI for multiple sequence analysis. *Comput. Appl. Biosci.* **10**: 671-675
- Steinman H** (1982a) Superoxide dismutases: protein chemistry and structure-function relationships. *In* LW Oberley, ed, *Superoxide Dismutase*, Vol I. CRC Press, Inc., Boca Raton, pp 11-68
- Steinman HM** (1982b) Copper-zinc superoxide dismutase from *Caulobacter crescentus* CB15. A novel bacteriocuprein form of the enzyme. *Journal of Biological Chemistry* **257**: 10283-10293
- Steinman HM** (1985) Bacteriocuprein superoxide dismutases in pseudomonads. *Journal of Bacteriology* **162**: 1255-1260
- Sterner RW, Smutka TM, McKay RML, Xiaoming Q, Brown ET, Sherrell RM** (2004) Phosphorus and trace metal limitation of algae and bacteria in Lake Superior. *Limnology and Oceanography* **49**: 495-507
- Sunda WG, Huntsman SA** (1986) Relationships among growth rate, cellular manganese concentrations and manganese transport kinetics in estuarine and oceanic species of the diatom *Thalassiosira*. *Journal of Phycology* **22**: 259-270
- Sunda WG, Huntsman SA** (1998) Interactive effects of external manganese, the toxic metals copper and zinc, and light in controlling cellular manganese and growth in a coastal diatom. *Limnology & Oceanography* **43**: 1467-1475
- Sundby C, McCaffery S, Anderson JM** (1993) Turnover of the photosystem II D1 protein in higher plants under photoinhibitory and nonphotoinhibitory irradiance. *Journal of Biological Chemistry* **268**: 25476-25482
- Takishita K, Ishida K-i, Maruyama T** (2004) Phylogeny of nuclear-encoded plastid-targeted GAPDH gene supports separate origins for the peridinin- and fucoxanthin derivative-containing plastids of dinoflagellates. *Protist* **155**: 447-458

- Telfer A, Barber J** (1994) Elucidation of the molecular mechanisms of photoinhibition by studying isolated photosystem II reaction centers. *In* N Baker, J Bowyer, eds, Photoinhibition of photosynthesis. BIOS Scientific Publishers, Oxford, pp 25-49
- Thompson JD, Gibson TJ, Plewniak F, Jeanmougin F, Higgins DG** (1997) The CLUSTAL\_X windows interface: flexible strategies for multiple sequence alignment aided by quality analysis tools. *Nucleic Acids Research* **25**: 4876-4882
- Thompson JD, Higgins DG, Gibson TJ** (1994) CLUSTAL W: improving the sensitivity of progressive multiple sequence alignment through sequence weighting, positions-specific gap penalties and weight matrix choice. *Nucleic Acids Research* **22**: 4673-4680
- Towbin H, Staehelin T, Gordon J** (1979) Electrophoretic transfer of proteins from polyacrylamide gels to nitrocellulose sheets: procedure and some applications. *Proceedings of the National Academy of Sciences* **76**: 4350-4354
- Twiner MJ, Trick CG** (2000) Possible physiological mechanisms for production of hydrogen peroxide by the ichthyotoxic flagellate *Heterosigma akashiwo*. *Journal of Plankton Research* **22**: 1961-1975
- Vance CK, Miller AF** (1998) Spectroscopic comparisons of the pH dependencies of Fe-substituted (Mn)superoxide dismutase and Fe-superoxide dismutase. *Biochemistry* **37**: 5518-5527
- Vance CK, Miller AF** (2001) Novel insights into the basis for Escherichia coli superoxide dismutase's metal ion specificity from Mn-substituted FeSOD and its very high E(m). *Biochemistry* **40**: 13079-13087
- Voelker BM, Sedlak DL, Zafiriou OC** (2000) Chemistry of superoxide radical in seawater: Reactions with organic Cu complexes. *Environmental Science & Technology* **34**: 1036-1042
- Voet D, Voet JG** (1990) *Biochemistry*. Wiley, New York
- Weatherburn DC** (2001) Manganese-containing enzymes and proteins. *In* I Bertini, A Sigel, H Sigel, eds, *Handbook on Metalloproteins*. Marcel Dekker, Inc., New York, pp 193-268
- Weiss J** (1935) Investigations on the radical HO<sub>2</sub> in solution. *Transactions of the Faraday Society* **31**: 668-681
- Whelan S, Goldman N** (2001) A general empirical model of protein evolution derived from multiple protein families using a maximum-likelihood approach. *Molecular Biology and Evolution* **18**: 691-699
- Whitfield M** (2001) Interactions between phytoplankton and trace metals in the ocean. *Advances in Marine Biology* **41**: 1-128

- Williams RJP** (2001) Chemical selection of elements by cells. *Coordination Chemistry Reviews* **216-217**: 583-595
- Williams RJP, Silva JJRFd** (1996) The natural selection of the chemical elements : the environment and life's chemistry. Clarendon Press ; Oxford University Press, Oxford  
New York
- Wolfe-Simon F, Grzebyk D, Schofield O, Falkowski PG** (2005) The role and evolution of superoxide dismutases in algae. *Journal of Phycology* **41**: 453-465
- Wu G, Wilen RW, Robertson AJ, Gusta LV** (1999) Isolation, chromosomal localization, and differential expression of mitochondrial manganese superoxide dismutase and chloroplastic copper/zinc superoxide dismutase genes in wheat. *Plant Physiology* **120**: 513-520
- Wuerges J, Lee J-W, Yim Y-I, Yim H-S, Kang S-O, Carugo KD** (2004) Crystal structure of nickel-containing superoxide dismutase reveals another type of active site. *Proceedings of the National Academy of Sciences of the United States of America* **101**: 8569-8574
- Yoon HS, Hackett JD, Ciniglia C, Pinto G, Bhattacharya D** (2004) A Molecular Timeline for the Origin of Photosynthetic Eukaryotes  
*Mol Biol Evol* **21**: 809-818
- Youn H-D, Kim E-J, Roe J-H, Hah YC, Kang S-O** (1996) A novel nickel-containing superoxide dismutase from *Streptomyces* spp. *Biochem J.* **318**: 889-896
- Zelko IN, Manriani YJ, Folz RJ** (2002) Superoxide dismutase multigene family: A comparison of the CuZn-SOD (SOD1), Mn-SOD (SOD2), and EC-SOD (SOD3) gene structures, evolution, and expression. *Free Radical Biol. Med.* **33**: 337-349
- Zepp RG, Faust BC, Holgne J** (1992) Hydroxyl radical formation in aqueous reactions (pH 3-8) of iron(II) with hydrogen peroxide: the photo-fenton reaction. *Environ. Sci. Technol.* **26**: 313-319
- Ziemann DA, Conquest LD, Olaizola M, Bienfang PK** (1991) Interannula variability in the spring phytoplankton bloom in Auke Bay, Alaska. *Marine Biology* **109**: 321-334
- Zigone AR, Casotti R, d'Alcala MR, Scardi M, Marino D** (1995) 'St Martin's Summer': The case of an autumn phytoplankton bloom in the Gulf of Naples (Mediterranean Sea). *Journal of Plankton Research* **17**: 575-593

## CURRICULUM VITAE

FELISA LAUREN WOLFE SIMON

### EDUCATION

2006 Ph.D. Oceanography, Rutgers University, New Brunswick, New Jersey.  
 2000 B.A. Biology (Chemistry), Oberlin College and Conservatory, Oberlin, Ohio.  
 2000 B.M. Oboe Performance (Ethnomusicology), Oberlin College and Conservatory, Oberlin, Ohio.

### APPOINTMENTS

2006- NSF Post-Doctoral Fellow, Dept. of Chemistry and Biochemistry and  
 Dept. of Geosciences, Arizona State University  
 2003-2006 Graduate Assistant, Dept. of Oceanography, Rutgers University  
 2001-2003 Teaching Assistant, Dept. of Oceanography, Rutgers University  
 2000-2001 Graduate Fellow, Dept. of Oceanography, Rutgers University

### REFEREED PUBLICATIONS

**F. Wolfe-Simon**, D. Grzebyk, O. Schofield, and P. G. Falkowski (2006). The role and evolution of superoxide dismutases in algae. *Journal of Phycology*, 41:453-465.

**F. Wolfe-Simon**, V. Starovoytov, J. R. Reinfelder, O. Schofield, and P. G. Falkowski (2006). Localization and role of manganese superoxide dismutase in a marine diatom. *Plant Physiology*, in revision.

**F. Wolfe-Simon**, D. Grzebyk, O. Schofield, and P. G. Falkowski (2006). The phylogenetic position of iron and manganese superoxide dismutase in secondary red algae. *Journal of Molecular Evolution*, in prep.

**F. Wolfe-Simon**, Ilana Berman-Frank, Liti Haramaty, O. Schofield, and P. G. Falkowski (2006). Characterization of superoxide dismutase in the marine photosynthetic diazotroph *Trichodesmium erythraeum* IMS101. *Journal of Bacteriology*, in prep.

**F. Wolfe**, K. Kroeger and I. Valiela (1999). Increased lability of estuarine dissolved organic nitrogen from urbanized watersheds. *Biological Bulletin*. 197:290-292.

### HONORS AND AWARDS

National Science Foundation- Minority Post-doctoral Research Fellowship, 2006-2008  
 Honorable mention NSF Graduate Student Fellowship, 2001  
 Excellence Graduate Fellowship (Rutgers University), 2000  
 Sigma Xi, Associate Member (2000)  
 National Science Foundation- Research Experience for Undergraduates (REU), 1999  
 Hope Hibbard Scholarship in Biology (Oberlin College), 1999  
 Leo S. Millar Prize in Biological Scholarship (Oberlin College), 1998

### SYNERGISTIC ACTIVITIES

President, Oceanography Graduate Student Association, 2003-2004

### TEACHING EXPERIENCE

Spring 2005 Oceanographic Scientific Inquiry: From biogeochemistry to genomes: Explorations at aquatic interfaces

Fall 2001, 2002 Chemical Oceanography (T.A.)

**CRUISE EXPERIENCE**

2003 RV Suncoaster

1997 RV Cape Henlopen

1996 RV Cape Henlopen